

**EVALUATING THE ROLE OF THE RAFFINOSE FAMILY OF  
OLIGOSACCHARIDES IN HYBRID POPLAR**  
*(Populus alba × grandidentata)*

by

Faride Unda

M.Sc, The University of British Columbia, 2006

A THESIS SUBMITTED IN PARTIAL FULFILLMENT OF  
THE REQUIREMENTS FOR THE DEGREE OF

DOCTOR OF PHILOSOPHY

in

The Faculty of Graduate Studies

(Forestry)

THE UNIVERSITY OF BRITISH COLUMBIA

(Vancouver)

October 2012

© Faride Unda, 2012

## Abstract

The raffinose family of oligosaccharides (RFO) function as transport carbohydrates in the phloem, storage compounds in sink tissues, and as putative metabolic agents that combat plant stresses. Research on the RFO pathway has focused on seed biology and plants that transport raffinose as their primary photoassimilate. In contrast, few studies have explored this pathway in woody species. As such, this thesis investigated the fundamental function of the RFO enzymes in hybrid poplar, with emphasis on galactinol synthase (GolS), an enzyme key to the pathway. Phylogenetic comparisons of *Populus* GolS with other known GolS suggest a putative role for these enzymes in stress response. Protein analysis of two heterologously expressed isoforms demonstrated that they are true GolS; with Pa×gGolSI possessing a broader pH and temperature range than Pa×gGolSII. Expression patterns also revealed that the *Pa×gGolSII* transcript abundance varied seasonally. Together, the results suggest that Pa×gGolSI may be involved in basic metabolic activities, while Pa×gGolSII is likely involved in seasonal mobilization of carbohydrates. To further elucidate the *in-planta* GolS function, transgenic trees with mis-regulated *GolS* were generated. Two *AtGolS3* over-expression (*OE*) transgenic lines showed effects on growth, while other lines appeared normal and possessed marginally modified cell wall characteristics. The extreme over-expressers were severely stunted and had cell wall traits characteristic of tension wood. *AtGolS3-OE* lines showed reduction in the microfibril angle, increase in cell wall crystallinity and possessed higher cellulose, and lower mannose and lignin contents. Interestingly, although galactinol and raffinose contents increased dramatically, they were not more tolerant to abiotic stress under the conditions tested. These results suggest that the over-expression of GolS and its product galactinol may serve as a molecular signal that

initiates different metabolic changes for combating stress, culminating in the formation of tension wood. Additionally, over-expression of raffinose synthase (*RFS*) resulted in increased biomass and total cellulose content. However, it does not appear to have a similar signalling role. Collectively, this research opens new insight about functions of the RFO in poplar, with the participation of GolS in stress signalling and consequent tension wood formation, and the importance of RFS to carbon allocation and growth.

## **Preface**

This thesis contains three chapters written with the intent of publication in peer-reviewed journals.

Chapter 2: Faride Unda helped on the design of the research project, performed the research, conducted data analysis, and prepared the manuscript. Lindsay Preston assisted in performing research. Thomas Canam helped on the design of the research project and on editing the manuscript. Shawn Mansfield was involved with identification and design of the research program, providing research opportunity, and with manuscript preparation. A version of chapter 2 has been published: Unda, F., Canam, T., Preston, L. and Mansfield, S.D. (2012) Isolation and characterization of galactinol synthases from hybrid poplar. *J. Exp. Bot.* 63, 5, 2059-2069.

Chapter 3: Faride Unda helped on the design of the research project, performed the research, conducted data analysis, and prepared the manuscript. Lindsay Preston, Foster Hart and Francis Raiche de Araujo assisted in performing research. Ji-Young Park assisted in designing the research project. Shawn Mansfield was involved with identification and design of the research program, providing research opportunity and with manuscript preparation.

Chapter 4: Faride Unda helped on the design of the research project, performed the research, conducted data analysis, and prepared the manuscript. Harman Sidhu and Nav Sidhu assisted in performing research. Shawn Mansfield was involved with identification and design of the research program, providing research opportunity, and with manuscript preparation.

## Table of contents

Abstract .....	ii
Preface.....	iv
Table of contents.....	v
List of tables.....	xi
List of figures .....	xii
List of symbols and abbreviations .....	xvi
Acknowledgements.....	xviii
Dedication .....	xix
Chapter 1: Introduction .....	1
1.1    The raffinose family of oligosaccharides (RFO) .....	1
1.1.1    Galactinol synthase .....	2
1.1.1.1 <i>Arabidopsis thaliana</i> .....	2
1.1.1.2 <i>Ajuga reptans</i> .....	3
1.1.1.3 <i>Coffea arabica</i> L.....	3
1.1.1.4 <i>Populus</i> spp.....	4
1.1.1.5 <i>Medicago sativa</i> L.....	4
1.1.1.6 <i>Boea hygrometrica</i> .....	5
1.1.1.7    Seeds .....	5
1.1.2    Raffinose synthase .....	6
1.2    Phloem loading and sugar translocation .....	6
1.3    Relationships between carbohydrate content and abiotic stress tolerance.....	9
1.4    Sugar signalling .....	12

1.5	Wood formation .....	14
1.5.1	Tension wood.....	15
1.6	Model organism .....	17
1.6.1	<i>Populus</i> spp.....	17
1.6.2	Goal and hypothesis .....	18
1.6.2.1	Chapter 2: Isolation and characterization of galactinol synthases from hybrid poplar .....	18
1.6.2.2	Chapter 3: Varied expression of the <i>Gols</i> in transgenic hybrid poplar ( <i>Populus alba</i> × <i>grandidentata</i> ).....	19
1.6.2.3	Chapter 4: Over-expression of the <i>CsRFS</i> in hybrid poplar .....	19
	Chapter 2: Isolation and characterization of galactinol synthases from hybrid poplar.....	21
2.1	Introduction.....	21
2.2	Materials and methods .....	23
2.2.1	Phylogenetic analysis.....	23
2.2.2	Cloning the galactinol synthase ( <i>Gols</i> ) from hybrid poplar ( <i>P. alba</i> × <i>grandidentata</i> ).....	24
2.2.3	Heterologous expression of <i>Gols</i> in <i>Pichia pastoris</i> .....	24
2.2.3.1	GolSI.....	24
2.2.3.2	GolSII.....	25
2.2.4	Enzyme assays and kinetics .....	26
2.2.5	Expression profile of <i>Gols</i> isoforms.....	27
2.2.6	Reverse-transcriptase PCR.....	27
2.2.7	Quantitative RT-PCR.....	28

2.2.8	Accession numbers .....	28
2.3	Results.....	28
2.3.1	Characterization and phylogeny of the galactinol synthase proteins.....	28
2.3.2	Heterologous expression in <i>Pichia pastoris</i> .....	30
2.3.3	Spatial and temporal expression profile of GolS isoforms .....	30
2.4	Discussion.....	32
2.4.1	Galactinol synthases from hybrid poplar .....	32
2.4.2	Phylogenetic analysis.....	33
2.4.3	Expression profiles.....	36
Chapter 3:	Varied expression of the <i>GolS</i> in hybrid poplar ( <i>P. alba</i> × <i>grandidentata</i> ) .....	48
3.1	Introduction.....	48
3.2	Materials and methods .....	50
3.2.1	Plasmid construction.....	50
3.2.2	Hybrid poplar transformations.....	51
3.2.3	Plant growth.....	52
3.2.4	Tissue collection .....	52
3.2.5	Molecular analysis .....	52
3.2.5.1	Genomic DNA extraction .....	52
3.2.5.2	RNA isolation .....	53
3.2.5.3	PCR analysis of putative transformants.....	53
3.2.5.4	Real Time- RT PCR.....	53
3.2.6	Phenotypic analyses .....	54
3.2.6.1	Growth measurements .....	54

3.2.6.2	Gas exchange .....	55
3.2.6.3	Water potential.....	55
3.2.7	Structural chemistry analysis .....	55
3.2.8	Soluble sugar analysis.....	56
3.2.9	Starch analysis .....	57
3.2.10	Cell wall characterization .....	57
3.2.11	Cross sectional staining and microscopy .....	58
3.2.11.1	Antibody labelling .....	59
3.2.12	Stress treatments .....	60
3.2.13	Leaf nutrient analysis.....	60
3.2.14	NMR .....	61
3.2.15	Statistical analysis.....	62
3.3	Results.....	62
3.3.1	Generation of transgenic poplar trees .....	62
3.3.2	Carbohydrate and lignin analysis.....	64
3.3.3	Soluble sugar analysis and starch .....	66
3.3.4	Cellulose characterization.....	68
3.3.5	Stress treatments and foliar nutrient analysis.....	68
3.4	Discussion.....	69
3.4.1	Wood properties of transgenic lines are characteristic of tension wood .....	70
3.4.2	<i>p</i> –hydroxybenzoate groups associated with S lignin absent from transgenic lines .....	73
3.4.3	Photosynthesis and leaf nutrient analysis .....	74

Chapter 4: Over-expression of the <i>Cucumis sativus</i> raffinose synthase in hybrid poplar ...	105
4.1 Introduction.....	105
4.2 Materials and methods .....	107
4.2.1 Plasmid construction.....	107
4.2.2 Hybrid poplar transformations.....	107
4.2.3 Plant growth .....	108
4.2.4 Tissue collection .....	108
4.2.5 Molecular analysis .....	109
4.2.5.1 Genomic DNA extraction .....	109
4.2.5.2 RNA isolation .....	109
4.2.5.3 PCR analysis of putative transformants .....	109
4.2.5.4 Real Time- RT PCR.....	110
4.2.6 Phylogenetic analysis.....	110
4.2.7 Phenotypic analyses .....	111
4.2.7.1 Growth measurements .....	111
4.2.7.2 Structural chemistry analysis .....	111
4.2.7.3 Wood density determination.....	112
4.2.7.4 Soluble sugar analysis.....	112
4.2.7.5 Starch analysis .....	112
4.3 Results.....	113
4.3.1 Phylogenetic analysis.....	113
4.3.2 Generation of transgenic poplar trees .....	114
4.3.3 Soluble sugar and starch analyses.....	115

4.3.4	Carbohydrate and lignin analysis.....	116
4.3.5	Total biomass.....	116
4.4	Discussion.....	117
4.4.1	Phylogenetic analysis.....	117
4.4.2	Structural carbohydrates and soluble sugars.....	118
Chapter 5: Conclusion.....		132
5.1	Thesis summary.....	132
5.2	Future research.....	136
5.2.1	Use of different promoters to drive the expression of <i>Gols</i> .....	136
5.2.2	Application of a cold stress treatment on <i>Gols</i> and <i>RFS-OE</i> lines.....	137
5.2.3	Double transformation of the <i>AtGols3</i> lines with a <i>RFS</i> construct.....	137
5.2.4	Grafting experiments using the <i>AtGols3</i> lines and wild-type trees.....	138
References.....		139

## List of tables

<b>Table 3.1</b> Gas exchange parameters and water potential for <i>AtGols3</i> transgenic and wild-type poplar trees. ....	78
<b>Table 3.2</b> Structural cell wall carbohydrates and total lignin content of wild-type, <i>AtGols3</i> over-expression transgenic trees and <i>RNAiGols</i> transgenic trees.....	85
<b>Table 3.3</b> Vessel count and measurements on cross sections of five-month old greenhouse-grown wild-type and <i>AtGols3</i> transgenic trees.....	87
<b>Table 3.4</b> Galacturonic acid percentage of five-month old greenhouse-grown wild-type and <i>AtGols3</i> transgenic trees.....	91
<b>Table 3.5</b> Starch content of five-month old wild-type and <i>AtGols3</i> transgenic poplar trees..	96
<b>Table 3.6</b> Crystallinity percentage of five-month old greenhouse-grown wild-type and <i>AtGols3</i> transgenic hybrid poplar trees. ....	101
<b>Table 3.7</b> Leaf nutrient analysis of source leaf of five-month old wild-type and <i>AtGols3</i> transgenic poplar trees.. ....	103
<b>Table 4.1</b> Concentration of starch (weight percentage) in source leaves and phloem tissues of six-month old wild-type and <i>CsRFS</i> transgenic poplar trees.....	128
<b>Table 4.2</b> Structural cell wall carbohydrates and total lignin content of six-month old wild-type and <i>CsRFS</i> transgenic poplar trees.....	129
<b>Table 4.3</b> Biomass and total cellulose content of six-month old wild-type and <i>CsRFS</i> transgenic poplar trees.. ....	130

## List of figures

<b>Figure 2.1</b> Schematic representation of the biosynthetic pathway of the Raffinose Family of Oligosaccharides (RFO).....	38
<b>Figure 2.2</b> Deduced amino acid sequence alignment of known GolS proteins. ....	39
<b>Figure 2.3</b> Phylogenetic analyses using the neighbour-joining method and based on predicted amino acid sequences of confirmed and putative GolS proteins. ....	41
<b>Figure 2.4</b> Enzymatic activity of the recombinant Pa×gGolSI and P×gGolSII in response to pH at 37.5°C.....	42
<b>Figure 2.5</b> Enzymatic activity of the recombinant Pa×gGolSI and Pa×gGolSII at different temperatures at optimal pH.....	43
<b>Figure 2.6</b> $V_{max}$ and $K_m$ values for the recombinant GolS enzymes Pa×gGolSI and Pa×gGolSII .....	44
<b>Figure 2.7</b> Annual expression profiles of hybrid poplar <i>GolS</i> isoforms in different tissues over the course of 1 year of growth.. ....	46
<b>Figure 2.8</b> Diurnal expression profiles of three <i>GolS</i> isoforms in hybrid poplar ( <i>P.alba</i> × <i>grandidentata</i> ) leaf and phloem tissue.. ....	47
<b>Figure 3.1</b> Height from the base of the stem to the apex, and diameter at 10 cm from the base of the stem of three-month old greenhouse-grown <i>AtGolS3</i> transgenic and wild-type hybrid poplar. ....	76
<b>Figure 3.2</b> Five months old greenhouse-grown transgenic poplar trees expressing the <i>Arabidopsis thaliana</i> galactinol synthase 3 gene ( <i>AtGolS3</i> ) and wild-type trees.....	77
<b>Figure 3.3</b> Transcript amount of the <i>Arabidopsis thaliana</i> galactinol synthase 3 gene ( <i>AtGolS3</i> ) in tissues of five months old greenhouse-grown hybrid poplar.....	79

<b>Figure 3.4</b> Transcript amount of the <i>Arabidopsis thaliana</i> galactinol synthase 3 gene ( <i>AtGols3</i> ) in phloem tissue of hybrid poplar .....	80
<b>Figure 3.5</b> Height from the base of the stem to the apex, and diameter at 10 cm from the base of the stem of six-month old greenhouse-grown <i>GolsRNAi</i> transgenic and wild-type hybrid poplar.. .....	81
<b>Figure 3.6</b> Transcript amount of the <i>Pa</i> × <i>g</i> <i>GolsII</i> gene in phloem tissue of <i>GolsRNAi</i> transgenic and wild-type hybrid poplar .....	82
<b>Figure 3.7</b> Transcript amount of the <i>Pa</i> × <i>g</i> <i>GolsII</i> gene in source leaf of wild-type hybrid poplar subjected to water stress for 7 days.. .....	83
<b>Figure 3.8</b> Transcript amount of the <i>Pa</i> × <i>g</i> <i>GolsII</i> , <i>IV</i> , <i>III</i> and <i>I</i> in source leaf of <i>GolsRNAi</i> transgenic and wild-type hybrid poplar subjected to cold stress for 7 days.. .....	84
<b>Figure 3.9</b> Auto-florescence and calcofluor staining of wild-type, <i>AtGols3</i> transgenic line 6 and transgenic line 11 hybrid poplar.....	86
<b>Figure 3.10</b> Immunofluorescence labelling of xylem tissue from wild-type; <i>AtGols3</i> transgenic line 6 and <i>AtGols3</i> transgenic line 11 hybrid poplar.....	88
<b>Figure 3.11</b> Polysaccharide anomeric regions of 2D <sup>13</sup> C– <sup>1</sup> H correlation (HSQC) spectra from cell wall gels in DMSO-d6/pyridine-d5.....	89
<b>Figure 3.12</b> Aromatic regions of 2D <sup>13</sup> C– <sup>1</sup> H correlation (HSQC) spectra from cell wall gels and soluble lignins from various samples in DMSO-d6/pyridine-d5 .....	90
<b>Figure 3.13</b> The concentration of galactinol in selected tissues of five-month old greenhouse-grown wild-type and <i>AtGols3</i> transgenic hybrid poplar.....	92
<b>Figure 3.14</b> The concentration of <i>myo</i> -inositol in selected tissues of five-month old greenhouse-grown wild-type and <i>AtGols3</i> transgenic hybrid poplar.. .....	93

<b>Figure 3.15</b> The concentration of sucrose in selected tissues of five-month old greenhouse-grown wild-type and <i>AtGols3</i> transgenic hybrid poplar.....	94
<b>Figure 3.16</b> The concentration of raffinose in selected tissues of five-month old greenhouse-grown wild-type and <i>AtGols3</i> transgenic hybrid poplar.....	95
<b>Figure 3.17</b> The concentration of stachyose and raffinose in source leaf of six-month old greenhouse-grown wild-type and <i>GolsRNAi</i> transgenic hybrid poplar exposed to 2°C for 7 days..	97
<b>Figure 3.18</b> The concentration of sucrose, glucose and <i>myo</i> -inositol in source leaf of six-month old greenhouse-grown wild-type and <i>GolsRNAi</i> transgenic hybrid poplar exposed to 2°C for 7 days.....	98
<b>Figure 3.19</b> The concentration of galactinol in source leaf of six-month old greenhouse-grown wild-type and <i>GolsRNAi</i> transgenic hybrid poplar exposed to 2°C for 7 days..	99
<b>Figure 3.20</b> Wood density and microfibre angle (MFA) of five-month old greenhouse-grown wild-type and <i>AtGols3</i> transgenic hybrid poplar.....	100
<b>Figure 3.21</b> Fibre length and width of five-month old greenhouse-grown wild-type and <i>AtGols3</i> transgenic hybrid poplar.....	102
<b>Figure 3.22</b> The maximum quantum yield of PSII, as judged by $F_v/F_m$ after stress treatment of leaf discs of <i>AtGols3</i> transgenic hybrid poplar and wild-type trees.....	104
<b>Figure 4.1</b> Phylogenetic analyses using the neighbour-joining method and based on predicted amino acid sequences of confirmed and putative RFS proteins..	122
<b>Figure 4.2</b> Transcript abundance of the <i>Cucumis sativus</i> raffinose synthase gene ( <i>CsRFS</i> ) in four tissue types of six months old greenhouse-grown hybrid poplar.....	123

**Figure 4.3** Concentration of raffinose in three tissue types of six-month old greenhouse-grown wild-type and *CsRFS* transgenic hybrid poplar..... 124

**Figure 4.4** Concentration of sucrose in three tissue types of six-month old greenhouse-grown wild-type and *CsRFS* transgenic hybrid poplar.. ..... 125

**Figure 4.5** Concentration of glucose in three tissue types of six-month old greenhouse-grown wild-type and *CsRFS* transgenic hybrid poplar.. ..... 126

**Figure 4.6** Concentration of fructose in two tissue types of six-month old greenhouse-grown wild-type and *CsRFS* transgenic hybrid poplar.. ..... 127

**Figure 4.7** Wood density of six-month old greenhouse-grown wild-type and *CsRFS* transgenic hybrid poplar.. ..... 131

## List of symbols and abbreviations

ABA	abscisic acid
Ac	carbon assimilation rate
ADP	adenosine diphosphate
BA	benzyl adenine
CBF	cold-responsive element binding factor
CC	companion cell
Ci	intercellular CO <sub>2</sub> content
DREB	dehydration-responsive element binding factor
DX	developing xylem
E	transpiration rate
$F_0$	minimal fluorescence
$F_m$	maximal fluorescence
$F_v/F_m$	ratio of variable fluorescence to maximal fluorescence
FQA	fibre quality analyzer
FTIR	Fourier transform infrared
RFO	raffinose family of oligosaccharides
GGT	galactan: galactan galactosyltransferase
GolS	galactinol synthase
GH	glycosyl hydrolase
$g_s$	stomatal conductance
HPLC	high performance liquid chromatography
HXK	hexokinase
HSF	heat shock transcription factor
$K_m$	Michaelis constant
$K_p$	whole-plant hydraulic conductance
MD	minimal dextrose medium
MFA	microfibre angle
NAA	1-naphthaleneacetic acid
NMR	nuclear magnetic resonance
<i>OE</i>	over-expression
PSII	photosystem II
PBS	phosphate-buffered saline
RFS	raffinose synthase
ROS	reactive oxygen species
RGI	rhamnogalacturan I
SE	sieve element
SEL	size exclusion limit
SPS	sucrose phosphate synthase
STS	stachyose synthase
SUT	sucrose transporters
TBST	Tris-buffered saline Tween-20
TDZ	thiadiazuron
TIF5A	translation initiation factor 5A
TW	tension wood

UDP uridine diphosphate  
 $V_{\max}$  maximum reaction rate  
WUE intrinsic water use efficiency  
WPM woody plant media  
 $\Psi_{\text{leaf}}$  leaf water potential

## **Acknowledgements**

I would like to start by thanking my supervisor, Dr. Shawn Mansfield, for all the invaluable guidance, support and patience during all these years. Thank you Dr. Mansfield for giving me the opportunity to join your lab, I enjoyed doing research under a great working environment. I will also like to thank my committee members, Drs. Lacey Samuels and Rob Guy for their helpful suggestions and assistance throughout this journey.

I am grateful to have had great lab colleagues; I really could not have done it without your support. Big thank yous to Drs. Thomas Canam and Ji-Young Park for all your scientific and technical support. To Drs. Heather Coleman, Lisa McDonnell and Victoria Maloney for all the encouragement, example and advice. To my office mates Rob, Maggie and Amanda for sharing all the ups and downs of every day. To my lab mates Foster, Francis and Charles for their technical support. To all my colleagues and friends in the lab, for their unconditional help and all the good memories.

This degree is for my kids, Faridita and Alejandro, for showing me every day the important things in life. For my parents, thank you for installing on me all the values to continue this journey. For my parents in law, for all their support throughout these years. For my Latin ladies, for their friendship.

Finally, my biggest “thank you” is for Mario, for all the love, encouragement, support and persistence. You are the only person that really knows how much this means to us.

*To my family*

## Chapter 1: Introduction

### 1.1 The raffinose family of oligosaccharides (RFO)

Typically, plants store fixed carbon as starch and/or translocate it as sucrose. However, many plant species also inherently possess the molecular architecture to synthesize other classes of carbohydrates, with the raffinose family of oligosaccharides (RFOs) being one of the most abundant (Kandler & Hopf, 1982; Keller & Pharr, 1996). The biosynthesis of the RFOs is initiated with the transfer of a galactosyl unit from a donor to an acceptor which could be sucrose, raffinose or higher homologues. Three possible galactosyl donors include UDP-D-galactose, galactinol and RFOs themselves, however, UDP-D-galactose, derived from the common nucleotide pathway via UDP-D-galactose 4'-epimerase (Joersbo *et al.*, 1999) is the main contributor (Peterbauer & Richter, 2001). The galactosyl residue of UDP-D-galactose is transferred to *myo*-inositol, yielding galactinol, which is the specific galactosyl donor to the RFOs, and as such the biosynthesis of galactinol is considered the crucial regulatory step in RFO synthesis (Keller & Pharr, 1996). Most of the studies biochemically describing the galactinol synthases (GalS EC 2.4.1.123) are from legume seeds and cucurbit leaves (Keller & Pharr, 1996). Galactinol synthase, raffinose synthase (RFS EC 2.4.1.82) and stachyose synthase (STS EC 2.4.1.67) are all cytosolic, while the next galactinol-independent RFO chain elongation appears to take place in the vacuole (Bachmann & Keller, 1995). This elongation is catalyzed by a different enzyme, galactan:galactan galactosyltransferase GGT (Gilbert *et al.*, 1997). Schneider & Keller (2009) showed that raffinose is present in the chloroplasts of cold-treated *Ajuga reptans* L., *Spinacea oleracea* L. and *Arabidopsis thaliana* L. plants using a compartmentalization study of leaf mesophyll protoplasts. Galactinol synthase and raffinose synthase were localized extra-chloroplastic (most likely cytosolic), suggesting that the chloroplast envelope contains a

raffinose transporter. The authors then confirmed that raffinose is certainly transported across the chloroplast envelope, and that this transport proceeds via an active process (Schneider & Keller, 2009).

Galactinol and stachyose synthases have been cloned and characterized from different plant species (Peterbauer & Richter, 2001). Comparatively, raffinose synthase has attracted less attention, because it is the least stable compared to the other enzymes in the pathway. Raffinose synthases, however, have been purified from seeds of *Vicia faba* (Lehle & Tanner, 1973), and from a crude preparation of *A. reptans* (Bachmann *et al.*, 1994). Additionally, raffinose synthase has been more recently cloned from *Pisum sativum* (Peterbauer *et al.*, 2002), and shown to have amino acid homology to stachyose synthases (Peterbauer *et al.*, 1999) and seed imbibition proteins (Anderson & Kohorn, 2001; Romo *et al.*, 2001).

### **1.1.1 Galactinol synthase**

#### **1.1.1.1 *Arabidopsis thaliana***

Seven *GolS* isoforms have been identified in *A. thaliana* (referred to as *AtGolS1*, 2, 3, 4, 5, 6, and 7). Among them, three genes have been shown to be induced by osmotic stress. Expression profiles of these *AtGolS* genes, demonstrated that drought and high-salinity stress induced the expression of *AtGolS1* and 2. Conversely, only cold but not drought or salt stress induced *AtGolS3* (Taji *et al.*, 2002). The same authors demonstrated that the over-expression of the *AtGolS2* in *Arabidopsis* augmented the levels of galactinol and raffinose, and improved drought tolerance. Panikulangara *et al.* (2004) showed that heat stress induced the expression of *GolS1* in a heat shock transcription factor (HSF)-dependent mode. Conversely, the expression of *GolS3* (cold inducible) seems to be controlled by dehydration-responsive element binding factor 1 $\alpha$ /cold responsive-element binding factor 3 (DREB1/CBF3) transcription factors, which are

involved in multiple plant reactions at low temperatures (Fowler & Thomashow, 2002). Over-expression of DREB1/CBF3 has been shown to improve frost tolerance and biochemical accumulation of osmoprotective substances (*e.g.* proline, sucrose, raffinose, glucose, and fructose) in transgenic *Arabidopsis* plants (Gilmour *et al.*, 2000)

#### **1.1.1.2 *Ajuga reptans***

*Ajuga reptans* is a frost-hardy evergreen labiate that innately possesses two different pools of RFOs. One is used for transport and the other for storage of carbohydrates. This species often serves as the model plant for studying RFO metabolism. Sprenger & Keller (2000) isolated two cDNAs encoding distinct galactinol synthases, *ArGolS1* and *ArGolS2*, and demonstrated that both isoforms were cold-inducible and furthermore that *ArGolS1* is expressed only in source leaves. *GolS1* expression correlates with the GolS activity, while *GolS2* expression was noticeably lower and only contributes marginally to the overall extractable GolS activity. *In situ* hybridization experiments revealed that the expression of *GolS1* was in the mesophyll, while *GolS2* transcripts were proximal the sieve elements of the phloem. These findings imply that *ArGolS1* primarily participates in the synthesis of storage RFOs, while *ArGolS2* is involved in the synthesis of transport RFOs.

#### **1.1.1.3 *Coffea arabica* L.**

The transcripts of the three *GolS* isoforms in *C. arabica* were shown to be differentially regulated by water, high salt and heat stress. *CaGoS1* showed the highest transcript abundance in leaves under normal growth and stress conditions (water, high salt and heat). *CaGolS2* increased when severe water deficit was applied or in reaction to high salt stress, suggesting a more specific role for this isoform. Transcripts of *CaGolS3* were detected under all stress conditions, but at much lower levels implying a minor role of this isoform (Bento dos Santos *et al.*, 2011).

#### **1.1.1.4 *Populus* spp.**

Studies with simulated herbivore feeding in hybrid poplar (*Populus trichocarpa* × *deltoides*) revealed differences in the transcript abundance of the *Populus GolS* isoforms, with individual patterns for each gene in source and sink leaves (Philippe *et al.*, 2010). Additionally, when drought treatment was imposed on *Populus balsamifera* clones, galactinol synthases were among the most significantly responsive genes (Wilkins *et al.*, 2009). Similarly, in *Populus euphratica*, salt stress resulted in an increase in the transcript levels of a galactinol synthase (*GolSI*), however, the concentrations of galactinol, raffinose, mannitol, etc. were shown to be too small to substantially affect the general osmotic adjustment (Ottow *et al.*, 2005). However, this does not rule out the significance of compatible solutes such as galactinol or raffinose in stress adaptation, as they have been implicated in the stabilization of membranes and proteins (Vinocur & Altman, 2005).

#### **1.1.1.5 *Medicago sativa* L.**

Fluctuations in the RFO levels in alfalfa roots were associated with increases in *GolS* transcripts (Cunningham *et al.*, 2003). *GolS* enzyme activity increased in early autumn, and showed higher overall transcript abundance in winter-hardy cultivars of alfalfa. Castonguay & Nadeau (1998) demonstrated a correlation of the sucrose phosphate synthase (SPS) activity with *GolS*, in addition to the amount of sucrose and RFOs in alfalfa crowns. However, there was a delay of at least two weeks between the onset of *GolS* activity and the accumulation of RFO. Additionally, Blochl *et al.* (2005) suggested that the accumulation of RFOs in alfalfa somatic embryos is associated with concentration of the phytohormone abscisic acid (ABA), and the authors further showed that the external application of ABA leads to an alteration of the activity of *GolS* and

consequently to an increase in the RFO levels. The central role of ABA in abiotic stress has been well documented, and as such links these two pathways.

#### **1.1.1.6 *Boea hygrometrica***

The *BhGolS1* and *BhWRKY1* genes were cloned from the resurrection plant *B. hygrometrica* (Wang *et al.*, 2009). Dehydration and ABA concentrations rapidly induced the expression of these two genes. When overexpressed, *BhGolS1* confers drought tolerance, and promotes the accumulation of both galactinol and raffinose. Previous studies revealed that *GolS* expression was regulated by HSF and CBF-type transcription factors in *Arabidopsis* (Taji *et al.*, 2002; Panikulangara *et al.*, 2004). Additionally, it was demonstrated that in *B. hygrometrica* the WRKY transcription factor interacts with the promoter region of *BhGolS1* and activates its expression. The authors further suggested that *BhWRKY1* may participate in the ABA-dependent signal pathway, which is in turn involved in activating *BhGolS1* expression in response to dehydration.

#### **1.1.1.7 Seeds**

Physiologically, the RFOs in seeds can be considered as storage carbohydrates. They have been shown to constitute as much as 16.2% of the dry mass (Muzquiz *et al.*, 1999), but more commonly are found in the range of 2-10% (Horbowicz & Obendorf, 1994). Galactinol synthase has also been purified to near homogeneity from the seeds of kidney bean (*Phaseolus vulgaris*) (Liu *et al.*, 1995). Furthermore, the seeds of developing tomato (*Lycopersicon esculentum* Mill.) have been shown to accumulate the *LeGolS1* mRNA during the period of maximum dry weight deposition which is correlated with increased desiccation tolerance. However, *LeGolS1* did not appear to be responsive during cold treatments. In contrast, both stresses induced the *LeGolS1* transcript levels in the leaves of seedlings (Downie *et al.*, 2003). Expression of the *GolS* genes

in maize was also shown to be temporarily controlled, with two of the three isoforms being detected in developing or germinating seeds under stress conditions. Similarly, pea *GolSI* revealed a comparable pattern during seed development (Peterbauer *et al.*, 2001). In maize, *ZmGols3* expression seems to be induced during the maturation desiccation process and the expression of *ZmGols2* is mainly related to post-imbibition dehydration stress (Zhao *et al.*, 2004).

### **1.1.2 Raffinose synthase**

Raffinose synthase catalyzes the reversible galactosylation of sucrose from galactinol, yielding raffinose and myo-inositol. The rice raffinose synthase gene has been cloned and expressed in *E. coli* (Li *et al.*, 2007). This recombinant protein shows an optimal activity at 45°C and pH 7.0, and has a requirement for a sulfhydryl group for proper catalytic activity. Similarly, the coding region of the pea raffinose synthase was cloned and inserted in *Spodoptera frugiperda* Sf21 insect cells (Peterbauer *et al.*, 2002), and shown to exhibit an optimal pH of 7.0 and similar kinetic properties ( $K_m$  galactinol 7.9 mM and  $K_m$  sucrose 22.6 mM) to the raffinose synthase partially purified from maturing seeds. In *Ajuga reptans*, kinetic studies revealed  $K_m$  values of 4.8 and 16.4 mM for galactinol and sucrose, respectively (Bachmann *et al.*, 1994).

## **1.2 Phloem loading and sugar translocation**

The conducting cells of the xylem are used for the mobilization of water and inorganic solutes, while the phloem is integral to the transport of sugars produced in source leaves during photosynthesis. The phloem is also responsible for long distance transport and allocation of nutrients and signals used in plant nutrition, growth and stress tolerance (Dinant & Lemoine, 2010). The sieve elements (SE), companion cells (CC) and parenchyma cells of the phloem of

angiosperms work in concert to direct the accumulation, storage, uploading and unloading of signal molecules and a range of metabolites (Van Bel, 2003).

The sieve element and the surrounding companion cells form a system that uses plasmodesmata to connect to the neighboring phloem parenchyma cells and other cell types. The conductivity of the plasmodesmata is influenced by tissue type and developmental stage. Plasmodesmata can be abundant and significantly permeable, or sparse and apparently closed to solute (Turgeon & Wolf, 2009). Generally, plasmodesmata are abundant in the phloem of symplastic loaders, but they can also be present in great number in certain apoplastic loaders (Turgeon & Medville, 2004). The size-exclusion limit (SEL) values allow for the calculation of the permeability (Fisher & Cash-Clark, 2000), however, measurements of SEL in the phloem can be difficult to obtain. The frequency of plasmodesmata is therefore often employed to measure the symplastic continuity, but without information of SEL, results can be inaccurate (Turgeon & Wolf, 2009).

Sucrose is the most commonly translocated carbohydrate, and it can be loaded either apoplastically or symplastically, with or without the use of a polymer trapping mechanism. In apoplastic phloem loaders, sucrose enters the cell wall space and is actively taken up by sucrose transporters (SUTs) localized in CCs that have few plasmodesmata and membrane protrusions (e.g. spinach) (Lohaus *et al.*, 1995; Truernit, 2001) or in companion transfer cells with wall ingrowths (e.g. pea) (Wimmers & Turgeon, 1991; Truernit, 2001). Much of the existing knowledge of the apoplastic loading mechanism is based on research conducted on uptake in the sucrose transporters, which co-transport sucrose with a proton using the energy stored in the transmembrane proton gradient (Dinant & Lemoine, 2010).

In a second active process, such as the one used by pumpkin (Volk *et al.*, 1996), sucrose diffuses into intermediary CCs assisted by abundant plasmodesmata and is then transformed to higher oligosaccharides (e.g. raffinose and stachyose) that are molecularly too large to diffuse back from the CC, creating the so-called “polymer trap” (Haritatos *et al.*, 2000; Turgeon & Medville, 2004; Amiard *et al.*, 2005). According to the polymer trap mechanism, energy is used to establish a concentration gradient between the mesophyll and the phloem, implying a thermodynamically active process but not an active transport process that moves ions across a membrane (Turgeon, 2010). Generally, in leaves, the RFO pathway is limited to intermediary cells. However, in certain species, such as *Ajuga reptans*, an additional pool of RFO is localized in the mesophyll, but the export of oligosaccharide occurs from the intermediary cell pool (Sprenger & Keller, 2000).

In the passive loading mechanism, diffusion alone appears to be sufficient. According to Munch (1927), the osmotically generated hydrostatic pressure is responsible for long-distance transport. The solutes (e.g. photoassimilate) are uploaded in the sieve tube and attract water by osmosis. The bulk flow of a solution is the result of the movement of the primary source metabolites synthesized by mature leaves, and the exit of water and solutes in sink tissues (e.g. roots and meristematic tissues). In sink tissues, phloem unloading appears to depend on sink strength, which requires substantial amounts of sucrose and/or hexoses for development or storage in a limited time period (Choi *et al.*, 1998).

Studies in dicotyledonous plants showed that the majority of herbaceous plants can use any of the two active loading mechanisms, while most of the tree species use the passive loading mechanisms (Gamalei, 1989; Rennie & Turgeon, 2009). For example, *Populus alba*, which showed abundant plasmodesmata in the minor veins loads sucrose passively (Russin & Evert,

1985). In the absence of active phloem loading, trees must establish a balance between low whole-plant hydraulic conductance ( $K_p$ ) and high concentration of foliar transport sugars as the moving force for sugar diffusion. Alternatively, in most herbaceous plants maintaining a high  $K_p$  allows the organism to lower the sugar concentrations in leaves which reduces the possible inventory cost, increasing growth but demanding an active phloem loading mechanism (Fu *et al.*, 2011). Although sucrose is the most commonly translocated sugar, polyol concentrations have on occasion been shown to exceed the concentration of sucrose in the phloem sap (Rennie & Turgeon, 2009; Nadwodnik & Lohaus, 2008). The most common sugar alcohols transported are mannitol and sorbitol. In celery and plantain the sugar alcohols are uploaded apoplastically using sugar proton symporters (Noiraud *et al.*, 2001; Ramsperger-Gleixner *et al.*, 2004). Alternatively, a passive symplastic mechanism is used by *Rosaceae* species to transport the sugar alcohols (Rennie & Turgeon, 2009). Polyols have been proposed to have a role as osmoprotectants and radical scavengers (Stoop *et al.*, 1996); however, their specific role in long distance transport is not fully understood.

### **1.3 Relationships between carbohydrate content and abiotic stress tolerance**

The accumulation of carbohydrates such as raffinose and stachyose has been shown to occur during cold acclimation in plants, especially in woody perennials. For example, in red osier dogwood (*Cornus sericea* L.) the accumulation of raffinose was demonstrated to be higher during cold acclimation in stem tissues. Furthermore, raffinose and sucrose concentrations increased in response to recurring low temperatures, with correlations highest for raffinose in four pine species: eastern white pine (*Pinus strobus* L.), eastern red cedar (*Juniperus virginiana* L.), Leyland cypress (*Cupressocyparis leylandii* Dallim.), and Virginia pine (*Pinus virginiana* L.) (Hinesley *et al.*, 1992). In alfalfa roots, changes in RFO concentrations were correlated with

the increase in galactinol synthase transcript abundance (Castonguay *et al.*, 1995). The endogenous levels of raffinose and stachyose in *Populus tremuloides* were shown to increase with lowering temperatures at the onset of winter and diminish when the temperatures rise in the spring. Additionally, the raffinose accumulation was significantly dependent on the occurrence of low temperatures during acclimation in dormant buds of *P. tremuloides* (Cox & Stushnoff, 2001).

In *Arabidopsis* three independent abiotic stresses have been shown to induce the accumulation of raffinose and galactinol to significant levels, however, stachyose was not accumulated. Additionally, raffinose and galactinol were not present in control plants grown under normal conditions, which is a strong indication that these molecules are involved in combating stress. Furthermore, over-expression of galactinol synthase 2 (*AtGols2*) in transgenic plants improved the drought tolerance of *Arabidopsis* (Taji *et al.*, 2002). The role that these oligosaccharides play in desiccation tolerance in seeds is based on the accumulation of raffinose and stachyose during seed development. For example, in maize the accumulation of raffinose during seed desiccation suggests a role in stress tolerance. On the other hand, the accumulation of sucrose was independent of the tolerance to desiccation. Additionally, without raffinose accumulation the desiccation tolerance in seeds was not reached (Brenac *et al.*, 1997). Furthermore, the slow dehydration of young excised soybean seeds induces the accumulation of stachyose which is significantly associated with the increase in stress tolerance (Blackman *et al.*, 1992). Non-reducing sugars such as sucrose and raffinose are ubiquitously present in relatively high concentration in dry orthodox seeds. They also increase in response to desiccation in resurrection plants (Leprince & Buitink, 2010). In general, soluble sugars are considered as osmotic regulators, with the non-reducing sugars most likely involved in membrane stability.

Furthermore, these carbohydrates are effective storage compounds and can accumulate in large quantities without affecting metabolic processes (Peters *et al.*, 2007). In contrast, the reducing sugars are more closely related with altered metabolism (Pence & Clark, 2005). Under stress conditions, the non-reducing sugars are less likely to react with other metabolites such as amino groups when they accumulate in high concentration.

Despite the fact that many of these studies highlighted a putative role for these oligosaccharides in abiotic stress tolerance, the specific physiological mechanisms are not well understood. For example, raffinose has been suggested to play a role in the delay of sucrose crystallization (Caffrey *et al.*, 1988). Additionally, raffinose was observed to be more efficient than sucrose or trehalose in hydrogen bonding to biomolecules (Gaffney *et al.*, 1988). The stabilization of not only proteins and membranes, but also entire cells, under freezing and dehydration stress has been demonstrated to be associated with the effectiveness of this hydrogen bonding mechanism (Carpenter & Crowe, 1989). In addition, glass formation has been proposed as the mechanism for natural cryoprotection of trees and shrubs by avoiding the formation of intracellular ice at temperatures below  $-20^{\circ}\text{C}$ . Hirsh *et al.* (1985; 1987) showed that the intracellular fluids of *Populus* form aqueous glasses, and suggest that specialized proteins appear to bind raffinose, stachyose and KCl which are present in very high concentrations in the intracellular fluids of dormant wood. In a recent study, Knaupp *et al.* (2011) revealed that some photosynthetic parameters in the *Arabidopsis* raffinose synthase mutant were remarkably reduced when leaves were subjected to cold stress. Among these parameters, the maximum quantum yield of PS II photochemistry was the most affected, and suggests that during freezing, raffinose is involved in stabilizing PSII of cold acclimatized cells.

The importance of ROS in various physiological processes has been well described in the literature (Joo *et al.*, 2001; Bolwell *et al.*, 2002). However, excess ROS can cause oxidative stress in plant cells (Blokhina *et al.*, 2003). Nishizawa *et al.* (2008) found that galactinol and raffinose were effective (*in vitro*) in protecting the salicylate from attack by hydroxyl radicals. The authors demonstrated, by a competitive trapping assay (Smirnoff & Cumbes, 1989), that the oxidative damage produced by methylviologen, salt or cold treatment is diminished by raffinose and galactinol which can act as hydroxyl radical scavengers to defend the plant cells.

#### **1.4 Sugar signalling**

Plants utilize different strategies to acquire stress tolerance, which is a complex process that generally starts with stress perception and signalling. The process continues with a sequence of molecular, biochemical and physiological changes. Moreover, plants are innately programmed to adapt and respond to a series of signalling molecules starting from seed germination and continuing throughout development. And, several metabolic responses are activated or regulated by sugar signalling. For example, sucrose, which is the major transport sugar, can also act as signal directly (Chiou & Bush, 1998), or the plant can sense the signal from its breakdown products (glucose or UDP-glc and fructose) (Rolland *et al.*, 2002). Sugars are also important for modulating growth by inducing or repressing gene expression in source and sink tissues, assuring optimal carbon allocation and effective use of energy resources (Stitt & Krapp, 1999). For example, sugar depletion can up-regulate the genes that participate in photosynthesis, carbohydrate remobilization, and nitrogen metabolism. Instead, an abundance of sugar induces the genes involved in carbohydrate import, use and storage, in addition to genes involved in starch and anthocyanin biosynthesis (Eveland & Jackson, 2012).

Seven of the nine different stereoisomeric forms of inositol occur in nature, with *myo*-inositol being the most abundant in biological systems (Dastidar *et al.*, 2006). *Myo*-inositol can be used to produce several compounds such as phosphatidylinositol, inositol polyphosphates, galactinol, RFOs, pinitol and cell wall polysaccharides (Karner *et al.*, 2004). As discussed previously, RFOs are the main transport sugars in some plant species; they can also be used as reserve compounds in seeds, or as agents against biotic and abiotic stress. Nevertheless, the exact mechanism of action of the RFOs is still unknown. They may act as direct signals or as true ROS scavengers (Foyer & Shigeoka, 2011; Knaupp *et al.*, 2011). Galactinol (Wang *et al.*, 2009) and raffinose synthase (Wu *et al.*, 2009) genes contain W-box cis-elements in their promoters and are bound by an abscisic acid-inducible WRKY. Furthermore, evidence has been presented for galactinol and raffinose to act as signals during pathogen-induced systemic resistance (Kim *et al.*, 2008). For example, *CsGolS1* transcript abundance was shown to coincide with increased galactinol levels in leaves challenge-inoculated with *Pseudomonas chlororaphis* O6. However, the accelerated accumulation of galactinol observed 12 h after the inoculation was rapidly returned to basal levels. These results suggest that the accelerated accumulation of galactinol may function transiently as a signalling molecule during the initial interaction between primed plant leaves and pathogen attack. Sucrose, the precursor for raffinose synthesis, was also suggested to be the endogenous signal that was responsible for the initiation of the defense reactions against pathogens in rice plants (Gomez-Ariza *et al.*, 2007). Valluru & Van den Ende (2011) proposed a model for the role of the RFOs as signal molecules working downstream of ROS signalling. In this model the free *myo*-inositol can be used to synthesize RFOs. First, an abiotic stress induces the rise of ROS levels that act either as a signalling molecule or can cause cellular damage. Both *myo*-inositol or galactinol and the RFOs could change these cell

responses. However, these mechanisms are mostly unknown. Additionally, there are two mechanisms that could be responding to the increase of ROS levels. Either galactinol/RFOs act as antioxidants, or the invertases localized in the cytosol or mitochondria and glucose act together to combat the ROS. The glucose produced by the stress-induced invertases might be used as substrate for hexokinase, which in turn may contribute to the steady-state recycling of ADP. Similarly, in the chloroplast the neutral invertases and hexokinase could possess comparable mechanisms to counteract ROS accumulation. Furthermore, galactinol and the RFOs are thought to be transported to the chloroplasts by a raffinose importer, which could aid in modulating ROS homeostasis. The transcript patterns of the *GolS* genes in plants under both abiotic and biotic stress, implicate galactinol synthase and its product (galactinol) in alterations of carbon metabolism and allocation induced by stress. On the other hand, it has also been suggested that galactinol could be a factor in systemic defense signalling (Philippe *et al.*, 2010).

## **1.5 Wood formation**

The macroscopic arrangement of the cells and the ultrastructural and chemical characteristics of cell walls are responsible for the structural properties of wood. Wood is the result of combination of developmental and physiological events that are highly reactive to environmental signals. Wood formation, or xylogenesis, is a product of secondary growth that starts after the elongation of stems during primary growth. Xylogenesis is initiated in the vascular cambium, which contains the meristematic cells organized in radial files and gives rise to the secondary xylem and phloem (Larson, 1994). The cambial fusiform initials divide periclinally to produce phloem mother cells centrifugally and xylem mother cells centripetally. Following origin, the new secondary xylem cells enter a phase of elongation, or 'apical intrusive growth'. The cells at this time have only primary cell walls containing mainly radially oriented cellulose microfibrils and

crosslinking hemicellulose glycan. The walls expand vertically under the pressure of protoplast turgor and the microfibrils are reoriented. The deposition of secondary cell wall starts after the expansion of the cell is finished. Secondary cell wall formation is controlled by the expression of a suite of genes responsible for the biosynthesis of four main components: polysaccharides (cellulose, hemicelluloses), lignins, cell wall proteins and soluble and insoluble compounds in a neutral solvent (Higuchi, 1997).

The chemical and ultrastructural composition, as well as growth parameters of *Populus* spp. wood can be influenced by both genetic and environmental factors. However, it is usually characterized by having low lignin content and high carbohydrates. *Populus* wood is commonly described as containing approximately 43-50% glucose, 17-21% xylans, 2-4% mannans and 19-24% lignin (Mansfield & Weineisen, 2007). Most of the hemicellulose in aspen is *O*-acetyl-(4-*O*-methylglucurono)-xylan, but also has *O*-acetylated glucomannan (Gustavsson *et al.*, 2001; Teleman *et al.*, 2003). *Populus* has syringyl-guaiacyl lignin, rich in syringyl units, with a syringyl monomer content of 65 to 72 mol% syringyl (Stewart *et al.*, 2006).

### **1.5.1 Tension wood**

As mentioned, environmental variations influence xylem development, manifesting in altered wood properties. For example, simple seasonal changes alter the annual rings of *Populus*, giving rise to thin secondary cell walls and larger lumens during spring and early summer, known as early wood. When water starts to be more limited, later in the summer, higher numbers of tracheary elements are produced with thicker cell walls and smaller lumens (Groover *et al.*, 2010). The differences of environmental factors across years are reflected as variation in the thickness of annual rings. Wood development can also be influenced by gravity and mechanical stress. In general, plants have the capacity to adapt to stress by modulating their growth. Some

angiosperm trees, like *Populus* spp, can respond to gravitational stimuli by differentiating a new layer in the secondary cell wall of the fibres, resulting in the formation of tension wood. Tension wood is typically produced as a response to a non-vertical orientation of the stem which could be caused by wind, snow, slope or asymmetrical crown shape (Telewski *et al.*, 1996). This type of wood is formed to re-orient a leaning stem or branch (Timell, 1986; Zobel & van Buijtenen, 1989). Tension wood shows properties distinct from wood produced under normal growth conditions (low lignin content, higher cellulose content), and is often defined as containing small vessels and fibres with an inner cell wall layer (G-layer) made primary of cellulose (Telewski *et al.*, 2006). Recent studies indicate that the G-layers in *Populus* are largely composed of crystalline cellulose and matrix polysaccharides, accounting for approximately 75 and 25%, respectively, of their total dry weight (Nishikubo *et al.*, 2007; Kaku *et al.*, 2009, Mellerowicz & Gorshkova, 2012), with minor proportions of proteins (~ 3%) and ash, but no detectable lignin (Kaku *et al.*, 2009).

The mechanism of how tension wood generates longitudinal tensile force remains unknown. Recent progress has been made towards elucidating G-fibre functions with two main theories. In the G-layer swelling or pressure hypothesis, the G-layer exerts outer pressure on the cell wall S-layers, producing their longitudinal shrinkage due to their high MFA (Goswami *et al.*, 2008; Burgert & Fratzl, 2009). In the second hypothesis, the G-layer longitudinal shrinkage hypothesis, tensile stress is generated by the crystallization of adjacent microfibrils with short sections of matrix polysaccharides trapped between them, producing strain in the cellulose lattice. The tensional stress in the G-layer fibrils is distributed to the entire fibre because of the contact between the G-layers and the adjacent S-layers. Shortening of fibrils is complemented by

a return to the normal lattice spacing (Sugiyama *et al.*, 1993; Okuyama *et al.*, 1994; Clair *et al.*, 2006; Mellerowicz *et al.*, 2008).

## **1.6 Model organism**

### **1.6.1 *Populus* spp.**

Poplars belong to the angiosperm genus *Populus*. Poplars are frequently diploid and deciduous pioneers which are spread in the Northern hemisphere. Canada is considered the centre of poplar diversity, with 7 of the 29 global *Populus* species occurring naturally, and other species being introduced (Cooke & Rood, 2007). *Populus* species and hybrids are intensively cultivated for different purposes, such as biomass production, carbon sinks, phytoremediation, and for buffering against nutrient leaching (Johansson & Karacic, 2011). Large *Populus* stands are found in every Canadian province, and *Populus* is estimated to represent over 50% of all hardwoods and approximately 11% of the entire Canadian timber resource (Peterson & Peterson, 1995). *Populus*'s rapid growth rate (as high as 35 m<sup>3</sup>/ha/yr for hybrids, under optimal conditions) and lower age of maturation result in shorter rotation times compared to other hardwood species grown in similar environments (Cisneros *et al.*, 1996). *Populus* has also become a model system in forest tree biotechnology. The recent molecular-based research has been partly based on the objective of improving the state of commercial poplar applications, however its rise in importance for molecular research also stems from the responsiveness of this genus to experimental manipulation (Richardson *et al.*, 2007). *Populus* is one of the few trees that can be transformed, regenerated, propagated and grown to tree size in short time which facilitated different functional genomic studies (Brunner *et al.*, 2004). The complete genome sequence is another advantage for the use of this model tree in extensive comparative genomic studies among species that will help elucidate its genome reorganization and gene family evolution (Tuskan *et*

*al.*, 2006). *Populus* is found in the Angiosperm Eurosida I clade together with *Arabidopsis* (Jansson & Douglas, 2007). Even with its relatively close relation to *Arabidopsis*, *Populus* offers new prospects to study additional biological processes such as xylem development, formation and functioning of the vascular cambium, secondary xylem development, and seasonality of growth and phenology; in addition to traits like sex determination, flowering and biotic comparative interactions (Jansson & Douglas, 2007).

## **1.6.2 Goal and hypothesis**

While the raffinose family of oligosaccharides (RFOs) has been studied in several plant species (Lehle & Tanner 1973; Bachmann *et al.*, 1994; Peterbauer *et al.*, 2002), very little work has been conducted evaluating woody species, or transgenics expressing these genes in woody plants. More specifically, to date there have been no reports of over-expression or down-regulation of this gene family (RFO) in *Populus* or any other tree species. The main goal of this project was to understand the function(s) of the enzymes that are involved in the biosynthesis of the raffinose family of oligosaccharides (RFO) in hybrid poplar. To achieve this goal the research was divided into three different studies, as follows:

### **1.6.2.1 Chapter 2: Isolation and characterization of galactinol synthases from hybrid poplar**

The goal of these experiments was to identify the galactinol synthases from hybrid poplar (*P. alba* × *grandidentata*), describe the phylogenetic relationships of GolS and characterize the spatial and temporal transcript expression of *Pa*×*gGolS* isoforms in an attempt to understand the physiological roles of these enzymes. The hypothesis was that galactinol synthase isoforms will be expressed in different tissues at different times of the day and year. Based on the available literature I predicted that these enzymes will show higher levels of expression when the trees are

preparing for dormancy. Furthermore, in this chapter, I characterized two galactinol synthases from hybrid poplar in a heterologous expression system (*Pichia pastoris*) and conclusively show that they are true galactinol synthases. Additionally, these two cloned genes were compared phylogenetically with known GolS from other species. Finally, transcript expression was analyzed diurnally and annually in selected hybrid poplar tissues.

### **1.6.2.2 Chapter 3: Varied expression of the *GolS* in transgenic hybrid poplar (*Populus alba* × *grandidentata*)**

The goal of these experiments was to investigate the effects of mis-regulation of a *GolS* gene in hybrid poplar. The underlying hypothesis was that an alteration in this enzyme will manifest in changes in carbon allocation, since carbohydrate metabolism is modified toward the accumulation of storage compounds and cryo-protecting or dehydration-protecting solutes when active growth begins to arrest. Based on the available literature I predicted that transgenic plants altered in *GolS* would increase/decrease RFO synthesis and consequently influence pools of these carbohydrates under stress conditions. In order to achieve this objective, I inserted the *A. thaliana GolS* gene in an over-expression construct and measured the effect of the transgene on cell wall characteristics, wood chemistry and physiological parameters of transgenic plants. Additionally, a *Pa×gRNAi* construct was created and tested on hybrid poplar under stress conditions.

### **1.6.2.3 Chapter 4: Over-expression of the *CsRFS* in hybrid poplar**

The goal of this experiment was to study the effect of the over-expression of the second enzyme in the RFO pathway, raffinose synthase. The hypothesis being tested in this work was that the altered expression of the raffinose synthase will correlate with accumulation of its corresponding product (raffinose) and again modify carbon allocation in hybrid poplar, but not act as an overall

plant signal similar to galactinol. To examine the effects, I measured changes in wood chemistry, soluble sugars and cell wall characteristics of transgenic raffinose synthase hybrid poplar.

## Chapter 2: Isolation and characterization of galactinol synthases from hybrid poplar

### 2.1 Introduction

Plants have the innate ability to store and translocate most of the fixed carbon derived from photosynthesis, affording them the plasticity required to grow and survive in a variety of environments and under a myriad of conditions. Typically, they do this by synthesizing starch for storage and translocating sucrose for metabolism and the synthesis of integral structural moieties. However, other types of translocatable soluble carbohydrates exist in the plant kingdom, with the raffinose family of oligosaccharides (RFOs) being the most prominent (Keller & Pharr, 1996). Chemically, the RFOs are natural extensions of sucrose to which varying numbers of alpha-galactosyl residues are attached. As non-reducing carbohydrates they are good storage compounds that can accumulate in large quantities without affecting primary metabolic processes (Peters, 2007). The potential role of RFOs in stress tolerance has been intensively studied in seeds, mainly with respect to desiccation tolerance and longevity in the dehydrated state (Downie *et al.*, 2003). Additionally, RFO accumulation has commonly been associated with abiotic stress conditions such as cold, heat or drought in several plant species. In *Populus tremuloides* endogenous raffinose and stachyose levels have been shown to increase as temperatures drop in early winter and diminish as temperatures rise in spring. Furthermore, raffinose accumulation has been shown to be strongly dependent on low temperatures during acclimation (Cox & Stushnoff, 2001). In addition, in *Populus balsamifera* clones, galactinol synthases were among the genes with most significant differences when trees were subjected to drought treatment (Wilkins *et al.*, 2009). The RFOs also appear to play a prominent role in the response of plants to biotic stresses. For example, a recent report (Philippe *et al.*, 2010)

demonstrated the accumulation of galactinol and raffinose in hybrid poplar (*Populus trichocarpa* × *deltoides*) plants subjected to simulated feeding by the forest tent caterpillar *Malacosoma disstria*. Transcriptome analysis revealed a strong induction of numerous *GolS* genes. Correspondingly, expression analysis by qPCR in source and sink leaves showed differential transcript accumulation for the various isoforms examined.

Galactinol synthase (GolS EC 2.4.1.123) catalyzes the first step in the biosynthesis of RFOs, by reversibly synthesizing galactinol from UDP-D-galactose and *myo*-inositol (Saravitz *et al.*, 1987; Keller & Pharr, 1996) (Figure 2.1). The only known function for galactinol is as a substrate for the formation of the larger soluble oligosaccharides: raffinose, stachyose and verbascose (Saravitz *et al.*, 1987). GolS has primarily been characterized biochemically from legume seeds and cucurbit leaves (Keller & Pharr, 1996). However, this enzyme has also been isolated and described in other plants, including: common bugle [*Ajuga reptans*] (Bachmann *et al.*, 1994); zucchini squash [*Cucurbita pepo*] (Smith *et al.*, 1991); kidney bean [*Phaseolus vulgaris*] (Liu *et al.*, 1995); soybean [*Glycine max*] (Ribeiro *et al.*, 2000); and cucumber [*Cucumis sativus*] (Wakiuchi *et al.*, 2003). Based on these findings, it appears that the enzyme has a pH optimum between 7 and 8, a temperature optimum between 35°C and 50°C, and requires manganese ions and dithiothreitol. In addition to the native expression studies, there have also been studies employing recombinant galactinol synthase protein. For example, Taji *et al.* (2002) expressed three *A. thaliana* *GolS* genes in *E. coli* and demonstrated that *AtGolS1*, 2 and 3 all encode for galactinol synthases, however, enzyme kinetics were not discussed. Biologically, it was shown that the transcript abundance of *AtGolS1* and 2 were induced by drought and increasing salinity, but not by cold. Alternatively, *AtGolS3* was induced by cold, but not by drought or high salinity. Furthermore, over-expression of *AtGolS2* increased the pools of

galactinol and raffinose in *Arabidopsis* and improved the overall drought tolerance of *Arabidopsis* plants.

Herein we characterize the spatial and temporal transcript expression of three hybrid poplar (*P. alba* × *grandidentata*) galactinol synthase homologues, diurnally and annually. Furthermore, we describe the phylogenetic relationships of *Populus* genes and compare them to all known galactinol synthases. Two galactinol synthase genes were heterologously expressed in *Pichia pastoris* and their enzyme kinetics were analyzed. These results expand our knowledge about the physiological roles of these enzymes in hybrid poplar.

## **2.2 Materials and methods**

### **2.2.1 Phylogenetic analysis**

Amino acid sequences obtained from GenBank and Phytozome were used for multiple sequence alignment using MAFFT from <http://www.ebi.ac.uk/>. The evolutionary history was inferred using the Neighbor-Joining method (Saitou & Nei, 1987). The N-J method was chosen because it can handle a large number of sequences, is applicable to most types of evolutionary distance data, and produces a unique final tree that can include a bootstrap test. The optimal trees with the sum of branch length = 0.79 and = 2.99 are shown in Figure 3A and B, respectively. The percentage of replicate trees in which the associated taxa clustered together in the bootstrap test (1000 replicates) is shown next to the branches (Felsenstein, 1985). The trees are drawn to scale, with branch lengths in the same units as those of the evolutionary distances used to infer the phylogenetic trees. The evolutionary distances were computed using the Poisson correction method (Zuckerka & Pauling, 1965) and are in the units of the number of amino acid substitutions per site. The analysis involved 10 and 35 amino acid sequences, respectively. All positions containing gaps and missing data were eliminated. There were a total of 323 and 266

positions, respectively, in the final dataset. Evolutionary analyses were conducted in MEGA5 (Tamura *et al.*, 2011). Amino acid percentage similarity was calculated in ClustalW.

## **2.2.2 Cloning the galactinol synthase (*GolS*) from hybrid poplar (*P. alba* × *grandidentata*)**

ESTs obtained from the Treenomix project of Genome BC (*P. trichocarpa*, WS02549\_C18, WS01812\_P18, WS02432\_H16, WS01212\_F01, WS0141\_H15, WS02543\_G16, WS0231\_K19, WS0189\_A11, WS0146\_B17, and WS01710\_L22) were sequenced and used to design primer sets that amplified the full-length coding region of the *GolS* genes from hybrid poplar. The primers used to amplify *GolSI* from leaf cDNA were: *GolSLGX.Fw* 5'-ATGGCTCCAGGAGTGCCCATGGA-3' and *GolSLGX.Rv* 5'-TTAAGCAGCAGATGGCGCAGA-3', while *GolSII* was amplified with: *GolSLGXIII.Fw* 5'-ATGGCTCCTCATATTACAACTGC-3' and *GolSLGXIII.Rv* 5'-CTAAGCGGCGGATGGGGCGG-3'. The 1014 bp products amplified by PCR were cloned into the ZERO Blunt vector (Invitrogen Canada Inc., Burlington, ON). Plasmids containing both *GolS* genes were then used for heterologous expression studies.

## **2.2.3 Heterologous expression of *GolS* in *Pichia pastoris***

### **2.2.3.1 *GolSI***

The *GolSI* gene was modified by polymerase chain reaction to include two restriction sites, *SnaBI* and *AvrII*, using the primer pair *P39GolSI.SnaBI* 5'-TCATACGTAATGGCTCCAGGAGTG-3' and *P39GolSI.AvrII* 5'-TCCCCTAGGTTAAGCAGCAGATGG-3'. The 1022 bp product, amplified by PCR, was cloned into the pCR®IIBlunt-TOPO®, (Invitrogen Canada Inc., Burlington, ON). The fragment spanning the *SnaBI* and *AvrII* sites was then subcloned in frame with the secretion signal ( $\alpha$  factor) into the pPIC9K expression vector (Original *Pichia* Expression Kit, Invitrogen) and then transformed into *E. coli*. Colonies were

screened using 5'AOX1 and 3'AOX1 primers (as per manufacturer's instructions) and sequenced with the 3'AOX primers to confirm that the *GolSI* sequence was in frame with the  $\alpha$  factor secretion signal, and thereby including the Kex2 cleavage site. The pPIC9K-*GolSI* plasmid was harvested from *E. coli* and linearized with *Sall*, and then transformed into electrocompetent *P. pastoris* strain GS115 according to the manufacturer's specifications with the following modifications: 15  $\mu$ g of linearized DNA was transformed into 80  $\mu$ l electrocompetent *P. pastoris* cells using the Electroporator 2510 (Eppendorf, Mississauga, ON), at the following settings: voltage (1500 V) and time constant (5 ms). Transformed colonies were selected on MD (Minimal Dextrose medium) plates, and screened for positive *GolSI* inserts by PCR with total genomic DNA employing the 5'AOX1 and 3'AOX1 primers.

The positive GS115-pPIC9K-*GolSI* colony was grown at 28°C and 250 rpm in MD media overnight, and then for 4 days in MM (Minimal Methanol) induction media with the addition of 500  $\mu$ l (0.5% v/v) of methanol each day. On the fourth day, the culture was centrifuged and the supernatant containing the secreted proteins was concentrated using the Amicon Ultra-15 filter devices (Millipore, Billerica, MA), and partially purified with size-exclusion chromatography using the Econo-Pac® 10DG desalting columns (Bio-Rad Laboratories Canada Ltd., Mississauga, ON). The desalting buffer contained 50 mM Hepes (pH 7), 10 mM DTT and 0.2% (v/v) BSA. The desalted enzyme solution was used for all enzyme kinetic assays.

### **2.2.3.2 GolSII**

The second gene was similarly amplified by PCR to include the *SnaBI* and *AvrII* restriction sites into the amplicon, and a 6xHis tag at the 3' end using the following primers *P39GolSIISnaBI* 5'-TTCTACGTAATGGCTCCTCATATTACAACCTACCTTGCTAAC-3' and *P39GolSII-AvrIIhist* 5'-TGGCCTAGGCTAATGATGATGATGATGATGAGCGGCGGATGG-3'. The

PCR product was cloned as per *GolSI*, and ligated in frame with the  $\alpha$  factor of the pPIC9K vector. *Pichia* strain GS115 was transformed with the construct as previously described for *GolSI*.

#### **2.2.4 Enzyme assays and kinetics**

Enzyme assays were based on Ribeiro *et al.* (2000) with minor modifications, including: the reaction contained 30  $\mu$ l of galactinol synthase desalted enzyme solution, with either 50 mM Hepes NaCl, MES, or TRIS to achieve different pH (5.5 to 7.5), 50 mM *myo*-inositol, 3 mM DTT, 2 mM MnCl<sub>2</sub>, and 10 mM UDP-galactose. The reaction was allowed to proceed overnight at various temperatures (30-60°C), and terminated by placing the tubes in boiling water for 2 min. To each tube, 500  $\mu$ l of water, 10  $\mu$ l of potato apyrase (0.3 U, Sigma, St. Louis, MO), and 150  $\mu$ l of apyrase reaction mixture (250 mM Tris HCl (pH 7.5), 25 mM KCl, 7.5 mM CaCl<sub>2</sub>, 0.5 mM Na<sub>2</sub>EDTA, and 50 mM glucose) was added and incubated for 10 min at 37°C. The apyrase reaction was stopped by the addition of 60  $\mu$ l of 75% (v/v) TCA. The tubes were cooled on ice for 10 min, centrifuged at 3000  $\times g$  for 10 min and the amount of P<sub>i</sub> in the supernatant was determined by a modified Fiske & Subbarow (1925) method. Briefly, to each tube 100  $\mu$ l of 2.5% (w/v) ammonium molybdate dissolved in 2 N HCl and 100  $\mu$ L of Fiske and SubbaRow reducer was added, and after 2 min (at room temperature) 40  $\mu$ l of 34% (w/v) sodium citrate·2H<sub>2</sub>O solution was added and the absorbance measured at 660 nm. The steady-state kinetics ( $V_{\max}$  and  $K_m$ ) were calculated using the Michaelis-Menten nonlinear regression model of GraphPad Prism 5.00 program (GraphPad, San Diego, California). The standard curve was constructed measuring the inorganic phosphate from KH<sub>2</sub>PO<sub>4</sub>.

### **2.2.5 Expression profile of *GolS* isoforms**

Hybrid poplar trees were planted in the University of British Columbia (Vancouver, British Columbia, Canada) greenhouse in July 2006. After one year of growth they were moved outdoors to experience seasonal conditions, and samples were collected monthly from September 2007 to August 2008. All sampling was done between 5:30 to 7:30 am. Leaf, phloem (includes bark, phloem tissue and cambial cells), lateral apical and young stem were cut, and immediately placed in liquid nitrogen and stored at -80°C until further use. Total RNA was isolated as per Kolosova *et al.* (2004). TURBO DNA-free Kit (Ambion Inc. Life Technologies Corporation, Carlsbad, CA) was used to eliminate contaminating DNA. RNA treated with DNase was quantified and 1 µg was used to generate cDNA using the iScript cDNA synthesis kit (Bio-Rad). The resulting cDNA was stored at -20°C. The same trees were used for diurnal profiling, the samples were taken hourly in July 31st 2009, and cDNA was generated according to the protocol previously described.

### **2.2.6 Reverse-transcriptase PCR**

PCR reactions contained 1 µl cDNA, 10 pmol of forward and reverse primers, 2mM dNTPs, and 1 µl of Taq polymerase (New England Biolabs, Ipswich, MA) with thermo buffer in a total reaction volume of 20 µl. The primer sequences were as per Philippe *et al.* (2010), and corresponded to *PtGolS1.2* (same clade as *Pa×gGolSI*), *PtGolS3.1* (homologue to *Pa×gGolSII*), and *PtGolS6.1* (homologue to *Pa×gGolSIII*). PCR was performed using a PTC 200 thermocycler (MJ Research, Waltham, MA), with the following conditions: 94°C for 4 min, followed by 35 cycles of 94°C for 30 s, 58°C, 55°C or 60°C (respectively) for 1 min and 72°C for 1 min. An aliquot of 12 µl of each reaction was run on a 2% (w/v) gel in TAE buffer. Gels were visualized with EtBr and captured with the AlphaImager 2200 (Alpha Inotech, San Leandro, CA).

### 2.2.7 Quantitative RT-PCR

Quantitative RT-PCR reactions consisted of 10 µl of SsoFast™ EvaGreen® Supermix (Bio-Rad), 5 pmol of forward and reverse primers for the *PtGolS1.2*, *PtGolS3.1*, *PtGolS6.1* (described above), and *TIF5A* genes, 1µl of a 1-in-5 cDNA dilution, and water to a total volume of 20 µl. RT-PCR was performed in the CFX96 Real-Time PCR Detection System (Bio-Rad). The following thermal cycler conditions were used to amplify the 92, 186, and 110 bp fragments of the *PtGolS1.2*, *PtGolS3.1*, *PtGolS6.1* transcripts, respectively: 1 cycle of 30 seconds at 95°C, 39 cycles of 95°C for 5 seconds, 58°C, 55°C and 60°C for 5 seconds, followed by 1 cycle of 55°C to 95°C for 5 seconds to calculate the melting curve. Relative expression was calculated using the following equation  $\Delta ct = 2^{-(ct_{\text{target gene}} - ct_{\text{TIF5A}})}$ , where *TIF5A* is used as the reference gene (Coleman *et al.*, 2009).

### 2.2.8 Accession numbers

GenBank accession numbers: *Pa×gGolSI* (JF499886) and *Pa×gGolSII* (JF499887).

## 2.3 Results

### 2.3.1 Characterization and phylogeny of the galactinol synthase proteins

The full-length sequences of two galactinol synthase homologues from hybrid poplar (*P. alba* × *grandidentata*) were isolated, cloned and subsequently named *Pa×gGolSI* and *Pa×gGolSII*. The complete coding region of *Pa×gGolSI* comprises 1014 nucleotides and includes an ORF that encodes a polypeptide of 337 amino acid residues. The second gene, *Pa×gGolSII*, encodes for a polypeptide of the same length. The deduced amino acid sequences were aligned to compare consensus regions with other known galactinol synthases (*Arabidopsis thaliana* GolS1 and 5, *Oryza sativa* GolS1, *Cucumis sativus* GolS1 and *Ajuga reptans* GolS1 and 2), which displayed characteristics common to known galactinol synthases (Figure 2.2). The MAFFT program was

used to align the sequences and the Neighbor-Joining method was used for phylogenetic analysis. A bootstrap value of 70 is used to define clades. The nine poplar GolS isoforms are positioned in four groups (Figure 2.3A). The first group contains *Populus trichocarpa* PtGolS3 (homologue to Pa×gGolSII), which has 89% similarity with PtGolS5. The second group is formed by PtGolS8 and PtGolS9, which share 88% similarity. The third group is formed by PtGolS7 and PtGolS6, which share 93% similarity. Finally, PtGolS2 (homologue to Pa×gGolSI) has 92% similarity to PtGolS1. The PtGolS4 gene was not included in the analysis as it is a tandem repeat of PtGolS3 (Philippe *et al.*, 2010).

A second tree grouping all known and putative galactinol synthases (Figure 2.3B) clusters the proteins in eight main clades. The first clade groups the *Populus trichocarpa* GolS3 and 5, with the hybrid poplar Pa×gGolSII galactinol synthase. The second clade includes PtGolS8 and 9 galactinol synthases. The CmGolS1 (*Cucumis melo*) has a low bootstrap value and could not be considered part of this clade. The third group is formed by ThGolS1 (*Theellungiella halophila*) and AtGolS (*Arabidopsis thaliana*) 2 and 3. The fourth clade is formed by GmGolS (*Glycine max*), AmGolS1 (*Ammopiptanthus mongolicus*), and MsGolS1 (*Medicago sativa*) galactinol synthases; this group shares 81% to 85% similarity. The ArGolS2 (*Ajuga reptans*) galactinol synthases demonstrated a rather low bootstrap value and is not considered as part of this clade. The fifth clade is formed by PtGolS6, 7, PsGolS1 (*Pisum sativum*), AtGolS1, and BnGolS1 (*Brassica napus*). The highest similarity within this group is 93% (the two *Populus* proteins). The sixth clade is formed primarily by three monocot species *Zea mays* (ZmGolS1, 2, and 3 with similarities between 74% and 90%), *Triticum aestivum* (TaGolS1 and 2 with 97% similarity) and *Oryza sativa* (OsGolS1 and OSGolS3) galactinol synthases. The *Xerophyta viscosa* (XvGolS1) galactinol synthase has a low bootstrap value and is not consider part of this

clade. The seventh clade groups PtGolS1 and 2, Pa×gGolSI, ArGolSI (*Ajuga reptans*), AtGolS4 and 7. Pa×gGolSI and ArGolSI share 80% similarity, while the *Arabidopsis* proteins share 72% similarity. Finally, AtGolS5 and 6 clustered in the last clade with 90% similarity. The LeGolS1 (*Lycopersicon esculentum*) galactinol synthase stands by itself and was used as the root of the tree.

### **2.3.2 Heterologous expression in *Pichia pastoris***

*GolSI* and *GolSII* from hybrid poplar were cloned and expressed in the methylotrophic yeast *P. pastoris* (GS115). Both isoforms were able to catalyze the reaction of UDP-galactose with *myo*-inositol to form galactinol. GolSI displayed greater pH stability, ranging from 5.5 to 9.0, with an optimum of 7 and only losing a small percentage of its original activity at the extreme pH (Figure 2.4). In contrast, GolSII displayed a very narrow pH tolerance, with activity decreasing considerably when the pH deviated from the 7.5 optimum (Figure 2.4). A similar pattern was apparent when the enzyme activity was measured at different temperatures: GolSI was more stable at different temperatures than GolSII, showing maximal activity at 45°C and 37°C, respectively (Figure 2.5).

The  $V_{\max}$  and  $K_m$  values of the GolSI for UDP-galactose were 657.5 nM min<sup>-1</sup> and 0.80 mM (Figure 2.6A), while GolSII had a  $V_{\max}$  and  $K_m$  of 1245 nM min<sup>-1</sup> and 0.65 mM for the same substrate, at their optimum enzyme conditions (Figure 2.6B). The  $V_{\max}$ ,  $K_m$  values, optimal pH and temperature profiles determined in this study are similar to those previously reported from other plants (Bachmann *et al.*, 1994; Liu *et al.*, 1995; Ribeiro *et al.*, 2000; Wakiuchi *et al.*, 2003).

### **2.3.3 Spatial and temporal expression profile of GolS isoforms**

Semi-quantitative and quantitative RT-PCR were used to investigate the expression of three hybrid poplar galactinol synthase isoforms, representing three out of four clades of poplar

galactinol synthases. *Pa×gGolSIII*, which is homologous to *PtGolS6* (LGII: 15155825-15157384; Philippe *et al.*, 2010) was expressed in source leaves sampled from May to November, showing a slightly higher expression during the autumn months. *Pa×gGolSII*, which is homologous to *PtGolS3* (LGXIII: 362675-364038; Philippe *et al.*, 2010), and *Pa×gGolSI* that is in the same clade as *PtGolSI* (LGVIII: 13321952-13323592; Philippe *et al.*, 2010) were also expressed during these same months. However, the latter showed higher overall expression (Figure 2.7A). In contrast, in the lateral apical tissue, which includes the apical meristem, small sink leaves and the three first internodes of the stem, differences in expression of the second homologue (*Pa×gGolSII*) were detected. Specifically, this homologue was expressed during both spring and fall, but was not detectable during the summer. Additionally, of the three genes, *Pa×gGolSI* had the highest expression during this same time period (Figure 2.7B).

The profile in the stem (apex without buds) during the winter period showed the highest expression of the *Pa×gGolSII* compared to the other two galactinol synthases genes (Figure 2.7C). Finally, in the phloem, the expression patterns of *Pa×gGolSIII* and *Pa×gGolSI* were similar and consistent for the entire annual cycle, while the expression of *Pa×gGolSII* was limited to the winter months (Figure 2.7D).

The relative expression levels of the three isoforms were also analyzed over the course of a full diurnal cycle to investigate daily changes in expression using quantitative RT-PCR. Two tissues were analyzed for this purpose: source leaf and phloem. The levels of the three galactinol synthase transcripts in leaves started to increase in the early morning before reaching maximum levels around 10 am. Thereafter, expression decreased in the afternoon to reach a low in the evening (Figure 2.8). It was also apparent that expression of the *Pa×gGolSI* isoform in source leaves was much higher than the expression of the other two isoforms (*Pa×gGolSII* and *III* with

differences on the highest relative expression of 139 and 590 times, respectively). Generally, expression of the transcripts in the phloem was lower than the expression in the leaf, for all isoforms during the summer.

## **2.4 Discussion**

### **2.4.1 Galactinol synthases from hybrid poplar**

The main goal of this chapter was to identify and characterize the galactinol synthase genes from hybrid poplar. Using the *Populus trichocarpa* genome sequence (Tuskan *et al.*, 2006), nine putative galactinol synthase genes were identified. Based on the predicted amino acid sequence, the nine putative *GolS* genes appear to have evolved from four ancestral genes through genome duplication (Philippe *et al.*, 2010).

Two homologues of the *PtGolS* genes were cloned from a hybrid poplar clone (*P. alba* × *grandidentata*). Pa×gGolSI shares 97% similarity at the amino acid level with its homologue PtGolS2, while the second isoform Pa×gGolSII has 91.7% similarity to PtGolS3. The predicted protein sequences of both cloned isoforms clearly show the serine phosphorylation site at position 274 and the pentapeptide hydrophobic domain ASAAP characteristic of all known galactinol synthases (Sprenger & Keller, 2000). Furthermore, the predicted isoelectric points for both enzymes were 5.27 and 5.48, respectively, which are similar to the galactinol synthase purified from zucchini leaves (Smith *et al.*, 1991) and characteristic of other plant GolS.

To confirm the identity of the putative *Pa×gGolS* isoforms and characterize the enzymatic properties of the proteins, the cloned genes were heterologously expressed in *Pichia pastoris*. The *P. pastoris* system represents a very useful experimental tool for protein research, as it can produce sufficient amounts of the recombinant protein(s) in soluble form, and offers correct folding and appropriate post-translational modification (Daly & Hearn, 2005). The

recombinant galactinol synthase  $V_{\max}$ ,  $K_m$  values, optimal pH and temperature profiles were similar to those previously reported from other plants. For example, Smith *et al.* (1991) determined a pH optimum of 7.5 for purified galactinol synthase isolated from mature zucchini (*Cucurbita pepo*) leaves. In addition, the purified galactinol synthase was shown to bind specifically to UDP-galactose ( $K_m = 1.8$  mM). *Phaseolus vulgaris* (kidney beans) galactinol synthase has also been purified and characterized (Liu *et al.*, 1995), and shown to have a pH optimum of 7.0 and a  $K_m$  of 0.4 mM for UDP-galactose. A crude and partially purified soybean seed galactinol synthase activity was shown to exhibit a maximal activity at pH 7.0 and 50°C. This enzyme showed  $K_m$  and  $V_{\max}$  values (for the UDP-galactose) of 5.2 mM and 195 nmol  $\text{min}^{-1}$ , respectively (Ribeiro *et al.*, 2000). The *Cucumis sativus* galactinol synthase extracted from leaves has similarly been shown to have optimal pH between 7-8 and highest activity at 40°C (Wakiuchi *et al.*, 2003). Based on our results, we can conclude that the two hybrid poplar isoforms encode true galactinol synthases, and functionally display similar properties to other known galactinol synthases.

#### **2.4.2 Phylogenetic analysis**

The predicted amino acid sequences of Pa×g GolS, PtGolS(s) and other confirmed and putative galactinol synthases from dicotyledonous and monocotyledonous plant species were used to perform a phylogenetic analysis using the Neighbor-Joining method. The results showed that the nine galactinol synthases from *P. trichocarpa* and the seven galactinol synthases from *A. thaliana* are distributed among all the clades, demonstrating as much variation within as among species. The *P. trichocarpa* GolS are positioned in pairs into four clades, following the pattern of genome duplication of *Populus* (Tuskan *et al.*, 2006). The two cloned isoforms from hybrid

poplar (*P. alba* × *grandidentata*) are representative of two different clades. Pa×gGolSI and II are homologues to the PtGolS2 and 3, respectively, with 66% similarity at the amino acid level.

Many galactinol synthase genes have been shown to be stress related. For example, the *PtGolS* genes were recently shown to be highly responsive to biotic stress and showed differential induction with gene-specific patterns in source and sink leaves (Philippe *et al.*, 2010). Similarly, three of the seven *Arabidopsis thaliana* galactinol synthases (*GolS1*, 2 and 3) were previously shown to be stress-responsive genes (Taji *et al.*, 2002).

The *Ajuga reptans* *GolS* genes 1 and 2 are also distributed in different clades, and have been proposed to inherently possess distinct biological functions (Sprenger & Keller, 2000). *ArGolS1* (grouped with *PaxgGolSI*) was predicted to be involved in the synthesis of storage RFOs, while *ArGolS2* was implicated in the synthesis and transport of RFOs. The galactinol synthase from *Cucumis melo* (that has 74% similarity with *PaxgGolSII*) has been shown to be present in developing melon seeds during the active formation of raffinose and stachyose (Volk *et al.*, 2003). Additionally, the galactinol synthase promoter isolated from *Cucumis melo* has been shown to drive gene expression in the minor-vein companion cells of both transgenic tobacco (*Nicotiana tabacum*) and *Arabidopsis*. Neither of these plants use galactinol in a phloem-loading process, suggesting that the promoter responds to a minor-vein-specific regulatory cascade that is highly conserved across a broad range of eudicotyledons (Ayre *et al.*, 2003). This is an interesting observation, since this gene was previously predicted to cluster phylogenetically (Zhao *et al.*, 2004) with the *C. pepo* galactinol synthase that is localized in the intermediary cells (Beebe & Turgeon, 1992). Based on phylogenetic clustering and the functional data available, it is indeed possible that the two galactinol synthases from hybrid poplar have different biological roles.

The *Glycine max*, *Ammopiptanthus mongolicus* and *Medicago sativa* *GolS* clustered together in our analysis. These genes have been shown to be strongly associated to stress-tolerance. In *A. mongolicus*, a woody species, only one form of the *GolS* gene (*AmGolS*) has been found, which was induced significantly by cold, drought, NaCl and ABA application (Cao *et al.*, 2009). Similarly, the transcript induction of the *MsGolS* was higher in winter-hardy alfalfa cultivars (Cunningham *et al.*, 2003).

Galactinol synthase from *Thellungiella halophila* was found to group together with two genes from *A. thaliana* (*GolS* 2 and 3). Similar to these *AtGolS* genes, shown to be stress related, the *ThGolS* is suggested to be a putative salinity stress-regulated gene (Wang *et al.*, 2004). Among the dicot species, the *Lycopersicon esculentum* galactinol synthase (*LeGolS*1) amino acid sequence was the most divergent, and interestingly, the expression of this transcript was shown to be induced by dehydration in germinating seeds and by dehydration coupled with cold in seedling leaves (Downie *et al.*, 2003). This may suggest a seed-specific role for some *GolS* isoforms in plant growth and development.

The similarity of the galactinol synthases from monocot species was evident from the close association observed in the cluster analysis. In particular, the cluster contains three maize galactinol synthases that have been studied during seed development and germination. Two of the three *GolS* gene family members in maize were also detected in stressed seeds, while the other *GolS* was mainly expressed during seed development (Zhao *et al.*, 2004). Another member of this tightly associated clade is the rice *GolS*, which was found to be expressed under chilling conditions (Takahashi *et al.*, 1994). Additionally, the *Xerophyta viscosa* *GolS* showed an increase in expression in leaf tissue experiencing water deficit (Peters, 2007).

Based on the phylogenetic relationships of the two hybrid poplar *GolS* isolates and the galactinol synthases from other species, we suggest a potential role of these enzymes during biotic or abiotic stresses in hybrid poplar. Furthermore, the distinct grouping of these isoforms implies different roles for the two galactinol synthases.

### **2.4.3 Expression profiles**

The raffinose family of oligosaccharides has long been suggested to act as biological agents to combat abiotic (Taji *et al.*, 2002; Cunningham *et al.*, 2003; Panikulangara *et al.*, 2004) and biotic stress (Philippe *et al.*, 2010). The three different galactinol synthase isoforms analyzed in this study are homologues to genes that belong to different clades of the *P. trichocarpa* galactinol synthases. The *Pa×gGolSII* homologue (to *PtGolS3*) showed seasonal expression and seems to be temperature-regulated based on the abundance of the transcript during the spring and autumn in the shoot tip along with elevated expression during the winter in the phloem. Additionally, expression in branch tips during winter was higher than that of the other genes. The expression differences during day and night in source leaf poplar revealed that the transcript abundance is much higher during the day, reaching a maximum near 10 am and then decreasing in the afternoon until reaching its lowest level in the evening. Similar patterns were also found in *Ajuga reptans*, where the *GolS* activity extracted from pre-dawn leaves represented only 30 to 50% of the *GolS* activity usually extracted during the day. (Bachmann *et al.*, 1994), hypothesized that galactinol synthases may obey a light /dark regulation by protein modification similar to sucrose-phosphate synthase (Huber, 1983).

The expression of the *Pa×gGolSI* homologue was constitutively higher in source leaves compared to the other two galactinol synthases. Interestingly, the same isoform was present throughout the year in most of the tissues, and it seems that its expression was not altered by cold

acclimation. Additionally, when the kinetics of the enzyme were analyzed at different pH and temperatures, the activity was more stable over a wide range of conditions compared to the *Pa×gGolsII* isoform, which displayed a very narrow temperature tolerance, indirectly suggesting that this enzyme may be highly temperature-related. Overall, the variation in seasonal expression of the *Pa×gGols* isoforms suggests that each enzyme may play different physiological roles. The persistent expression of the *Pa×gGolsI* transcript throughout the year could be associated with the synthesis of RFOs for storage, while the *Pa×gGolsII* may be involved with seasonal mobilization of carbohydrates. However, additional studies of the galactinol synthases are required to further elucidate the specific roles of this important enzyme group in phloem transport and storage in poplar.

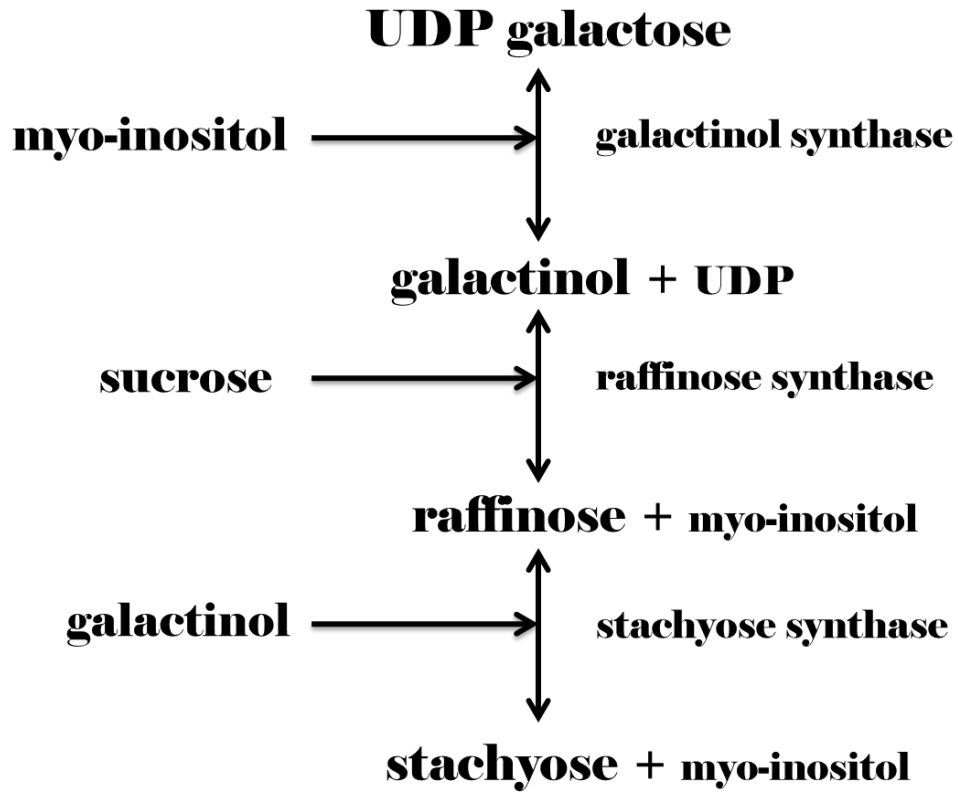


Figure 2.1 Schematic representation of the biosynthetic pathway of the Raffinose Family of Oligosaccharides (RFO).

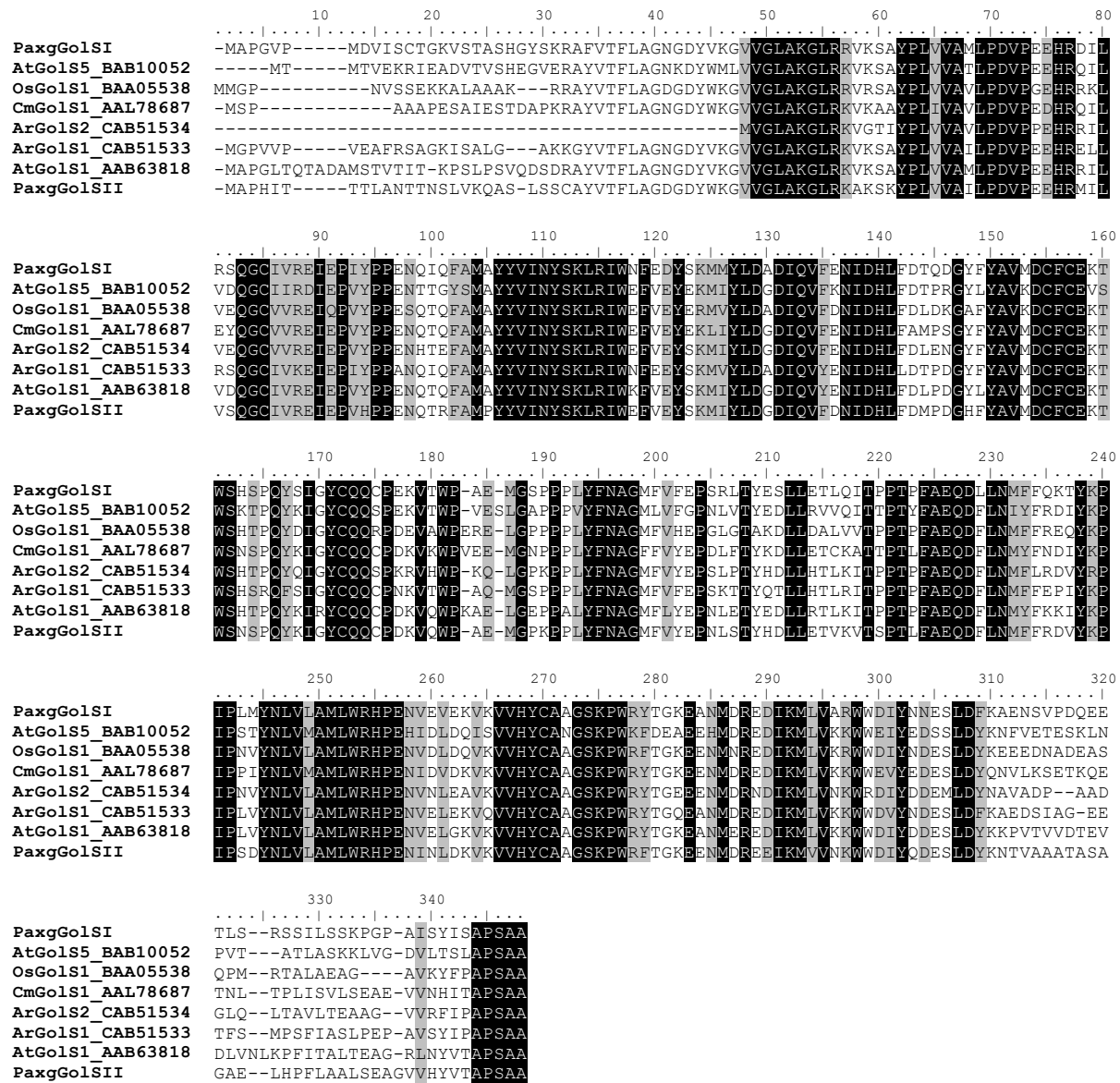
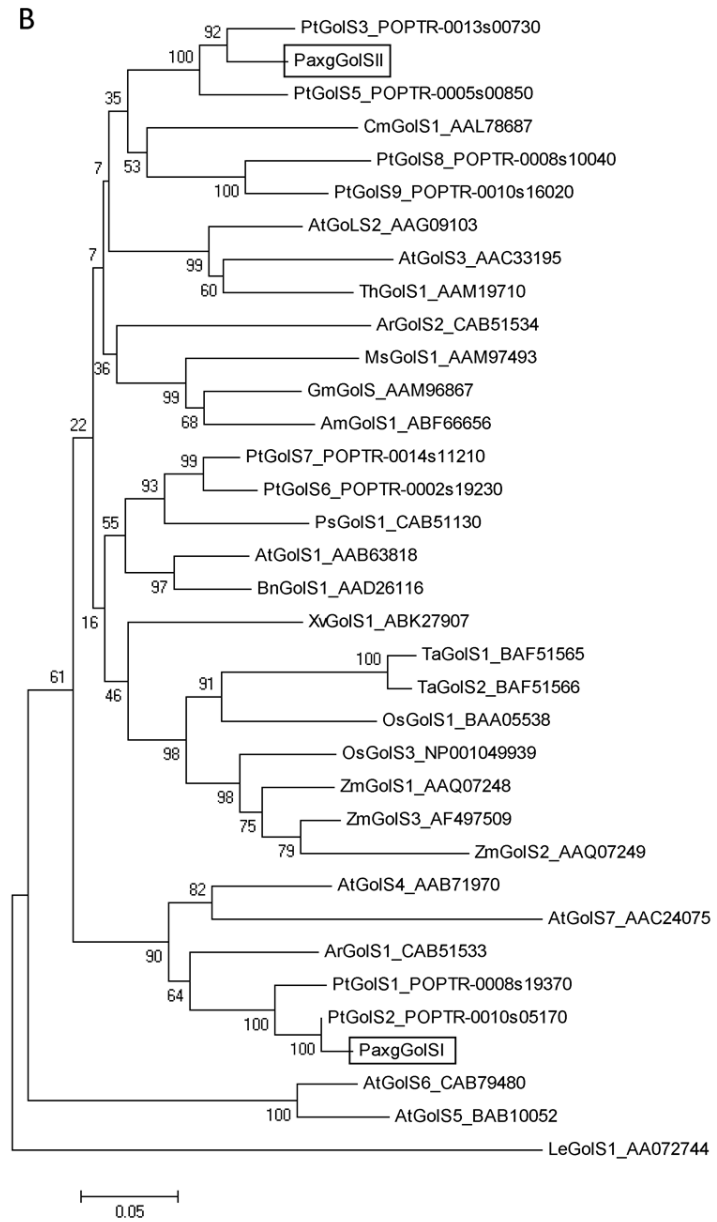
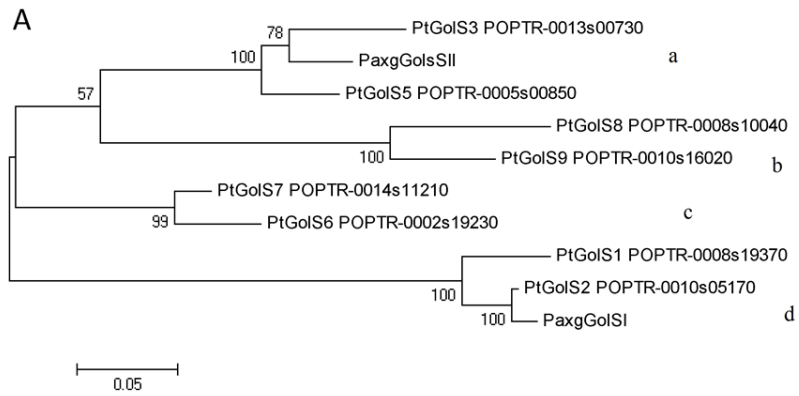
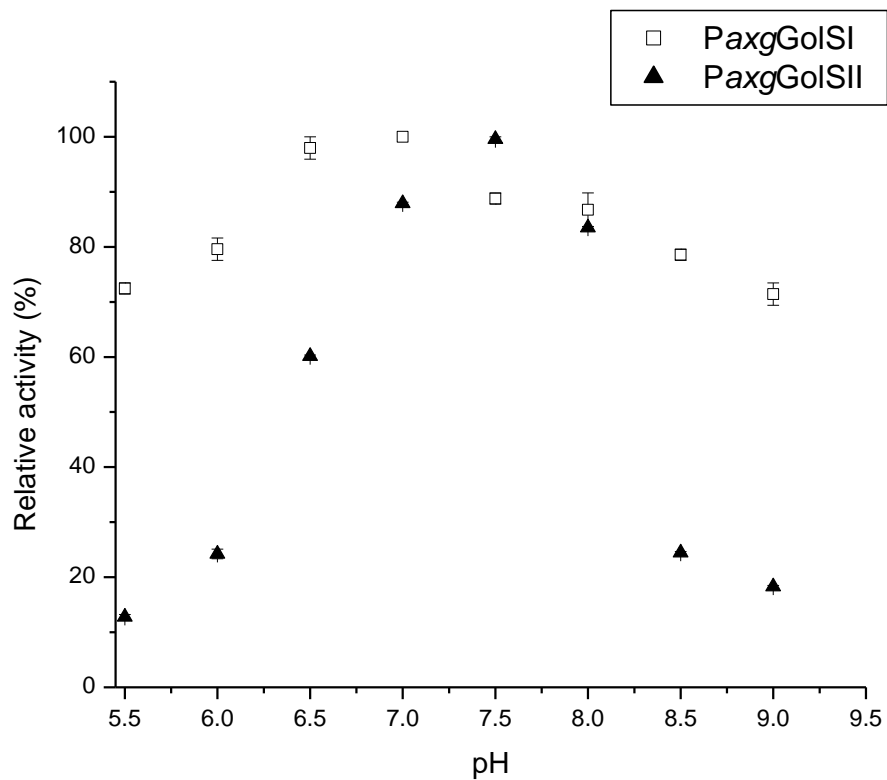


Figure 2.2 Deduced amino acid sequence alignment of known GolS proteins from *Arabidopsis thaliana* (AtGolS1 and -5), *Ajuga reptans* (ArGolS1 and -2), *Oryza sativa* (OsGolS1), *Cucumis melo* (CmGolS1) and the two GolS proteins isolated from the *P. alba* × *grandidentata* hybrid poplar (PaxgGolSI and PaxgGolSII). There is a conserved putative serine phosphorylation site (S) at position 274, and the characteristic hydrophobic pentapeptide (APSAA) is located at the end of the sequence. Identical amino acids are shaded in black and similar residues are shaded in grey.



**Figure 2.3 Phylogenetic analyses using the Neighbour-Joining method and based on predicted amino acid sequences of confirmed and putative GolS proteins. (A) GolS proteins from *Populus* grouped in four clades (a–d). (B) GolS proteins from different plant species. Phytozome accession numbers are provided for the *Populus trichocarpa* GolS proteins and GenBank accession numbers are provided for the remaining proteins. The two GolS proteins cloned from hybrid poplar (*P. alba*×*grandidentata*) are denoted in rectangles in (B). Bootstrap values are based on 1000 replicates. Bars, 0.05 amino acid substitutions per site.**



**Figure 2.4** Enzymatic activity of the recombinant PaxgGolSI (homologue of PtGolS2) and PaxgGolSII (homologue of PtGolS3) in response to pH at 37.5°C. Relative activity (%) was determined colorimetrically (Ribeiro *et al.*, 2000). Error bars correspond to the standard error of the mean.

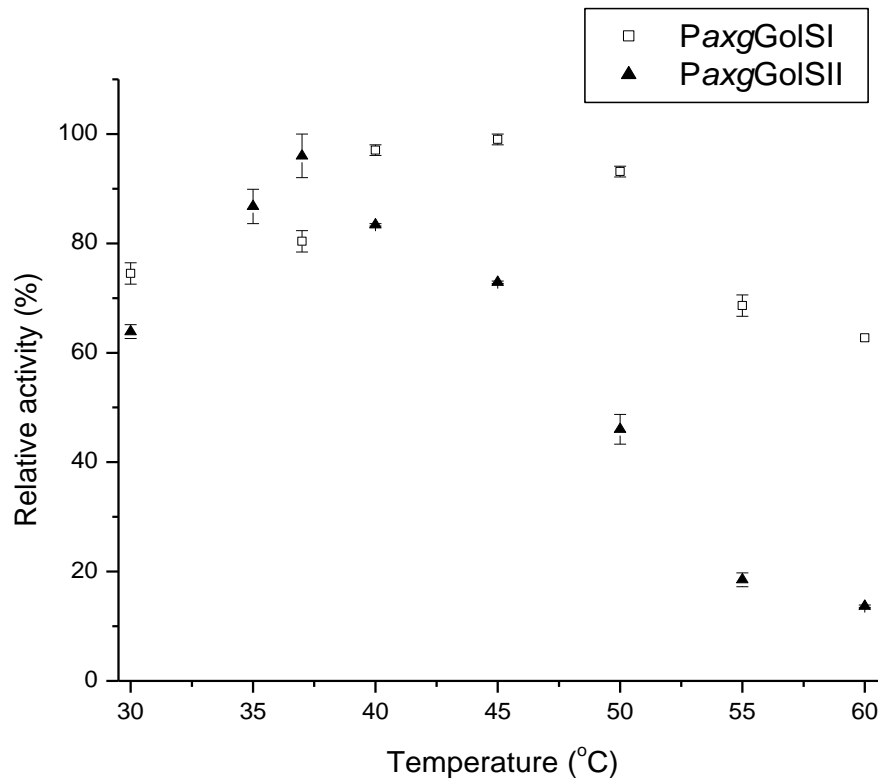


**Figure 2.5 Enzymatic activity of the recombinant PaxgGolSI (homologue of PtGolS2) and PaxgGolSII (homologue of PtGolS3) at different temperatures at optimal pH. Relative activity (%) was determined colorimetrically (Ribeiro *et al.*, 2000). Error bars correspond to the standard error of the mean.**

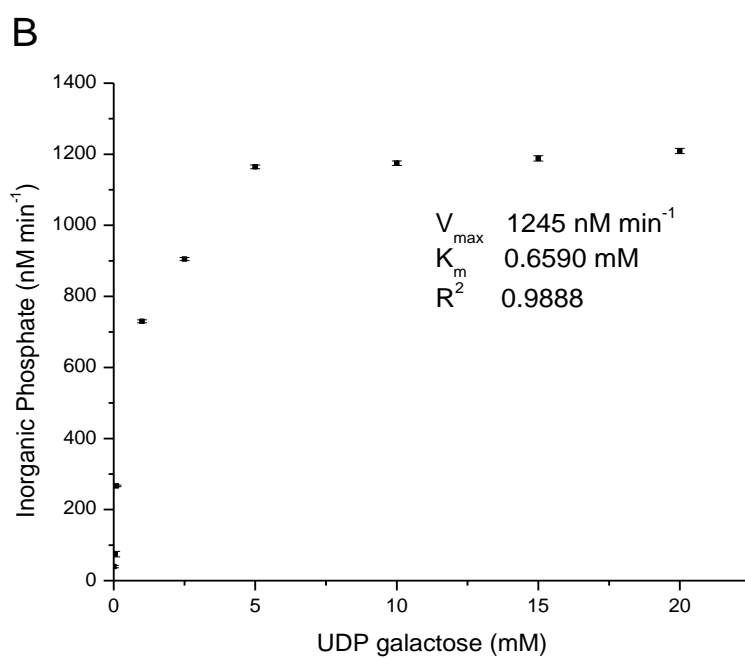
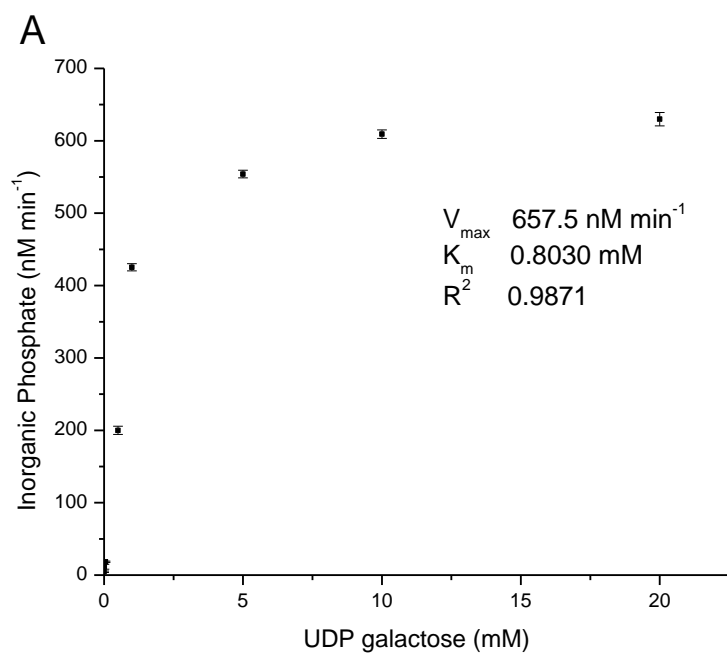


**Figure 2.6**  $V_{\max}$  and  $K_m$  values for the recombinant GolS enzymes Pa×gGolSI (A) and Pa×gGolSII (B). Error bars represent the standard error of the mean ( $n=6$  and  $n=4$ , respectively).

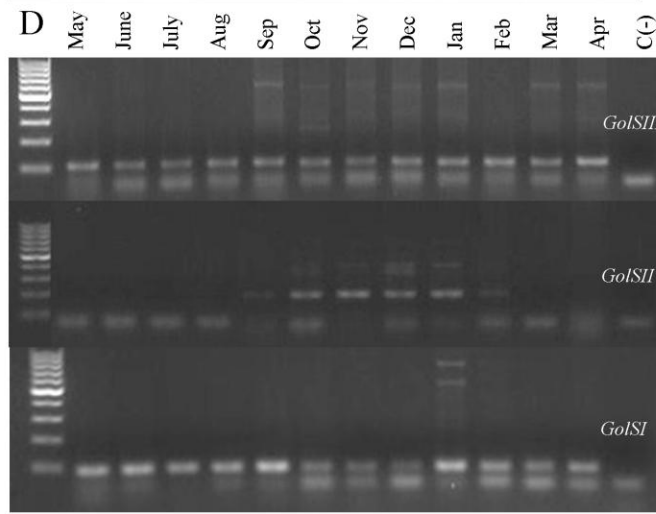
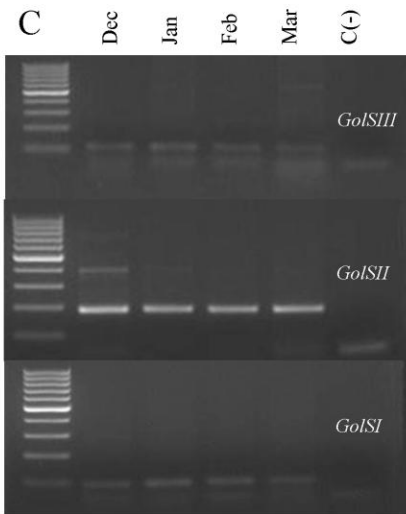
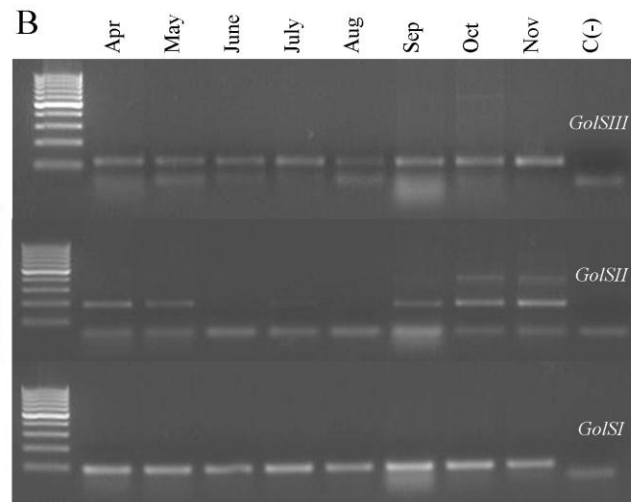
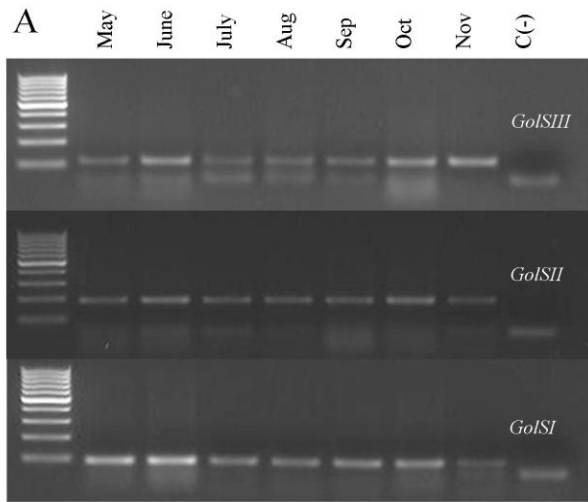


**Figure 2.7 Annual expression profiles of hybrid poplar *GolS* isoforms in different tissues over the course of 1 year of growth. (A) Source leaf, (B) lateral apical stem (first three nodes), (C) branch tip (without buds), (D) phloem. Primers used in the RT-PCRs amplified one member of the following three clades (based on Fig. 3A): clade a *Pa×gGolSII*, clade c *Pa×gGolSIII* and clade d *Pa×gGolSI*. PCR mix without template was used as the negative control [C(-)]. Lower bands correspond to primer dimer.**

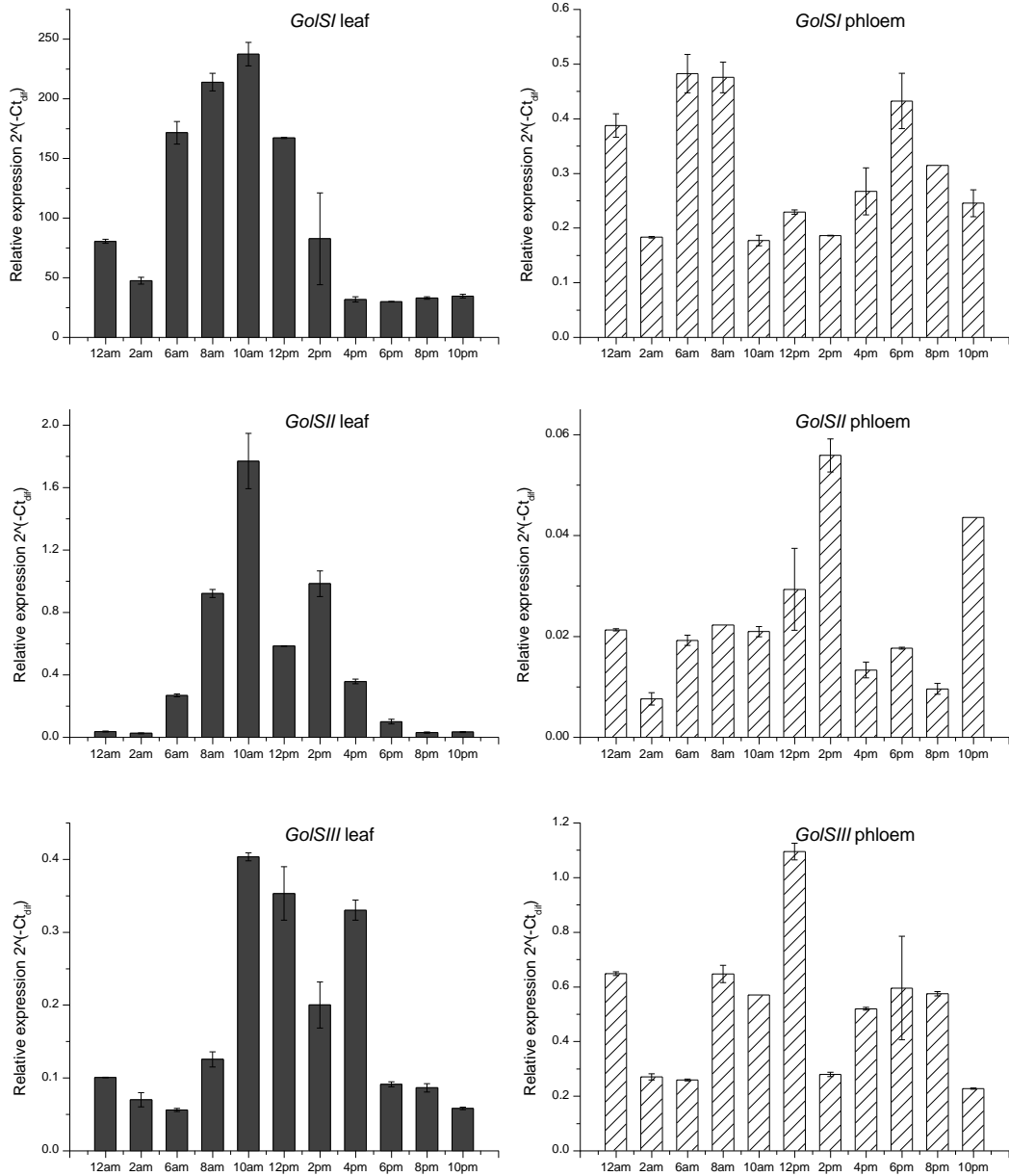


**Figure 2.8 Diurnal expression profiles of three *GoIS* isoforms in hybrid poplar (*P. alba* × *grandidentata*) leaf and phloem tissue. Error bars correspond to standard error of the mean, based on three replicates.**

## Chapter 3: Varied expression of the *GolS* in hybrid poplar (*Populus alba* × *grandidentata*)

### 3.1 Introduction

Generally, growth in plants is restricted to defined zones containing newly formed cells derived from meristematic divisions. Cell division in the apical meristems and subsequent elongation and maturation of the new cells defines primary growth; a phase of plant development that gives rise to new organs and to the basic plant form. Following primary growth, secondary growth may occur, producing radial polarity. Secondary growth involves two lateral meristems: the vascular cambium and the cork cambium. Secondary xylem is formed by a sequence of five major steps, named cell division, cell expansion (elongation and radial enlargement), cell wall thickening (involving cellulose, hemicellulose, and lignin deposition), programmed cell death, and finally heartwood formation (Plomion *et al.*, 2001). During elongation the cell wall consists of only a thin layer (primary cell wall) of radially orientated cellulose microfibrils that are crosslinked by hemicellulose glycan. Deposition of secondary cell wall begins once the cell shape is established, and occurs in a programmed manner that results in distinct zones, the outer (S<sub>1</sub>), middle (S<sub>2</sub>) and inner (S<sub>3</sub>) layers. The molecular underpinnings governing the regulation of these defined secondary wall layers remains a mystery, despite the distinct ultrastructural characters of each. In general, the secondary wall as a whole is characterized by a cellulose rich layer that intricately interacts with hemicellulose and lignin to form a network of cross-linked fibres in the cell wall (Popper & Fry, 2008; Uraki *et al.*, 2007). In numerous angiosperm trees, including *Populus* spp., normal secondary wall development is substantially modified when tension wood (TW) is formed in response to stem stresses, such as wind or snow load (Telewski *et al.*, 1996; Hellgren *et al.*, 2004; Mellerowicz *et al.*, 2001). In general, the overall lignin content

of TW is lower while the cellulose content is enriched, and ultrastructurally the cellulose synthesized is of higher crystallinity (Norberg & Meier, 1966; Bentrup *et al.*, 1969). In addition, the orientation of the microfibrils (MFA) is lower than that of corresponding normal wood (Nobushi & Fujita, 1972). In some species, such as *Populus* spp, a gelatinous layer or G layer can be formed between the lumen and the S3 layer (Nobushi & Fujita, 1972). Most of this G layer is made of cellulose with a very low MFA. Throughout maturation, longitudinal shrinkage occurs in this layer creating tensile stress in the cell.

Galactinol and the raffinose family of oligosaccharides (RFOs) are almost ubiquitous in plants. The RFOs have been shown to fulfill at least two major physiological roles in plants; storage and translocation of carbon. In addition, they have been implicated in possible roles related to combating biotic and abiotic stress, including drought and cold stress tolerance (Taji *et al.*, 2002; Cunningham *et al.*, 2003; Panikulangara *et al.*, 2004). However, substantial debate exists on the exact mechanism of action of these metabolites. For example, it has commonly been postulated that these metabolites may act as molecular signals or could act as true reactive oxygen species (ROS) scavengers when they accumulate at elevated concentrations in particular locations (e.g. vicinity of chloroplast thylakoid membranes) (Foyer & Shigeoka, 2011). Substantial evidence also implicates galactinol and/or raffinose as a signal during pathogen induced systemic resistance, suggesting a role in defense against biotic stress (Kim *et al.*, 2008). Application of exogenous galactinol increases pathogen resistances and stimulates defense related gene transcripts (e.g. *PR1a* and *b*) in tobacco (Kim *et al.*, 2008). Additionally, cucumber plants primed against *Corynespora cassiicola* showed an increase in *CsGolS1* gene transcript and accumulation of galactinol in challenge-inoculated leaves. However, the high level of galactinol fell back to normal levels within 12 h after pathogen attack, implying that galactinol can function

transiently as a signal molecule during early plant-pathogen interaction (Kim *et al.*, 2008). Although there is indirect evidence supporting the signalling role of galactinol and RFOs under abiotic stress, the exact mechanism and its direct targets remain unclear. It is, however, apparent that both biotic and abiotic elicitors share a substantial proportion of features in their stress mechanisms. We hypothesized that the galactinol signalling function may be related to a global stress response, and that altered expression of galactinol synthase will have an impact on carbon allocation and plant development.

In this chapter, I examine the effects of both over-expression and down-regulation of galactinol synthase (*GolS*) on hybrid poplar development and cell wall characteristics. Two transgenic lines possessing the highest transcript abundance in the phloem, clearly displayed significant physiological effects. Additionally, the occurrence of tension wood was clearly apparent in the transgenic lines which manifested in alteration in wood chemistry and fibre properties. Taken together, we discuss the possible role of *GolS* in cell wall development.

## **3.2 Materials and methods**

### **3.2.1 Plasmid construction**

The *A. thaliana GolS3* (At1g09350), which was previously shown to be cold inducible (Taji *et al.*, 2002), was cloned from Columbia ecotype (CO) cDNA using primers: *AtGolS3.Fw* 5'-CGCGGATCCATGGCACCTGAGATGAACAACAAGTTG-3' and *AtGolS3.Rv* 5'-CGCGAGCTCCTGGTGTGACAAGAACCTCGCTC-3'. The galactinol synthase transformation vector was constructed by ligating the cloned *AtGolS3* gene into the pSM3 vector (pCambia 1390 with double 35S promoter, Mansfield Lab, UBC) using the *BamHI* and *SacI* restriction enzymes. The vector was then subjected to genomic sequencing to confirm gene,

frame and orientation, and then transformed into *Agrobacterium tumefaciens* C58 strain, which was used for plant transformation.

The  $P_{a \times g}GolS$ -RNAi construct was generated using primers: *GolSXhXb* 5'-CTCGAGTCTAGACGGTTTGCTATGCCTTATTAT -3' and *GolSKpBa* 5'-GGTACCGGATCCTGC CAGCATTGAAGTAGAGAG -3'. The forward primer included the *XhoI* and *XbaI* restriction sites and the reverse primer included the *KpnI* and *BamHI* restriction sites, which were used to amplify a 288 bp fragment of a conserved region of the galactinol synthase family. The fragment was digested with the appropriate enzymes and ligated to the pKANNIBAL cloning vector (Helliwell & Waterhouse, 2003). The *NotI* fragment from the pKANNIBAL vector containing the hpRNA cassettes was then sub-cloned into the binary vector pART27 (Gleave, 1992). Once the vector (pART27  $P_{a \times g}GolSRNAi$ ) was confirmed by sequencing, it was transformed into *Agrobacterium tumefaciens* EHA105 strain and used for plant transformations.

### 3.2.2 Hybrid poplar transformations

*Populus alba* × *grandidentata* (P39) leaf discs were harvested from four week-old tissue culture-grown plants using a cork borer. Twenty plates containing 25 leaf discs (7 mm<sup>2</sup>) per genotype were co-cultivated with 30 ml of bacterial culture in 50 ml Falcon tubes for 30 min at 28° C in a gyratory shaker (100 rpm). Following co-cultivation, the explants were blotted dry on sterile filter paper and placed abaxially on WPM 0.1 NAA, 0.1 BA and 0.1 TDZ μM culture medium. The plates were cultured in the dark for two days at room temperature. On the third day, residual *Agrobacterium* was eliminated by transferring the leaf discs to WPM media containing 250 mg l<sup>-1</sup> cefotaxime and 500 mg l<sup>-1</sup> carbenicillin. All plates were kept in the dark for an additional two days. Explants were then transferred to WPM selection media containing 250 mg l<sup>-1</sup> cefotaxime, 500 mg l<sup>-1</sup> carbenicillin and 25 mg l<sup>-1</sup> hygromycin (*AtGolS3* over-expression) or 50 mg l<sup>-1</sup>

kanamycin (*GolSRNAi* down-regulation). After emergence, only one shoot per leaf disc was excised and placed on WPM selection media. After 6 weeks growth, explants were transferred to fresh medium with the same composition, and permitted to develop. Plants were confirmed as transgenic by genomic DNA screening, and those identified as positive were then subcultured and multiplied on antibiotic free WPM media.

### **3.2.3 Plant growth**

Transgenic trees were multiplied in WPM media until approximately eight to ten plants of each transgenic event were of similar size, along with the appropriate control, non-transformed trees. The trees were then moved to 2 gallon pots containing perennial soil (50% peat, 25% fine bark and 25% pumice; pH 6.0), where they were maintained on flood tables with supplemental lighting (16 h days) and daily water with fertilized water in the UBC greenhouse, Vancouver, BC.

### **3.2.4 Tissue collection**

Source leaf was collected using the leaf plastochron index (PI=5). Where PI=0 was defined as the first leaf greater than 5 cm in length and where PI=1 is the leaf immediately below PI=0. Sink leaves are the smallest and not fully expanded leaves. Phloem tissue included the bark, phloem tissue and cambial cells. Developing xylem corresponded to a slight scarring of the stem.

### **3.2.5 Molecular analysis**

#### **3.2.5.1 Genomic DNA extraction**

The CTAB (Sigma-Aldrich Co.) extraction method was used to isolate hybrid poplar P39 DNA. Briefly, the tissue was frozen with liquid N<sub>2</sub> and ground to a powder with 1 ml extraction buffer (2% w/v CTAB, 1.4 M NaCl, 20 mM EDTA, 100 mM Tris-HCl, 1% PVP, and 0.2% v/v β-

mercaptoethanol). The DNA concentration was measured with a GeneQuant *pro* (BioChrom Labs. Inc. Terre Haute, IN) and/or a spectrophotometer ND1000 (NanoDrop Technologies, Inc. DE, USA). DNA was stored at -20° C until use.

### **3.2.5.2 RNA isolation**

Hybrid poplar RNA was isolated as per Kolosova *et al.* (2004), using source and sink leaves, phloem, and developing xylem tissue. The RNA concentration was calculated using a GeneQuant *pro* machine or a ND1000 spectrophotometer. DNase I DIGEST kit (Ambion Inc.) was used to eliminate contaminating DNA. RNA treated with DNase was then quantified, and 1 µg was used to generate cDNA using the SuperScript II RT kit (Invitrogen Canada Inc.) or iScript cDNA synthesis kit (Bio-Rad Laboratories, CA, USA). The resulting cDNA was stored at -20° C.

### **3.2.5.3 PCR analysis of putative transformants**

Hybrid poplar plants that survived antibiotic selection were evaluated for the presence of the transgene. Transgene detection was established by PCR screening of genomic DNA using gene specific primers: *AtGols3scFw* 5'-AGCCTCCCCACTTATTACAAC-3' and *AtGols3scRv* 5'TGCACAGTAATGAACAACCTT-3'. *GolsRNAi* plants were screened with primers specific for a 773 bp fragment located just outside of the hairpin structure. *773Fw* 5'-TCCCACAAAAATCTGAGCTTAA-3' and *773Rv* 5'-TACCTTTTTAGAGACTCCAATC-3'.

### **3.2.5.4 Real Time- RT PCR**

*AtGols3* lines. Real Time RT-PCR reactions consisted of 12.5 µl of SYBR<sup>®</sup> Green QRT-PCR master mix (Invitrogen, Carisbad, CA), 20 pmol of *AtGols3scFw* and *AtGols3scRv* primers (described above), 1µl of cDNA, and distilled deionized water to a total volume of 25 µl. RT-PCR was performed on an Mx3000P<sup>®</sup> QPCR System (Stratagene, La Jolla, CA) using the

following thermal cycler conditions to amplify the 201 bp fragment of the *AtGols3* transcript: 1 cycle of 5 min at 95° C, 40 cycles of 95° C for 30 seconds, 55° C for 1 min, and 72° C for 30 seconds, followed by 1 cycle of 95° C for 1 min, 55° C for 30 sec, and 95° C for 30 sec.

*GolsRNAi* lines. The primer sequences were as per Philippe *et al.* (2010), and corresponded to PtGolS1.2 (same clade as *Pa×gGolSI*), PtGolS3.1 (homologue to *Pa×gGolSII*), PtGolS6.1 (homologue to *Pa×gGolSIII*), and a new primer for *Pa×gGolSIV* (same clade as *Pa×gGolSII*)  
*Fw* 5'-AACCTTTTGATTTCTCTAACC-3' and *Rv* 5'-AAGGGAGTTGGTGTGTTACG-3'  
Real Time RT-PCR reactions consisted of 10 µl of SsoFast Eva Green® Supermix (Bio-Rad Laboratories, CA, USA), 20 pmol of primers, 1µl of cDNA, and distilled deionized water to a total volume of 20 µl. RT-PCR was performed on a CFX 96 System® (Bio-Rad Laboratories, CA, USA). The following thermal cycler regime was used to amplify the 92, 186, 110 and 115 bp fragments of the *Pa×gGolSI*, *II*, *II* and *IV* transcripts, respectively: 1 cycle of 30 sec at 95° C, 39 cycles of 95° C for 5 seconds, and 58° C for 30 sec, followed by 1 cycle of 95° C for 30 sec, and a melt curve cycle of 58° C to 95° C increment of 0.5° C for 5 sec. Relative expression was calculated using the following equation  $\Delta ct = 2^{-(ct_{\text{target gene}} - ct_{\text{TIF5A}})}$ , where *TIF5A* is used as the reference gene (Coleman *et al.*, 2009).

### **3.2.6 Phenotypic analyses**

#### **3.2.6.1 Growth measurements**

After either three months (*AtGols3* over-expression) or six months (*GolsRNAi* down-regulation) greenhouse growth, tree height from root collar to the apex of the tree was recorded, while stem diameter was measured using digital calipers at 10 cm above the root collar (soil level). *AtGols3* transgenic lines and corresponding wild-type trees were harvested after 5 months of growth, and

tissues were kept on  $-80^{\circ}\text{C}$  until used. *GolSRNAi* transgenic lines and wild-type trees were harvested after six months of growth.

### **3.2.6.2 Gas exchange**

Gas exchange variables were measured using a LI-6400 portable gas-exchange system (LI-COR Biosciences, Lincoln, NB, USA). Measurements were conducted between September 3-11-2008, before noon. An artificial light source (LI-COR6400-02B LED Light Source) was used to ensure a constant light at saturation ( $1000\ \mu\text{mol quanta m}^{-2}\ \text{s}^{-1}$ ). Leaf chamber conditions were:  $\text{CO}_2$  concentration at  $380\ \mu\text{l l}^{-1}$ ; relative humidity between 38-45%; and block temperature between  $19\text{-}20^{\circ}\text{C}$ . A fully-expanded leaf from the upper stem of each tree was measured twice to calculate an average for each tree. Measured parameters included net photosynthesis ( $A$ ,  $\mu\text{mol CO}_2\ \text{m}^{-2}\ \text{s}^{-1}$ ), transpiration rate ( $E$ ,  $\text{mmol H}_2\text{O m}^{-2}\ \text{s}^{-1}$ ), stomatal conductance ( $g_s$ ,  $\text{mol H}_2\text{O m}^{-2}\ \text{s}^{-1}$ ), and intercellular  $\text{CO}_2$  concentration ( $C_i$ ,  $\mu\text{mol CO}_2\ \text{mol air}^{-1}$ ). The instantaneous intrinsic  $\text{WUE}_i$  ( $\mu\text{mol CO}_2\ \text{mol H}_2\text{O}^{-1}$ ) was calculated as the ratio of net photosynthesis to stomatal conductance, or  $A/g_s$  (McDermitt, 1990).

### **3.2.6.3 Water potential**

Leaf water potential was measured at midday for each tree using a pressure bomb (Soilmoisture Equipment Corp., Santa Barbara, CA, USA).

### **3.2.7 Structural chemistry analysis**

Dried wood samples from 5 or 6 months old greenhouse-grown trees were used to determine lignin and carbohydrate content following a modified Klason method (Cullis *et al.*, 2004). Samples were ground in a Wiley mill to pass a 40 mesh screen, treated with acetone overnight using a Soxhlet and then dried for 24 h at  $105^{\circ}\text{C}$ . Approximately 200 mg of dried extractive-free tissue was treated with 72% sulphuric acid for 2 h, diluted to ~3% with 112 ml DI water and

autoclaved at 121°C for 60 min. The mixture was filtered through a medium coarseness crucible and the retentate dried at 105°C. The acid-insoluble lignin was determined by weighing the retentate, while the acid-soluble lignin was measured from an aliquot of the filtrate using an UV spectrophotometer at 205 nm. Carbohydrate contents were determined by HPLC analysis of the filtrate. Glucose, xylose, mannose, galactose, arabinose and rhamnose were analyzed using a Dx-600 anion-exchange HPLC (Dionex, Sunnyvale, CA, USA) with a CarboPac PA1 column (Dionex) at 1 ml min<sup>-1</sup> and post column detection (100mM NaOH min<sup>-1</sup>). Sugar concentrations were calculated from standard curves created from external standards. Normalizations of the calculations were done using fucose as internal standard.

### **3.2.8 Soluble sugar analysis**

Phloem, developing xylem, source and sink leaf frozen tissues were ground using a mortar and pestle in the presence of excess liquid nitrogen. After which, the tissue was lyophilized for 24 h, weighed and treated with 4 ml of methanol:chloroform:water (12:5:3) overnight at 4°C.

Following incubation, the solution was centrifuged at 2770 × g for 10 min, and supernatant collected. The pellet was washed twice with 4 ml of the same solution and supernatants pooled (12 ml), while the pellet was dried and kept for starch analysis. Water (5 ml) was added to the pooled supernatant, mixed and centrifuged at 2770 × g for 5 min to induce phase separation. An aliquot (1 ml) of the upper phase was collected and dried using a vacuum centrifuge. For the *AtGOLS3* transgenic lines, the pellet was resuspended in 1 ml of water and analyzed for sucrose, raffinose, galactinol and *myo*-inositol on an Dionex HPLC fit with a PA 200 (sucrose and raffinose) and MA-1 (*myo*-inositol and galactinol) column (Dionex) with 600mM NaOH at 0.5 ml min<sup>-1</sup>. Fucose was added as internal standard. For the *GolsRNAi* lines, sugars were separated

on a Rezex RPM column (Phenomenex, CA, USA) with a flow rate of  $0.270 \text{ ml min}^{-1}$ . Fucose or galactitol were added as internal standards.

### **3.2.9 Starch analysis**

The pellet retained from the soluble sugar isolation was dried overnight in a  $50^{\circ}\text{C}$  oven, weighed and incubated with 5 mL of 4% sulfuric acid. The solution was then autoclaved at  $121^{\circ}\text{C}$  for 3.5 min, cooled and centrifuged at  $20 \times g$  for 5 min. An aliquot of the supernatant was analyzed by HPLC to quantify glucose release, representing the starch that was hydrolyzed by the acid treatment, using the same conditions as described in section 3.3 (above). Fucose was again added as an internal standard.

### **3.2.10 Cell wall characterization**

Fibre length was determined on a 1 cm segment isolated 10 cm above the root collar. Samples were macerated in Franklin solution (1:1, 30 % peroxide:glacial acetic acid) for 48 h at  $70^{\circ}\text{C}$ . Following the reaction, the residual solution was decanted and the tissue washed extensively with DI water under vacuum until a neutral pH was achieved. The fibrous sample was then resuspended in 10 ml of DI water and diluted to attain a fibre count of 25-40 fibres per second on the Fibre Quality Analyzer (FQA; OpTest Equipment Inc. Hawkesbury, Ont. Canada). Fibre length (in mm) was established for each sample by measuring 10,000 fibres.

Wood density was determined by X-Ray Densitometry (Quintek Measurement System Inc. Knoxville, TN, USA). Bark to bark samples isolated 9 cm above the root collar were first cut to 1.68 mm thickness on a pneumatic saw, Soxhlet extracted overnight with hot acetone, and allowed to acclimate to 7% moisture prior to X-Ray profiling. Density was measured on both sides of the pith and averaged for each sample.

Microfibril angle and cell wall crystallinity were determined by X-ray diffraction using a Bruker D8 Discover X-ray diffraction unit equipped with a general area detector diffraction system (GADDS) on the same samples prepared for density profiling. Wide-angle diffraction was used in transmission mode, and the measurements were performed with CuK $\alpha$ 1 radiation ( $\lambda = 1.54 \text{ \AA}$ ), the x-ray source fit with a 0.5-mm collimator, and the scattered photon collected by a GADDS detector. Both the X-ray source and the detector were set to theta = 0° for microfibril angle determination. The average T-value of the two 002 diffraction arc peaks was used for microfibril angle calculations, as per the method of Megraw *et al.* (1998). In contrast, the 2 theta (source) was set to 17° for wood crystallinity determination. Crystallinity was determined by mathematically fitting the data using the method of Vonk (1973). Crystallinity measures were precalibrated by capturing diffractograms of pure *A. xylinum* bacterial cellulose (known to be 87% crystalline).

### **3.2.11 Cross sectional staining and microscopy**

Wood samples from six months old *AtGols3* transgenic poplar trees were soaked overnight in dH<sub>2</sub>O. Samples were then cut into 40  $\mu\text{m}$  cross sections with a Spencer AO860 hand sliding microtome (Spencer Lens Co., Buffalo, NY, USA) and stored in microfuge tubes with dH<sub>2</sub>O until visualized. Sections were treated with 0.01% Calcofluor white in 1x PBS for 3 min, and then washed 3 x 5 min in 1x PBS (Falconer and Seagull, 1985). Sections were also treated with a saturated solution of phloroglucinol in 10% HCl. The sections were mounted onto glass slides and visualized with a Leica DRM microscope (Leica Microsystems, Wetzlar, Germany). The pictures were taken with a QICam camera (Q-imaging, Surrey, Canada) and analyzed with OpenLab 4.0Z software (PerkinElmer Inc., Waltham, USA).

Vessel number, length and area were calculated from the 40 $\mu$ m cross sections stained with phloroglucinol. Three trees per line were analyzed. Four pictures were taken in different zones of the sections and approximately 180 vessel areas were measured per tree. The sections were analyzed on the Carl Zeiss Jena “Jenamed” 2 fluorescence microscope (Carl Zeiss Microscopy LLC, NY, USA). Photos were taken with an Infinity 3 camera (Lumenera Corporation, Ottawa, Canada) and analyzed with the associated Infinity capture program.

### **3.2.11.1 Antibody labelling**

The prepared cross section samples described above were also subject to antibody labelling. Briefly, non-specific protein binding was blocked with 5% BSA in TBST (10 mM Tris-buffer, 0.25 M NaCl, pH 7, with 0.1% Tween) for 20 min. Sections were then treated with diluted primary antibody (1:50) anti- $\beta$ -(1–4)-D-mannan (catalogue #400-4) monoclonal antibody (Biosupplies Australia Pty Ltd, Melbourne, Australia), anti-xylan LM10 antibody (kind gift of Dr. J. Paul Knox; [www.plantprobes.co.uk](http://www.plantprobes.co.uk)) or CCRC-M7 against RGI (Puhlmann *et al.*, 1994) at room temperature for 1 hour. The sections were then washed twice with TBST for 5 minutes. The diluted secondary antibody (Alexa 543: antirat or antimouse) 1:50 was then added, incubated for 1 hour and washed twice with TBST. Samples were mounted on glass slides with 90% glycerol or anti-fade mounting media. Fluorescent localization was observed on a Leica DRM (Leica Microsystems, Wetzlar, Germany) light microscope using a Texas Red filter, and images captured with a QICam camera (Qimaging, Surrey, Canada) and analyzed with OpenLab 4.0Z software (Perkinelmer Inc., Waltham, USA). The antibody tagged sections were stored at 4°C in TBST 1x in microfuge tubes if they were not used immediately.

### 3.2.12 Stress treatments

AtGolS3 lines Heat and cold stresses were imposed on trees grown under normal greenhouse conditions. Greenhouse leaves were cut into discs using a #13 cork borer, placed into 12 cell well plates and sealed with parafilm to avoid dehydration. Leaf discs were subjected to cold (-4, -6, and -8°C) for 24 hours, or heat treatment (38, 40, and 42°C) for 4 hours. All treatments (n=6) were carried out in the dark and had a control plate at room temperature. Detection of chlorophyll fluorescence was accomplished on the dark-adapted leaves with a portable modulated chlorophyll fluorometer Os-30 (Opti-Sciences Inc. NH., USA). Fluorescence parameters ( $F_0$ , minimal fluorescence;  $F_m$ , maximal fluorescence) were measured.  $F_v/F_m$  (ratio of variable fluorescence to maximal fluorescence) was calculated with the following formula  $F_v/F_m = (F_m - F_0)/F_m$ .

GolSRNAi lines Greenhouse-grown trees were subjected to two abiotic stress treatments. Water stress was imposed on trees grown in the greenhouse for seven days by water withdrawal, after this period trees were re-watered. Leaf tissue was collected on day 0, 2, 4, 6 and 9. Cold treatment was achieved by placing the transgenic and control trees in a refrigerated room (2°C) with light ( $1.17 \mu\text{mol s}^{-1} \text{m}^{-2}$ ) for 12 days. Leaf samples were collected on days 4, 7 and 12. Source leaf tissue samples were used for RNA and soluble sugar extractions to measure transcript and product abundance of poplar *GolS*.

### 3.2.13 Leaf nutrient analysis

Leaf samples representing leaf plastochron index PI=5 were sent for plant nutrient analysis by Inductively Coupled Plasma (ICP) analysis at the Pacific Soil Laboratory, Richmond, BC.

### 3.2.14 NMR

NMR analysis was performed as per Mansfield *et al.* (2012). Briefly, plant biomass was air-dried to a constant moisture content and cryogenically pre-ground for 2 min at 30 Hz using a Retsch (Newtown, PA, USA) MM301 mixer mill. The pre-ground cell walls were extracted with distilled water and 80% ethanol using ultrasonication. Isolated cell walls (200 mg) were then finely milled using a Retsch PM100 planetary ball mill for 70 min in 10 min intervals with 5 min interval breaks. Approximately 30–60 mg of extract-free, ball-milled plant cell wall material was transferred to a 5-mm NMR tube, and 500  $\mu$ l of premixed DMSO- $d_6$ /pyridine- $d_5$  (4:1) was added directly into the NMR tube containing individual sample. The NMR solvent mixture was carefully introduced (via a syringe), spreading it from the bottom of the NMR tube, along the sides, and towards the top of the sample. The NMR tubes were then placed in an ultrasonic bath and sonicated for 1–5 h, until the gel became apparently homogeneous; the final sample height in the tube was ~4–5 cm. NMR spectra from the sol-gel- samples were acquired in a 2D  $^1\text{H}$ – $^{13}\text{C}$  HSQC spectra using a standard Bruker pulse program ('hsqcetgpsisp.2' or 'hsqcetgpsisp2.2'). The NMR spectra had the following parameters typical for plant cell wall samples: spectra were acquired from 11 to –1 ppm in F2 ( $^1\text{H}$ ) using 1078 data points for an acquisition time (AQ) of 60 ms, an interscan delay (D1) of 750 ms, 196 to –23 ppm in F1 ( $^{13}\text{C}$ ) using 480 increments (F1 acquisition time 5.78 ms) of 16 scans, with a total acquisition time of 6 h. Processing used typical matched Gaussian apodization in F2 and a squared cosine-bell in F1. Interactive integrations of contours in 2D HSQC /HMQC plots were carried out using Bruker's TopSpin 2.5 software, as was all data processing.

### 3.2.15 Statistical analysis

Parametric or non-parametric Student's t tests were performed (depending on equal or non-equal variances). Student's t test values were calculated with Microsoft Excel (Microsoft Corp., WA, USA). Significant differences were calculated between wild-type and transgenic lines at the 95% confidence level.

## 3.3 Results

### 3.3.1 Generation of transgenic poplar trees

The full length coding sequence of the *A. thaliana* *Gols3* (At1g09350) (Taji *et al.*, 2002) was cloned and inserted into the binary vector pSM-3 driven by the 35S promoter for over-expression (OE) analysis. In contrast, suppression of the *Pa*×*gGols* expression was achieved using a 288 bp hairpin RNAi construct designed from the cDNA-encoding *Pa*×*gGols*. *Agrobacterium*-mediated transformation of hybrid poplar yielded multiple *AtGols3-OE* and *GolsRNAi* transformants which were verified by genomic screening. After several weeks of growth, RNA was isolated; cDNA generated using reverse transcriptase, and transcript abundance determined by Real Time RT-PCR. Ten lines possessing the highest transcript abundance of the *AtGols3-OE* transgene and four lines with *Pa*×*gGols* down-regulation, based on RT-PCR, were transferred to antibiotic free-media and multiplied to obtain a minimum of eight clonal trees per transgenic line.

*AtGols3-OE* transgenic plants were transferred to the UBC greenhouse (March 2008), and after three months of growth the height and diameter of the stem was recorded (Figure 3.1). Lines 6 and 11, among the 10 transgenic lines, showed a distinct growth phenotype (Figure 3.2). These lines were severely stunted in height (0.86 m and 0.86 m, respectively) and had thinner (5.47 mm 5.71 mm, respectively) stem diameters compared to the wild-type trees (2.16 m of height and 12.92 mm of stem diameter).

After 5 months growth, physiological parameters were analyzed in four *AtGols3-OE* transgenic lines (3, 6, 8, and 11) and wild type. Net photosynthesis, stomatal conductance, and  $WUE_i$  were reduced in the phenotypic lines 6 and 11, while the other two transgenic lines (3 and 8) had values similar to those of the wild-type trees (Table 3.1).

Relative transcript abundance was again examined on greenhouse-grown plants, and clearly detected in all four *AtGols3-OE* transgenic lines examined, but not in wild type, as expected (Figure 3.3). Lines 6 and 11 had higher expression in the phloem and developing xylem than the other two non-phenotypic lines (3 and 8). The expression was different in source leaves where the non-phenotypic lines had higher expression than lines 6 and 11. Finally, lines 11 and 3 had higher expression in sink leaves than the other two transgenic lines. Gene expression was also checked in the other transgenic lines (1, 2, 4, 5, 7, 9, and 10) in phloem tissue (Figure 3.4). Lines 6 and 11 consistently showed the highest transgene expression compared to the other transgenic lines.

*GolsRNAi* transgenic plants were transferred to the UBC greenhouse in August 2010 and after six months of growth the height and diameter of the stem was measured (Figure 3.5). No statistical differences were found between transgenic lines and wild-type trees. However, line 16 appeared shorter than wild type.

Relative expression was also examined on greenhouse-grown *RNAiGols* plants. Endogenous expression of the *Pa $\times$ gGolsII* was very low in phloem tissue (Figure 3.6) of wild-type and transgenic trees, and it was not detected in the other tissues analyzed. The low endogenous expression of this gene made it difficult to confirm a down-regulation of the *Gols* genes. To further analyze the *Gols* transcript abundance, *GolsRNAi* transformants and wild-type trees were subject to two different abiotic stress treatments. The water stress treatment failed to

alter the transcript abundance of *Pa×gGolsII* in the source leaves of wild-type trees (Figure 3.7). Relative expression values were extremely low, and it was not possible to discriminate between the transgenic lines and wild-type trees. However, the expression of *Pa×gGolsII* in wild-type leaves seemed to be higher after four days of water removal. In contrast, when the cold stress treatment was then imposed on the hybrid poplar trees the transcript abundance of the *Pa×gGolsII* increased more than 1000 fold that of corresponding normal growth conditions (Figure 3.8A). Furthermore, transgenic lines 3, 4 and 11 displayed a significant reduction in the relative expression levels of the gene. The transcript abundance of members of *Pa×gGols* isoforms was measured to determine the impact of the RNAi-construct on overall *Gols* down-regulation by the RNAi suppression strategy. Relative expressions of the other isoforms (*Pa×gGolsIV*, *III* and *I*) were markedly lower compared to *Pa×gGolsII* when the trees were under cold stress (Figure 3.8B-D). Nevertheless, the expression trend of all *Gols* isoforms analyzed show a down-regulation in the transgenic lines.

### **3.3.2 Carbohydrate and lignin analysis**

The structural chemistry of the transgenic and control stem was analyzed using a modified Klason method (Table 3.2). *AtGols3* transgenic lines 3 and 8 were most similar to wild-type trees in cell wall composition, while lines 6 and 11 were markedly different (Table 3.2A). More specifically, the carbohydrate composition of lines 6 and 11 had higher arabinose and galactose levels, while rhamnose and xylose content were reduced. The most remarkable change was a massive reduction in mannose in the extreme lines compared to the other *AtGols3* transgenic lines and the wild type. Additionally, an increase in glucose content was observed in all transgenic lines compared to the wild-type, implying higher cellulose content. Further histochemical staining specific for cellulose of stem cross sections with calcofluor white (Figure

3.9) showed increased fluorescence for both lines 6 and 11, which is consistent with the results of the chemical analysis. Total lignin content of these two extreme phenotypic lines was also significantly decreased (Table 3.2A). In contrast, the *GolSRNAi* transgenic lines only showed slight reductions in the hemicellulose and pectic-derived sugars, arabinose, rhamnose and galactose under normal growth conditions (Table 3.2B).

Microscopic observations of stem cross sections of the *AtGolS3-OE* lines 6 and 11 showed irregular and smaller vessels, increased number of vessels per unit area (Table 3.3), and visible increases in the percentage of tension wood compared to wild-type trees. To further analyze the change in structural carbohydrate content, immuno-labelling of cross sections with antibodies LM10 (anti-xylan), CCRC-M7 (anti-rhamnogalacturan I) and anti-mannan was used to evaluate lines 6 and 11 relative to wild type. The anti-xylan antibody LM10 bound evenly to xylem tissue (fibres, vessels and ray parenchyma) (Figure 3.10 A-C). Fluorescence was similar in both the transgenic lines and wild type, but binding of the antibody was higher in areas of tension wood in all samples, and with all antibodies; especially with CCRC-M7 (RG-I) (Figure 3.10 D-F). The anti- $\beta$ -(1-4)-D-mannan binding was noticeably stronger in wild-type tissue compared to lines 6 and 11 (Figure 3.10 G-I), which is consistent with substantial reduction in mannose shown by cell wall chemistry analyses. In addition, it appears that in wild type the anti-mannan binding was enhanced in fibre cell walls when compared to vessels.

*AtGolS3* transgenic lines 6 and 11 and wild-type trees were also analyzed by 2D NMR to study the composition of the anomeric sugars and lignin without degrading the cell wall polymeric structures. The lignin monomer distribution and abundance were not considerably changed between the transgenic lines and wild-type trees; however, the syringyl monomers were

slightly reduced. The most striking difference was found in the *p*-hydroxybenzoates, which were present in the wild-type trees and totally absent in the transgenic lines (Figure 3.12)

Similarly high amount of the acid sugar, galacturonic acid or  $\alpha$ -D-GalpA (difficult to discriminate in the chemical assignments) in the phenotypic lines which was not present in the wild-type plants (Figure 3.11). Additionally, arabinose ( $\alpha$ -L-Araf) was present in small amounts in the transgenic lines, but not in wild-type trees. On the other hand, mannose ( $\beta$  D-Manp) was reduced considerably in the transgenic lines compared to wild-type trees, consistent with the compositional analyses. Further quantification of the galacturonic acid by HPLC in wild-type trees and *AtGols3* transgenic lines is presented in Table 3.4, showing similar levels in both wild-type and transgenic lines.

### **3.3.3 Soluble sugar analysis and starch**

Soluble sugars (galactinol, *myo*-inositol, sucrose and raffinose) were analyzed in four tissues (phloem, developing xylem, source leaves, and sink leaves) of wild-type and *AtGols3* transgenic lines. Galactinol increased in all *AtGols3* over-expressing transgenic lines compared to wild type in all tissues, as expected, while lines 6 and 11 possessed the highest amount in phloem and developing xylem tissues (Figure 3.13). *Myo*-inositol, which is one of the substrates participating in the reaction catalyzed by galactinol synthase was increased in all transgenic lines in the phloem and developing xylem, and reduced in lines 6 and 11 in leaf tissue compared to the wild-type trees (Figure 3.14). Sucrose was reduced in lines 6 and 11 in the phloem and developing xylem compared to the other transgenic lines and wild type (Figure 3.15). Raffinose was not present in the developing xylem and sink leaf in the wild-type trees, while it was apparent in all transgenic lines, in all tissues (Figure 3.16).

Interestingly, the overall amount of sucrose in the phloem of the wild-type hybrid poplar trees was 13 times higher than the amount of raffinose, confirming that sucrose is the major transporting sugar in poplar, despite the substantial number of plasmodesmata present in poplar phloem tissue (Russin & Evert, 1985). Starch was quantified and shown to be reduced in source leaf tissue in all transgenic lines when compared to wild-type trees (Table 3.5), while phloem starch was higher in all transgenic lines (significantly higher in line 8) compared to wild type, suggesting that carbon partitioning was substantially augmented by *GolS* over-expression in these transgenic poplar trees. Furthermore, it appears from the NMR analysis that the xylem was also enriched in starch, as the putative assignment of  $\alpha$ -D-GalpA was significantly elevated in the transgenic lines.

In the *GolSRNAi* transgenic lines the soluble sugars (galactinol, sucrose, stachyose and raffinose) were analyzed in four separate tissues (phloem, developing xylem, source leaves, sink leaves) when the trees were subject to normal growth conditions. No statistical differences were apparent in sucrose content in the transgenic lines compared to wild-type trees. Galactinol was slightly reduced in line 16 sink leaves and developing xylem tissue. Furthermore, raffinose was increased in phloem tissue in the transgenic lines and reduced in source leaves (data not presented). The transgenic and wild-type trees were then subject to cold treatment to assess the impact of this stress treatment on the differences in the amount of soluble sugars in source leaves. Stachyose in source leaves of trees subjected to cold treatment was reduced in most of the *GolSRNAi* lines, except line 11 (Figure 3.17). While raffinose was reduced in all *GolSRNAi* lines (Figure 3.17), and sucrose was generally higher in transgenic lines compared to wild-type trees (Figure 3.18). Finally, as anticipated, the *GolSRNAi* transgenic lines showed a reduction in the concentration of galactinol when compared to wild-type trees (Figure 3.19).

### 3.3.4 Cellulose characterization

The wood properties of the *AtGols3* over-expressing transgenic lines and wild-type trees were compared. All transgenic lines had higher wood densities, with lines 6 and 11 showing substantially higher wood densities (564.1 and 549.2 Kg m<sup>-3</sup> respectively) compared to wild type (293.20 Kg m<sup>-3</sup>). Lines 3 and 8 also had increased wood densities showing average densities of 332.2 and 347.1 Kg m<sup>-3</sup>, respectively (Figure 3.20). The wood microfibril angle was reduced in lines 6 and 11 (7.69 and 7.44) when compared to 10.20 of wild type (Figure 3.20), while the percent cell wall crystallinity increased in the same lines (51.3 and 55%, respectively) compared to wild-type poplar (46.7%) (Table 3.6). Furthermore, the fibres of lines 6 and 11 were smaller and thinner than wild-type plants (Figure 3.21).

### 3.3.5 Stress treatments and foliar nutrient analysis

Wild-type hybrid poplar and *AtGols3* transgenic lines 3, 6, 8 and 11 were grown in greenhouse conditions and leaf discs were subjected to two stress treatments. The  $F_v/F_m$  was calculated, a parameter that provides an estimate of the PSII maximum efficiency in dark adapted material. After leaves were exposed to cold temperatures, the maximum quantum yield of PSII, as judged by  $F_v/F_m$ , was significantly decreased in wild type (from 0.82 to 0.75 at -8°C; Figure 3.22 A), depicting the sensitivity of PSII in poplar leaves to cold treatment. In contrast, the transgenic lines 6 and 11 showed  $F_v/F_m$  values of 0.71 and 0.65 respectively at room temperature, and dropped to 0.45 and 0.59 respectively when the trees were subject to -8°C conditions. These low values indicated that the transgenic lines were stressed prior to cold treatments; this is in accordance with the observation of chlorosis in the leaves of these transgenic lines. Furthermore, the  $F_v/F_m$  estimates demonstrate that increasing these “stress stimulated” metabolites did not improve the tolerance of poplar plants to stress treatments. A second stress treatment (heat) had

an even more significant effect on the leaves, as the  $F_v/F_m$  values dropped drastically to 0.40 and 0.20 in transgenic lines 6 and 11, respectively, at 42°C (Figure 3.22 B).

Leaf nutrient analysis revealed an increase in N, P, K and Cu in leaves of transgenic plants compared to wild-type trees (Table 3.7). In contrast, Ca, Mg, Fe and more significantly Mn and B were reduced in these same lines compared to wild-type trees. A deficiency in one or more of nutrients such as Mn, Fe and Zn may be the cause the leaf chlorosis observed in the transgenic trees. Microscopic observations of phloem structure in transgenic and wild-type plants (data not presented) showed irregular phloem cell structure, which could explain accumulation of the primary nutrients in leaves. This accumulation could also be caused by a lack of sites to use these primary nutrients in the plant.

### **3.4 Discussion**

The raffinose family of oligosaccharides (RFO) has been implicated in several intricate plant biological processes, including desiccation tolerance in seeds, transport of carbohydrates in the phloem, and protection of plants against a variety of stress scenarios. In the second chapter of this thesis I suggested that the galactinol synthase genes from hybrid poplar putatively play a role in the storage and seasonal mobilization of carbohydrates, in addition to a role in protecting against biotic and abiotic stress. To further understand the specific function of this gene *in planta*, we studied the changes in physiological parameters, wood properties, and carbohydrate content caused by over-expressing and down-regulating galactinol synthase in hybrid poplar.

In this study, the *Arabidopsis thaliana* galactinol synthase 3 gene (*AtGols3*) was over-expressed in hybrid poplar trees. Previously, this same gene was characterized (Taji *et al.*, 2002) and shown to be induced by cold stress in *Arabidopsis* plants. This gene was employed to create several individual transgenic lines, of which a limited group (based on expression levels)

were selected for comprehensive evaluation. Furthermore, two *AtGols3-OE* lines clearly showed unusual phenotypes with clear changes in height, photosynthetic rates, carbohydrate composition and chemical properties of the wood. These same phenotypic lines 6 and 11 displayed the highest transgene transcript abundance in the vascular tissues compared to all transgenic lines generated.

In the second part of this study, RNAi-mediated suppression was used for down-regulation of the galactinol synthase genes in poplar. Endogenous expression of different isoforms of galactinol synthase was described in the first chapter of this thesis. The *Pa×gGolsII* isoform was suggested to be temperature related (Unda *et al.*, 2012). This was confirmed when expression of *Pa×gGolsII* in wild-type trees was extremely low when grown under normal conditions. However, the transcript abundance of *Pa×gGolsII* was significantly increased when these same trees were subjected to cold, but not to drought stress. Similar results were found in *Arabidopsis*, as *AtGols3* was induced by cold stress but not by drought or salt stress. By contrast, *AtGols1* and 2 were induced by drought and salinity stress, but not by cold stress (Taji *et al.*, 2002). The RNAi construct employed here achieved the down-regulation of primarily *Pa×gGolsII* and also the other *Pa×gGols* genes analyzed. Commensurately, the amount of galactinol in source leaf tissue was reduced, as well as the higher oligosaccharides raffinose and stachyose.

#### **3.4.1 Wood properties of transgenic lines are characteristic of tension wood**

Cross sections of the *AtGols3* phenotypic lines showed smaller and irregular vessels compared to wild-type trees. The number of vessels significantly increased and there was the distinct presence of a G-layer in fibres, characteristic of tension wood formation in angiosperm trees. Commensurate with the visual observation, the microfibril angle was significantly reduced and

the crystallinity increased. In poplar, as in most temperate tree species, tension wood fibres are characterized by the existence of a G-layer (Jourez *et al.*, 2001; Fang *et al.*, 2008; Gorshkova *et al.*, 2010; Clair *et al.*, 2011). This layer has been shown in extreme cases to have microfibrils that are arranged almost parallel to the cell's long axis (Faruya *et al.*, 1970). In the current study, the MFA of the *AtGOLS3* transgenic lines 6 and 11 was reduced approximately 25% compared to wild-type trees. This is in accordance with the general consensus of tension wood in the G-layer of gelatinous fibres (Wardrop & Dadswell, 1948; Hillis *et al.*, 2004; Washusen *et al.*, 2005).

In addition to the ultrastructural phenotypic characteristics, the cell wall mannose content was extremely reduced in the *AtGOLS3* transgenic lines when compared to wild-type trees. Similar results were obtained by (Hedenstrom *et al.*, 2009) in aspen, showing that both mannose and 1,4- $\beta$ -mannan were approximately 2 to 3 fold lower in tension wood of G-fibres when compared to normal wood fibres. These biochemical findings are consistent with molecular findings, which showed that in *Populus* species, the inherent levels of mannan biosynthesis-related transcripts are lower in differentiating fibres forming a G-layer during tension wood formation (Andersson-Gunneras *et al.*, 2006). In addition to the observed reduction in mannose, there was a significant increase of galactan content. Tension wood is known to contain 2 to 4 fold more galactose than normal wood in many species, including *Eucalyptus gonicalyx* (Schwerin, 1958), *Betula pubescens* and *B. verrucosa* (Gustafsson *et al.*, 1952), and *Fagus sylvatica* (Meier, 1962). Ruel & Barnoud (1978) suggested that high galactose content is a strong indicator of G-fibre formation. Furthermore, it has been shown that the galactose isolated from tension wood is present as a highly complex structure with high degree of branching (Azuma *et al.*, 1983). Kuo & Timell (1969), showed that the G-fibre galactan in American beech largely consisted of  $\beta$ -(1 $\rightarrow$ 4)- and  $\beta$ -(1 $\rightarrow$ 6)-linked galactopyranosidic residues, with a smaller

component of galacturonic acid, rhamnose, and the disaccharide 2-*O*- $\alpha$ -D-GalAp-L-Rha, indicating the presence of Rhamnogalacturan I (RG I) (Meier, 1962; Kuo & Timell, 1969; Azuma *et al.*, 1983). Besides the total increase of galactose in the *AtGals3* transgenic lines, another important finding (2D NMR analysis) was the presence of galacturonic acid. Pectin polysaccharides containing (1-4)- $\alpha$ -D-galacturonic acid are one of the major components of the middle lamella and primary cell wall. Nevertheless, they are also present in small proportions in secondary cell wall, especially in secondary cell walls enriched in gelatinous type cells (Gorshkova *et al.*, 2010). Additionally, galacturonic acid together with rhamnose and galactose are present in the alkali-insoluble residue of flax fibre (Mooney *et al.*, 2001) suggesting that the pectic galactan can be tightly bound to cellulose of secondary cell wall. The high amount of galacturonic acid found in the *AtGals3-OE* lines and the presence of the G-layer in these lines is in line with these papers.

Immunofluorescence analysis of the *AtGals3* transgenic lines showed that the CCRC-M7 antibody, which has RGI as its epitope, bound more intensely to areas where tension wood was found. Similarly, immunochemical studies in sweetgum (*Liquidambar styraciflua*; Hamamelidaceae) and hackberry (*Celtis occidentalis*; Ulmaceae) showed that a number of antibodies that recognize arabinogalactan proteins and RG I-type pectin molecules bind to the G-layer (Bowling & Vaughn, 2008). The fact that the tissue is labelled with CCRC-M7 antibody, which recognizes RG I as well as both soluble and membrane-bound AGPs, supports the idea that tension wood is not entirely composed of crystalline cellulose. In our study, the *AtGals3* phenotypic lines (6 and 11) clearly formed tension wood. Based on the cumulative results, I hypothesized that the over-expression of galactinol synthase and/or its resulting biochemical product, galactinol, may act as a signal *in planta* to combat stress, and in consequence may also

be involved in initiating the formation of tension wood. The formation of tension wood is a mechanism that permits a tree to develop and react to the environment (Jourez, 1997). The inference that galactinol is a signal molecule was previously proposed in plants subjected to biotic stress, where galactinol was shown to function as a signalling factor for induced systemic resistance caused by *Pseudomonas chlororaphis* O6 root colonization (Kim *et al.*, 2008), and galactinol and/or RFOs activated jasmonate-dependent defense responses against *B. cinerea* infection in *Arabidopsis* (Cho *et al.*, 2010). Valluru & Van den Ende (2011) hypothesized that galactinol and RFOs function as signals that mediate stress responses in plants. Furthermore, the authors put forth a model suggesting that galactinol and the RFOs maintain reactive oxygen species (ROS) homeostasis in plants, and proposed that these sugars may function as endogenous signals acting downstream of ROS signalling and mediate ROS responses to cellular functions leading to acclimation or cell death.

### **3.4.2 *p*-hydroxybenzoate groups associated with S lignin absent from transgenic lines**

The total lignin content of the *AtGols3* transgenic plants was also shown to be significantly reduced. More detailed analysis using 2D NMR showed that the most noticeable change in the lignin structure was the absence of the *p*-hydroxybenzoate groups in the transgenic lines.  $\gamma$ -acylated G and S units have been identified in the lignins of several species. The lignin of grasses has  $\gamma$ -*p*-coumarate substituents on many lignin units. In poplar, willow, and palm the structural analyses of lignin have shown that  $\gamma$ -*p*-hydroxybenzoate esters are present (Meyermans *et al.*, 2000; Landucci & Ralph, 2001). In our study, the 2D NMR showed a slight reduction of S lignin in the galactinol synthase over-expressive lines; accordingly, there was an extreme reduction of its associated *p*-hydroxybenzoate. Further studies will be necessary to analyze the transferases that regulate the *p*-hydroxybenzoate groups in poplar.

### 3.4.3 Photosynthesis and leaf nutrient analysis

It was apparent in the two high expressing *AtGolS3* transgenic trees that there was a significant reduction in height and diameter of the stem. Additionally, these same trees had numerous sylleptic branches that grew like vines with noticeably chlorotic leaves. Nutrient analysis showed that these lines were low in calcium, and several authors have suggested that calcium supply in trees can impact wood formation, causing important changes in wood structure and chemistry. Westermark (1982) suggested that lignin polymerization is a calcium-dependent mechanism during secondary cell wall formation. More recently, Lautner *et al.* (2007) using Fourier transform infrared (FTIR) spectroscopy on poplar wood grown under calcium starvation, found evidence for the role of calcium in lignification based on the reduction in carbonyl and methoxyl groups from S-lignin. The comparison of the leaf nutrient analysis between the phenotypic *AtGolS3* transgenic lines and wild-type trees also revealed that the primary nutrients, N, P and K, had accumulated in the leaves of the transgenic lines. Similarly, Cu accumulated to double of the amount detected in wild type, suggesting that the transporting cells in the phloem could be altered. Microscopic observations of the phloem structure in transgenic lines showed irregular cells, which could affect mobilization of nutrients.

Photosynthetic parameters such as carbon assimilation rates (Ac) were significantly reduced in the transgenic lines. Stomatal conductance and transpiration rates were also reduced, but not at the same rate as assimilation rates. The decrease in photosynthetic rates in transgenic lines could be caused by non-stomatal effects (Teskey *et al.*, 1986). In our transgenic lines, some of the nutrients involved in chlorophyll formation, electron transport chains and photosynthesis (Mg, Zn, Fe and Mn) were reduced compared to wild-type trees, and could be one of the factors to explain the reduction in photosynthetic rate found.

In summary, we explored the effects of the mis-regulation of the galactinol synthase genes in hybrid poplar. Galactinol has been studied for the role that it has as the galactosyl donor for the synthesis of raffinose and higher oligosaccharides (*i.e.* stachyose). Our hypothesis was that the over-expression of galactinol synthase would increase RFOs and consequently the resistance of hybrid poplar to abiotic stress. The main alteration, however, was in xylem composition and tension wood formation. Collectively, the results suggest that the over-expression of *GolS* and its product galactinol may serve as a molecular signal that initiates different metabolic changes for combating stress, culminating in the formation of tension wood. Interestingly, the over-expression of raffinose synthase and its product raffinose (Chapter 4) did not have the same effect on cell wall development, suggesting that it must be the disaccharide galactinol and not its higher oligosaccharides acting as the signalling molecule for response to exogenous stresses. Some other interesting findings, such as the reduction of *p*-hydroxybenzoates groups in lignin in transgenic lines, offer new questions that could be the basis of further investigations.

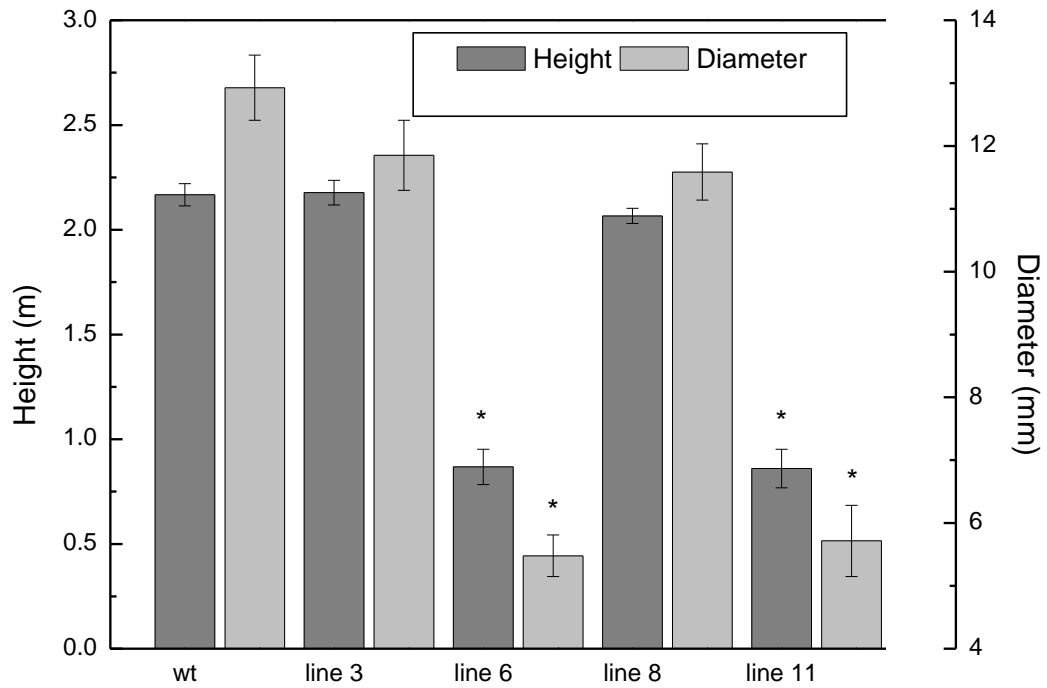


**Figure 3.1** Height from the base of the stem to the apex, and diameter at 10 cm from the base of the stem of three-month old greenhouse-grown *AtGols3* transgenic and wild-type hybrid poplar. Bars represent the standard error of the mean (n=10). Asterisks represent statistical difference from wild type (wt) at 95% level.



Figure 3.2 Five months old greenhouse-grown transgenic poplar trees expressing the *Arabidopsis thaliana* galactinol synthase 3 gene (*AtGolS3*) and wild type. Inset shows the vine-like growth pattern of the transgenic lines.

Lines	Photo ( $A_c$ )	Stomatal conductance ( $g_s$ )	WUE <sub>i</sub>	water potential ( $\Psi_{leaf}$ )
	$\mu\text{mol CO}_2/\text{m}^2\text{s}$	$\text{mol H}_2\text{O}/\text{m}^2\text{s}$	$\mu\text{mol CO}_2/\text{mol H}_2\text{O}$	MPa
wt	13.37 (1.40)	0.156 (0.03)	90.63 (10.09)	-0.97 (0.15)
line 6	<b>9.10 (0.97)</b>	0.132 (0.03)	70.91 (7.95)	-0.72 (0.07)
line 8	13.99 (1.64)	0.213 (0.07)	83.83 (13.91)	-0.91 (0.09)
line 11	<b>6.89 (0.64)</b>	0.117 (0.04)	74.87 (14.50)	-0.78 (0.11)

**Table 3.1 Gas exchange parameters and water potential for *AtGols3-OE* and wild-type poplar trees. Carbon assimilation rate Photo ( $A_c$ ), stomatal conductance ( $g_s$ ), intrinsic water use efficiency (WUE<sub>i</sub> =  $A / g_s$ ) and water potential ( $\Psi_{leaf}$ ). Values represent the mean and standard error of the mean with bold values corresponding to a statistical difference from wild type (wt) at 95% level (n=5).**

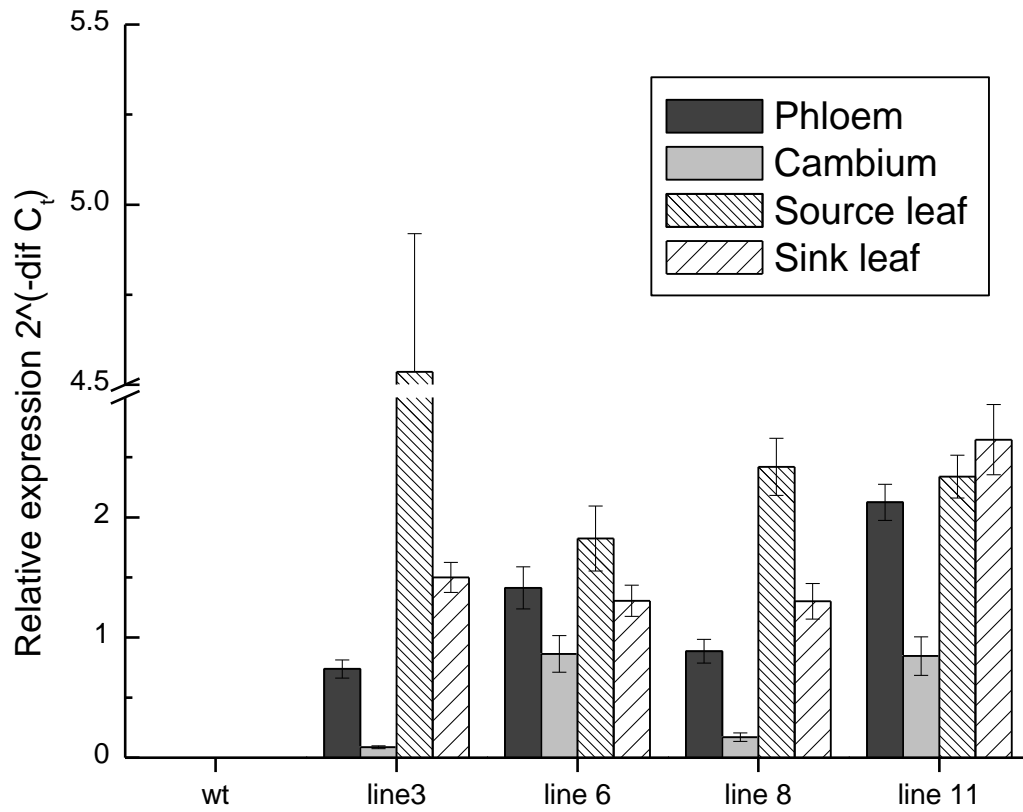
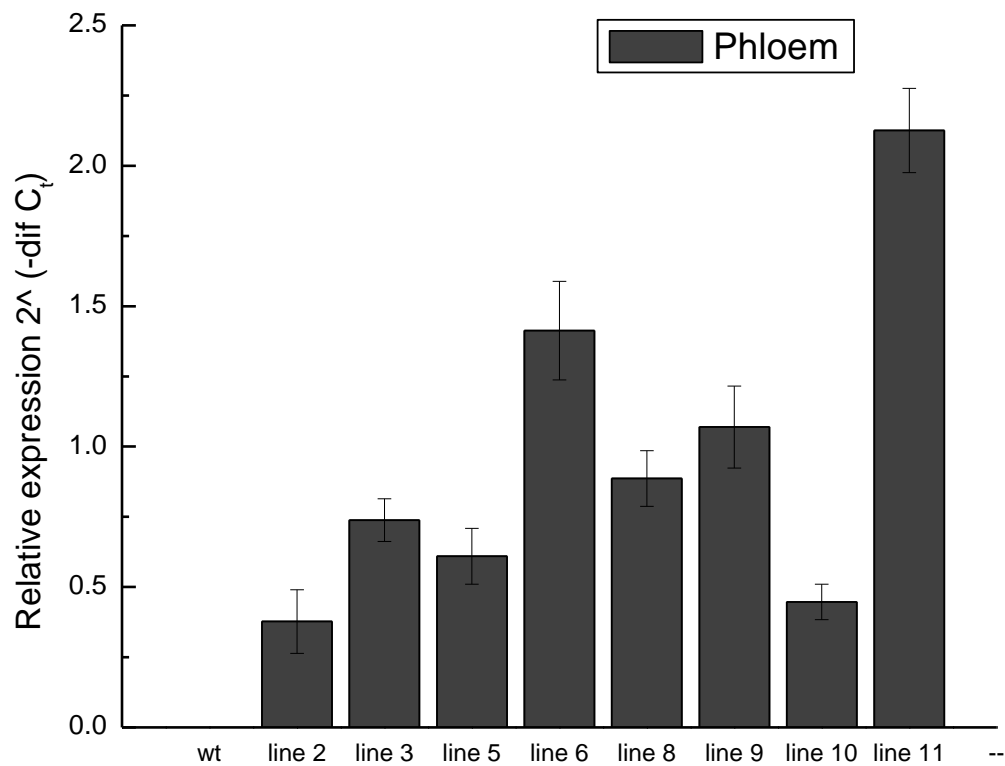
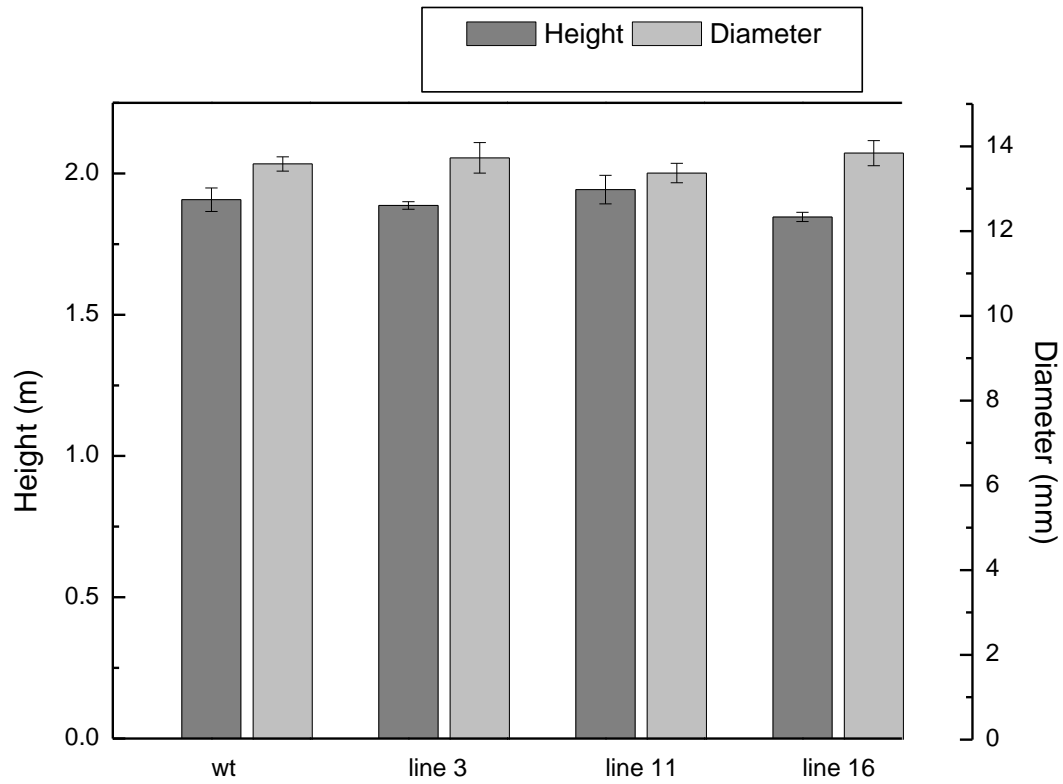


Figure 3.3 Transcript amount of the *Arabidopsis thaliana* galactinol synthase 3 gene (*AtGolS3*) in tissues of five months old greenhouse-grown hybrid poplar presented as expression relative to the translation initiation factor 5A (*TIF5A*= reference gene) using the formula  $2^{(-\Delta C_t)}$ . Bars represent the standard error of the mean (n=3).



**Figure 3.4** Transcript amount of the *Arabidopsis thaliana* galactinol synthase 3 gene (*AtGols3*) in phloem tissue of hybrid poplar presented as expression relative to the translation initiation factor 5A (*TIF5A*= reference gene) using the formula  $2^{(-\Delta C_t)}$ . Bars represent the standard error of the mean (n=3).



**Figure 3.5** Height from the base of the stem to the apex, and diameter at 10 cm from the base of the stem of six-month old greenhouse-grown *GolSRNAi* transgenic and wild-type hybrid poplar. Bars represent the standard error of the mean (n=8).

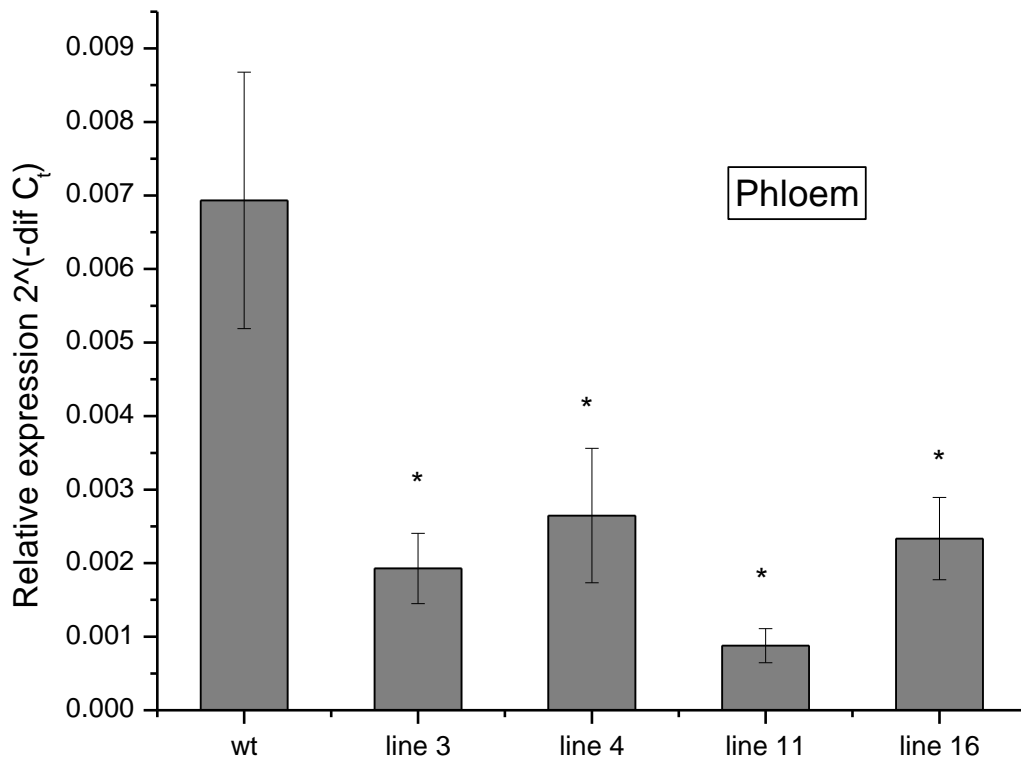


**Figure 3.6** Transcript amount of the *Pa×g GolsII* gene in phloem tissue of *GolSRNAi* transgenic and wild-type hybrid poplar presented as expression relative to the translation initiation factor 5A (*TIF5A*= reference gene) using the formula  $2^{(-\Delta C_t)}$ . Bars represent the standard error of the mean (n=3). Asterisks represent statistical difference from wild type (wt) at 95% level.

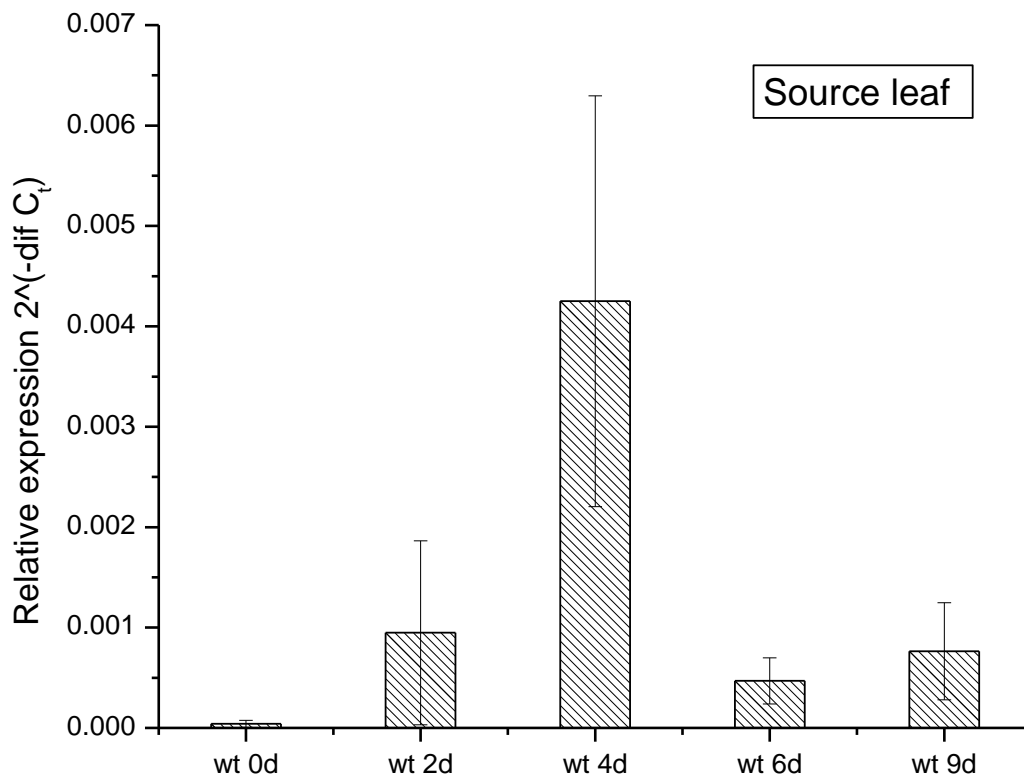


**Figure 3.7** Transcript amount of the *Paxg GolSII* gene in source leaf of wild-type hybrid poplar subjected to water stress for 7 days. Tissue was collected at 2 day intervals, until trees were watered on day 7 and a sample was collected after 2 days. Transcript is presented as expression relative to the translation initiation factor 5A (*TIF5A*= reference gene) using the formula  $2^{(-\Delta C_t)}$ . Bars represent the standard error of the mean (n=3).

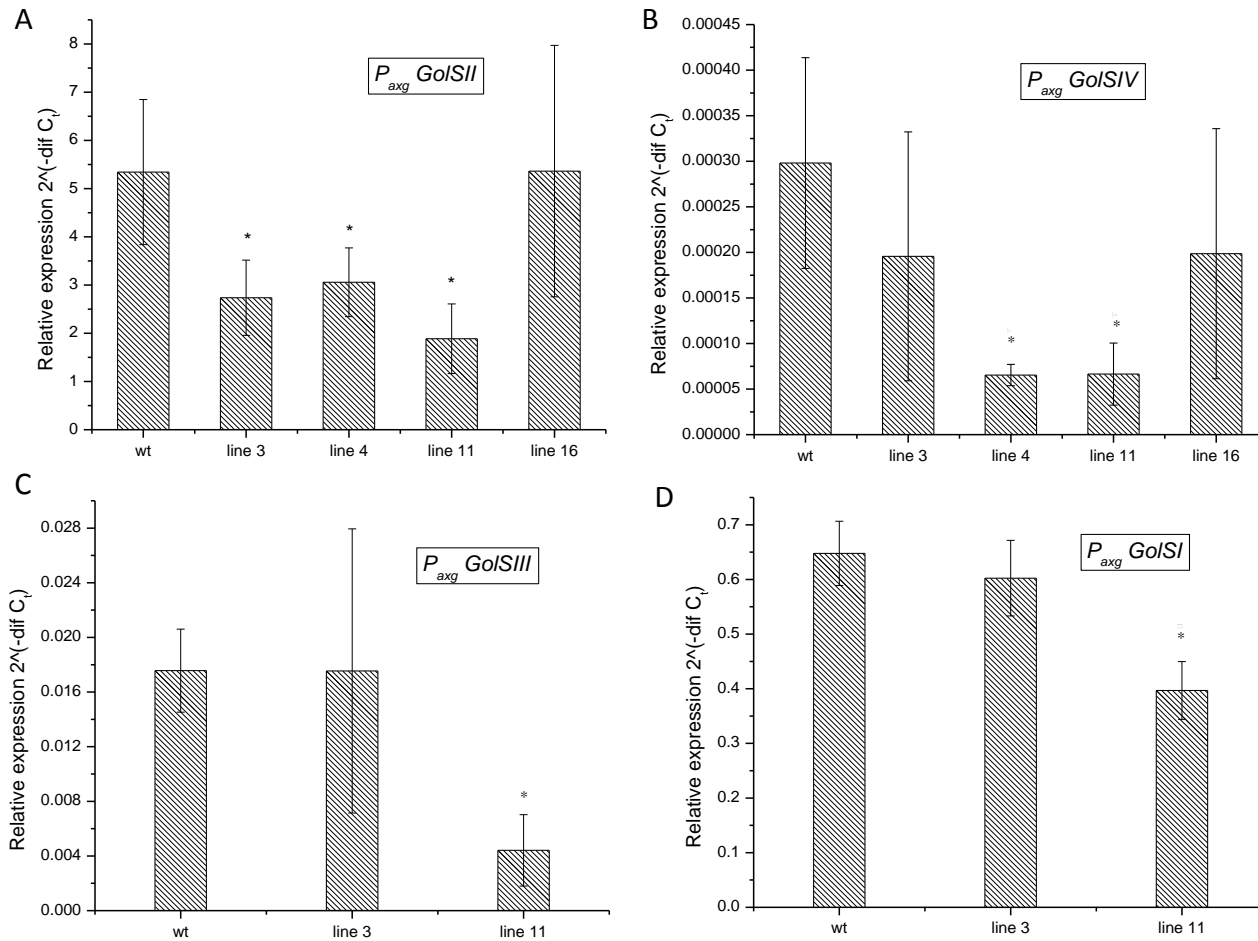


**Figure 3.8** Transcript amount of the  $P_{axg} \text{ GolSII}$ ,  $IV$ ,  $III$  and  $I$  in source leaf of  $\text{GolSRNAi}$  transgenic and wild-type hybrid poplar subjected to cold stress for 7 days. Transcript is presented as expression relative to the translation initiation factor 5A ( $TIF5A$ = reference gene) using the formula  $2^{(-\Delta Ct)}$ . Bars represent the standard error of the mean (n=3). Asterisks represent statistical difference from wild type (wt) at 95% level.

Lines	Arabinose µg/mg		Rhamnose µg/mg		Galactose µg/mg		Glucose µg/mg		Xylose µg/mg		Mannose µg/mg		Lignin %	
<b>A)</b>														
wt	3.12	(0.48)	6.63	(0.52)	8.65	(0.67)	466.16	(6.82)	161.37	(4.58)	24.64	(0.94)	24.79	(0.21)
line 3	3.00	(0.40)	6.37	(1.79)	10.80	(1.16)	<b>509.43</b>	<b>(10.59)</b>	151.57	(5.62)	<b>29.02</b>	<b>(0.84)</b>	23.06	(1.27)
line 6	<b>7.52</b>	<b>(0.71)</b>	4.63	(1.03)	<b>18.61</b>	<b>(2.79)</b>	<b>540.62</b>	<b>(23.77)</b>	<b>127.97</b>	<b>(4.87)</b>	<b>8.73</b>	<b>(0.80)</b>	<b>18.23</b>	<b>(0.40)</b>
line 8	3.12	(0.66)	5.28	(0.12)	10.06	(1.04)	481.09	(9.80)	151.54	(5.66)	22.54	(0.81)	23.58	(0.38)
line11	<b>8.67</b>	<b>(1.30)</b>	7.15	(1.35)	<b>17.02</b>	<b>(0.97)</b>	<b>509.45</b>	<b>(4.27)</b>	<b>134.61</b>	<b>(5.25)</b>	<b>11.39</b>	<b>(1.44)</b>	<b>19.38</b>	<b>(0.47)</b>
<b>B)</b>														
wt	3.49	(0.10)	3.77	(1.32)	10.03	(2.06)	499.83	(11.27)	190.75	(2.16)	28.49	(1.60)	20.90	(0.39)
line 3	<b>2.74</b>	<b>(0.10)</b>	1.41	(0.24)	6.16	(0.38)	493.60	(17.60)	183.74	(2.95)	28.44	(1.34)	20.03	(0.20)
line 4	3.70	(0.16)	4.10	(1.58)	7.30	(1.00)	477.90	(7.95)	197.50	(2.27)	24.40	(2.17)	20.83	(2.13)
line11	<b>2.40</b>	<b>(0.22)</b>	0.74	(0.38)	5.70	(0.63)	517.48	(8.71)	188.17	(4.98)	29.86	(0.52)	19.56	(1.08)
line16	3.36	(0.17)	5.31	(0.15)	8.58	(0.43)	491.37	(15.21)	193.53	(5.59)	25.30	(1.19)	21.28	(0.65)

**Table 3.2 Structural cell wall carbohydrates and total lignin content A) five- month old wild-type and *AtGolS3* over-expression transgenic trees and B) six-month old wild-type and *RNAiGolS* transgenic poplar trees. Values represent the mean and standard error of the mean in parenthesis with bold values corresponding to a statistical difference from wild type (wt) at 95% level (n=3).**

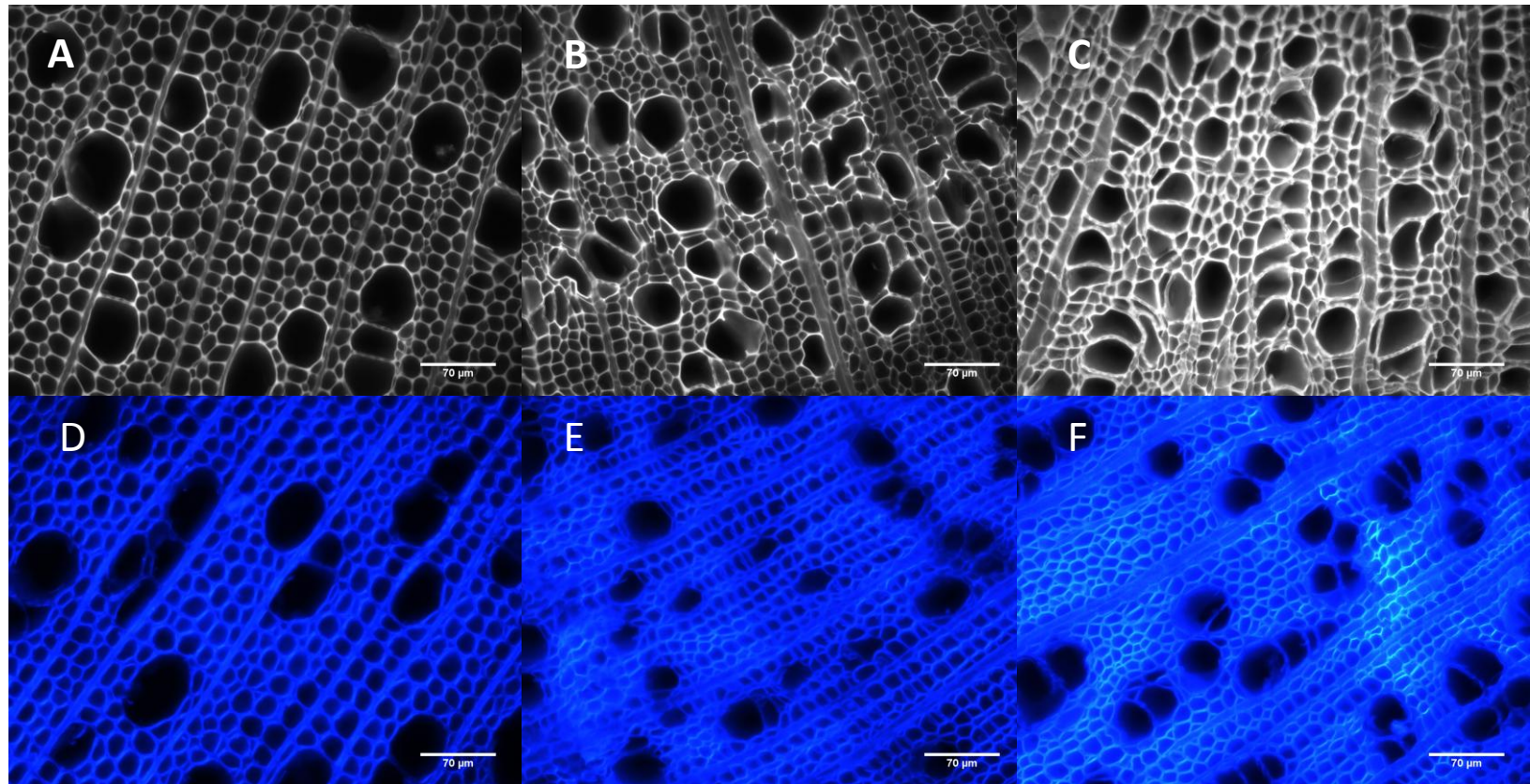


**Figure 3.9** Auto-fluorescence (A-C) and calcofluor (D-F) staining of wild type (A, D), *AtGols3* transgenic line 6 (B, E) and transgenic line 11 (C, F) hybrid poplar. Transgenic lines show an irregular vessel phenotype and increased cellulose staining with calcofluor. (Scale bars: 70 μm).

Lines	Area per vessel ( $\mu\text{m}^2$ )		Number (per 100000 $\mu\text{m}^2$ )		Length ( $\mu\text{m}$ )		Width ( $\mu\text{m}$ )	
wt	1536.02	(50.03)	9.99	(0.40)	48.73	(1.45)	35.22	(1.84)
line 6	<b>544.47</b>	<b>(16.31)</b>	<b>21.44</b>	<b>(1.87)</b>	<b>30.07</b>	<b>(0.82)</b>	<b>24.91</b>	<b>(0.78)</b>
line 8	1427.88	(54.416)	<b>8.17</b>	<b>(0.48)</b>	<b>44.61</b>	<b>(1.27)</b>	33.96	(0.92)
line 11	<b>338.83</b>	<b>(10.49)</b>	<b>23.00</b>	<b>(2.14)</b>	<b>20.15</b>	<b>(0.78)</b>	<b>17.76</b>	<b>(0.68)</b>

Table 3.3 Vessel count and measurements on cross sections of five-month old greenhouse-grown wild-type and *AtGolS3* transgenic trees. Values represent the mean and standard error of the mean in parenthesis with bold values corresponding to a statistical difference from wild type (wt) at 95% level (n=3).

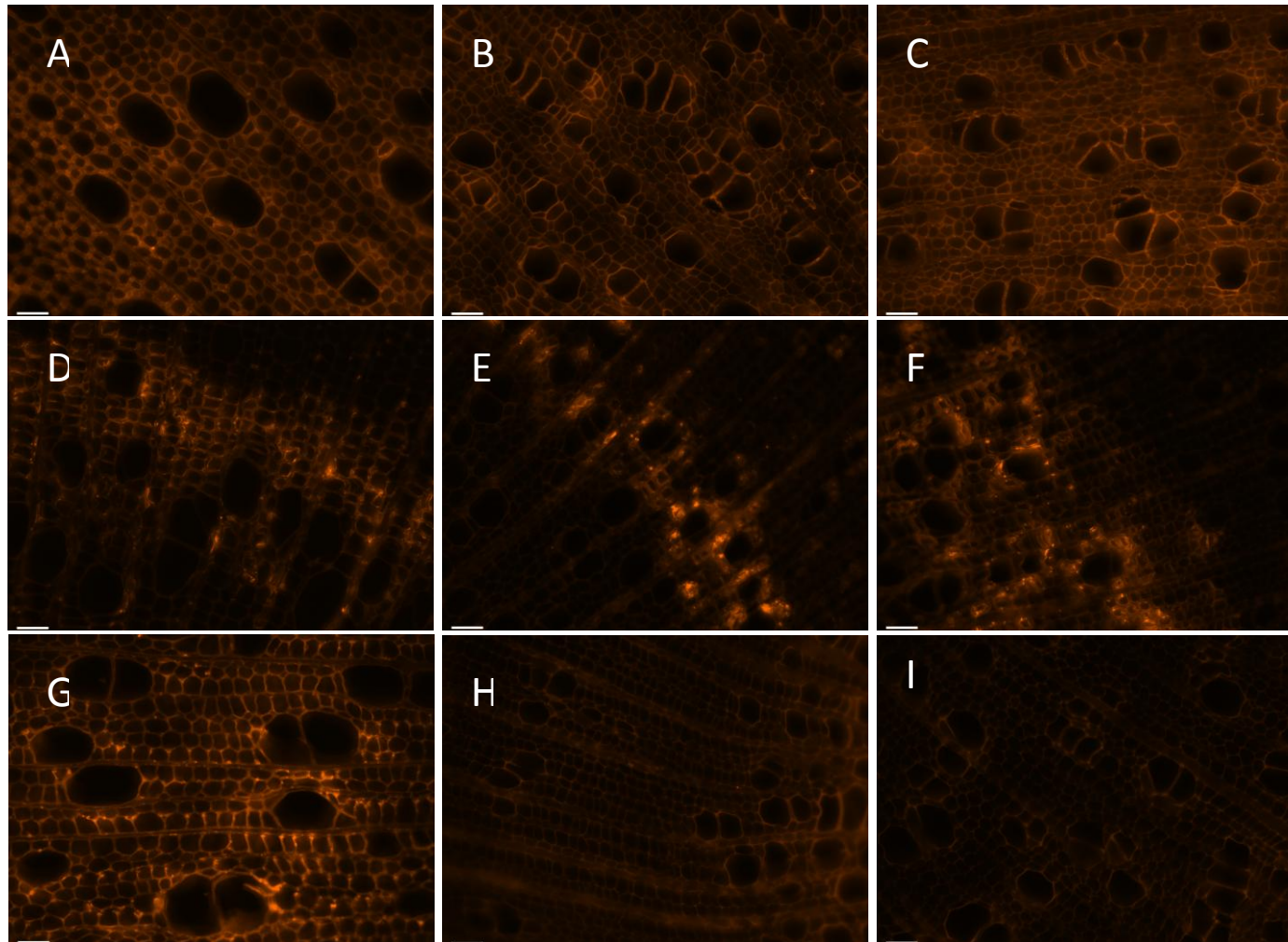


**Figure 3.10** Immunofluorescence labelling of xylem tissue from wild type (A, D and G); *AtGols3* transgenic line 6 (B, E and H) and *AtGols3* transgenic line 11 (C, F and I) hybrid poplar. Tissue was labelled with the anti-xylan LM10 antibody (A-C); the anti- RGI CCRCM7 antibody (D-F) and the anti-mannan antibody (G-I). Bars 40  $\mu\text{m}$ .

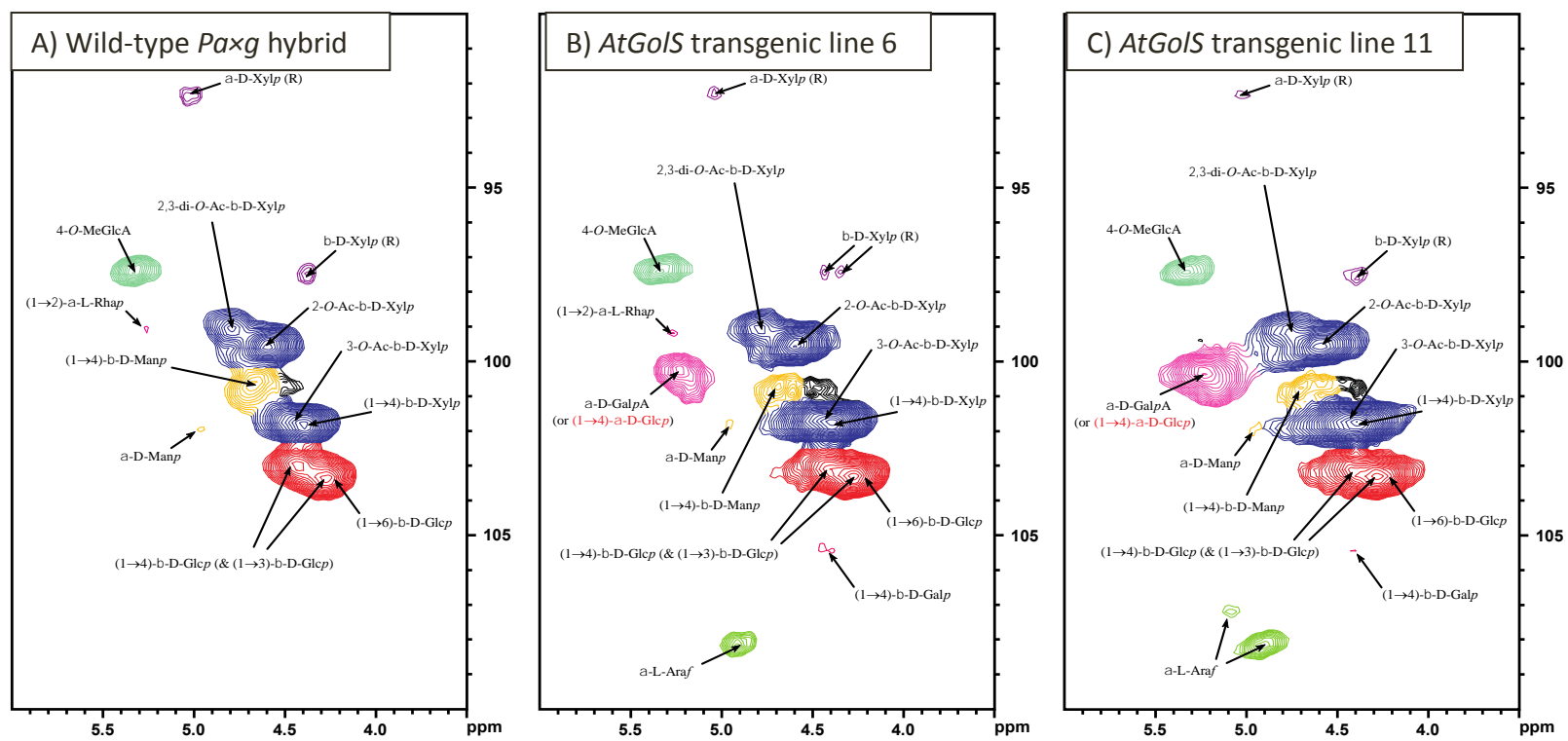


Figure 3.11 Polysaccharide anomeric regions of 2D  $^{13}\text{C}$ - $^1\text{H}$  correlation (HSQC) spectra from cell wall gels in DMSO- $d_6$ /pyridine- $d_5$ . A) wild-type *Paxg* hybrid poplar, B) *AtGolS3* transgenic line 6, C) *AtGolS3* transgenic line 11.  $\beta$ -D-Glcp,  $\beta$ -D-glucopyranoside;  $\alpha$ -D-Manp,  $\alpha$ -D-mannopyranoside;  $\beta$ -D-Manp,  $\beta$ -D-mannopyranoside;  $\beta$ -D-Xylp,  $\beta$ -D-xylopyranoside;  $\alpha$ -L-Araf,  $\alpha$ -L-arabinofuranoside;  $\alpha$ -L-Rhap,  $\alpha$ -L-rhamnopyranoside; 2-O-Ac- $\beta$ -D-Xylp, acetylated  $\beta$ -D-Xylp; 3-O-Ac- $\beta$ -D-Xylp, acetylated  $\beta$ -D-Xylp; 4-O-MeGlcA, 4-O-methyl- $\alpha$ -D-glucuronic acid;  $\alpha$ -D-GalpA,  $\alpha$ -D-galacturonic acid. R, reducing end; NR, non-reducing end.

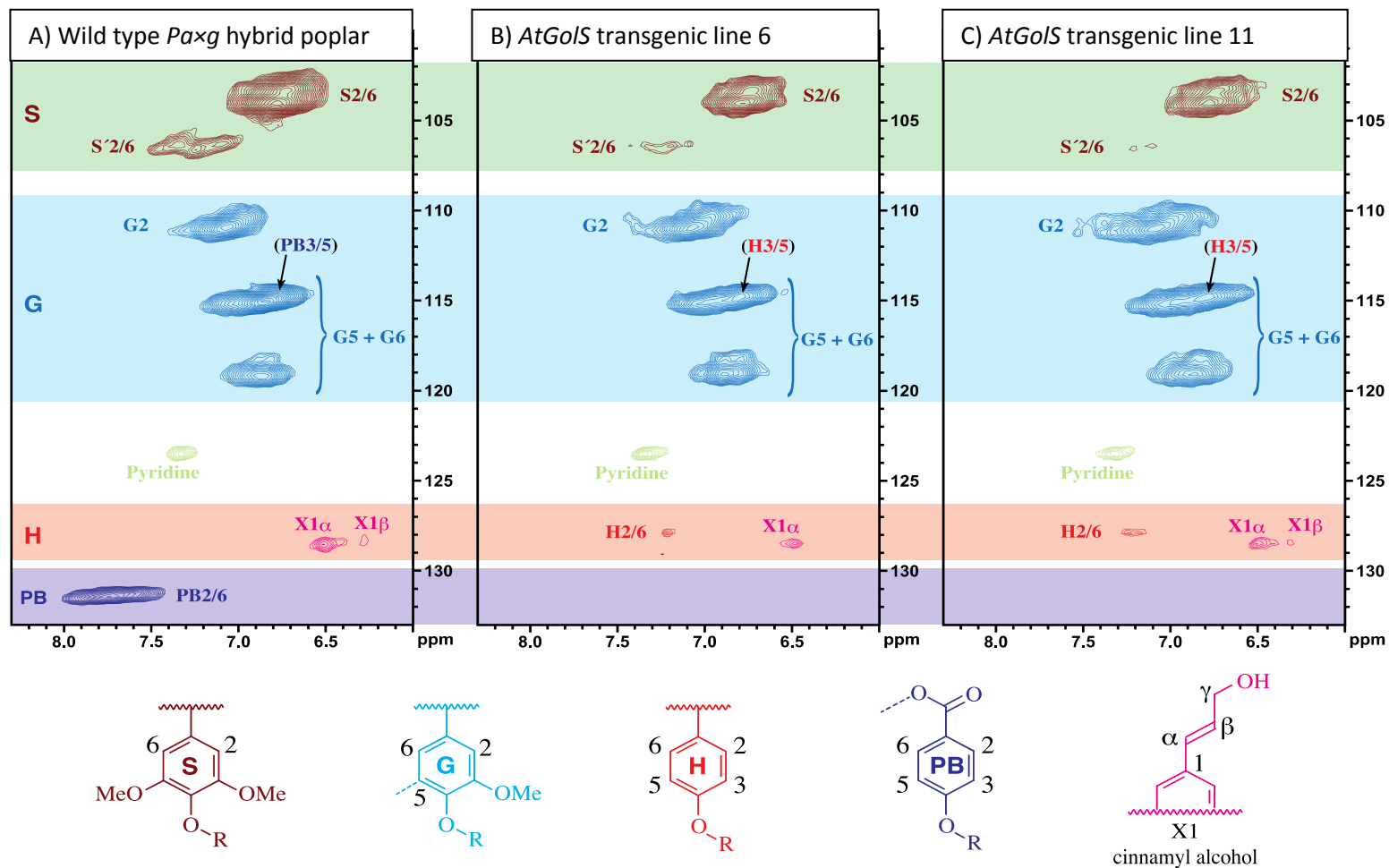
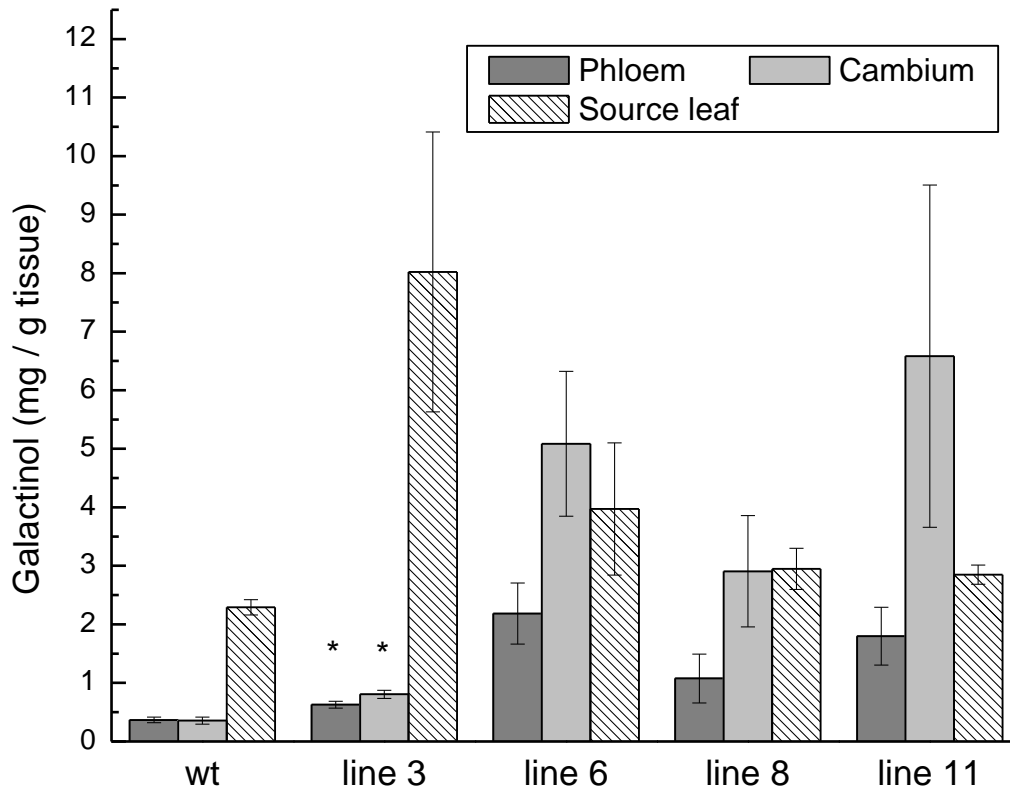


Figure 3.12 Aromatic regions of 2D  $^{13}\text{C}$ - $^1\text{H}$  correlation (HSQC) spectra from cell wall gels and soluble lignins from various samples in DMSO- $d_6$ /pyridine- $d_5$ . A) wild-type *Pa*×*g* hybrid poplar, B) *AtGoIS3* transgenic line 6, C) *AtGoIS3* transgenic line 11. Correlations from the aromatic rings are well dispersed and can be categorized by the type of aromatic units (syringyl S, guaiacyl G, p-hydroxyphenyl H, p-hydroxybenzoate PB; color coding is according to the structures shown).

<b>Lines</b>	<b>GalAc</b>
	<b>%</b>
<b>wt</b>	2.24 (0.39)
<b>line 3</b>	1.72 (0.15)
<b>line 6</b>	2.66 (0.09)
<b>line 8</b>	2.37 (0.47)
<b>line 11</b>	2.35 (0.25)

**Table 3.4 Galacturonic acid percentage of five-month old greenhouse-grown wild-type and *AtGalS3* transgenic trees. Values represent the mean and standard error of the mean in parenthesis (n=3).**



**Figure 3.13** The concentration of galactinol in selected tissues of five-month old greenhouse-grown wild-type and *AtGols3* transgenic hybrid poplar. Bars represent the standard error of the mean (n=3). Asterisks represent statistical difference from wild type (wt) at 95% level.

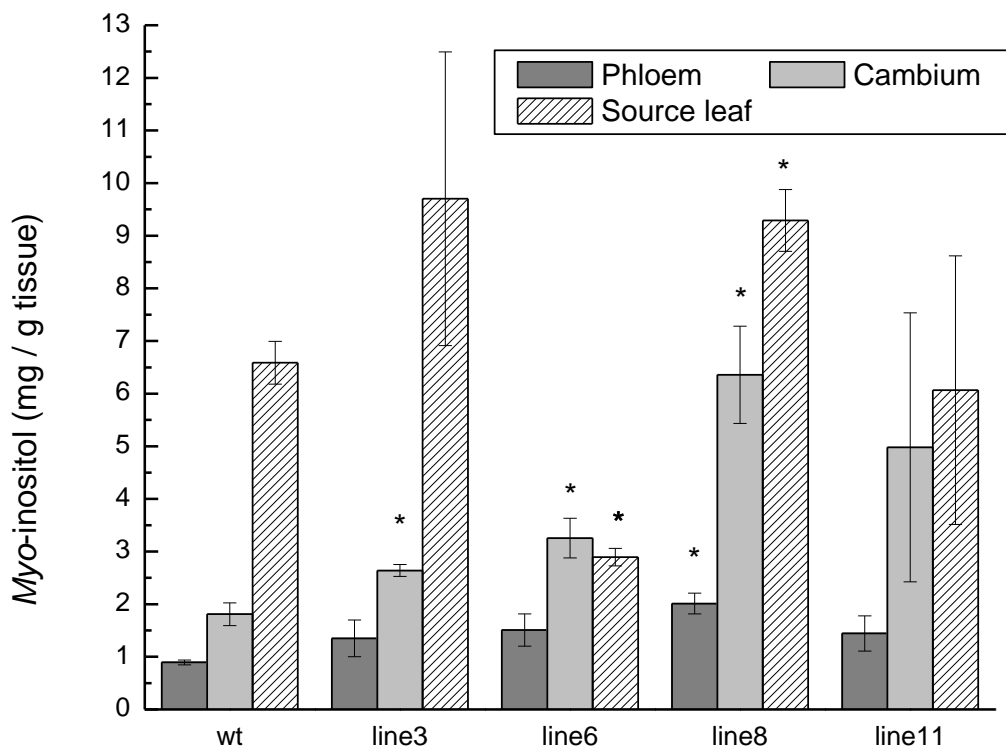
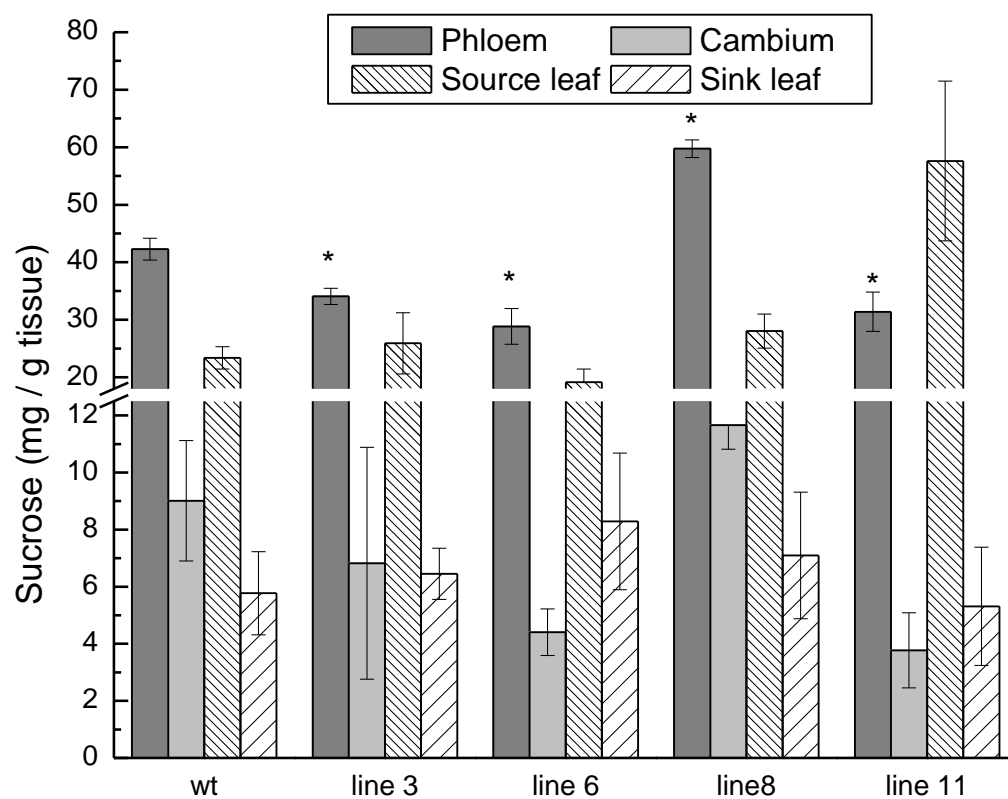
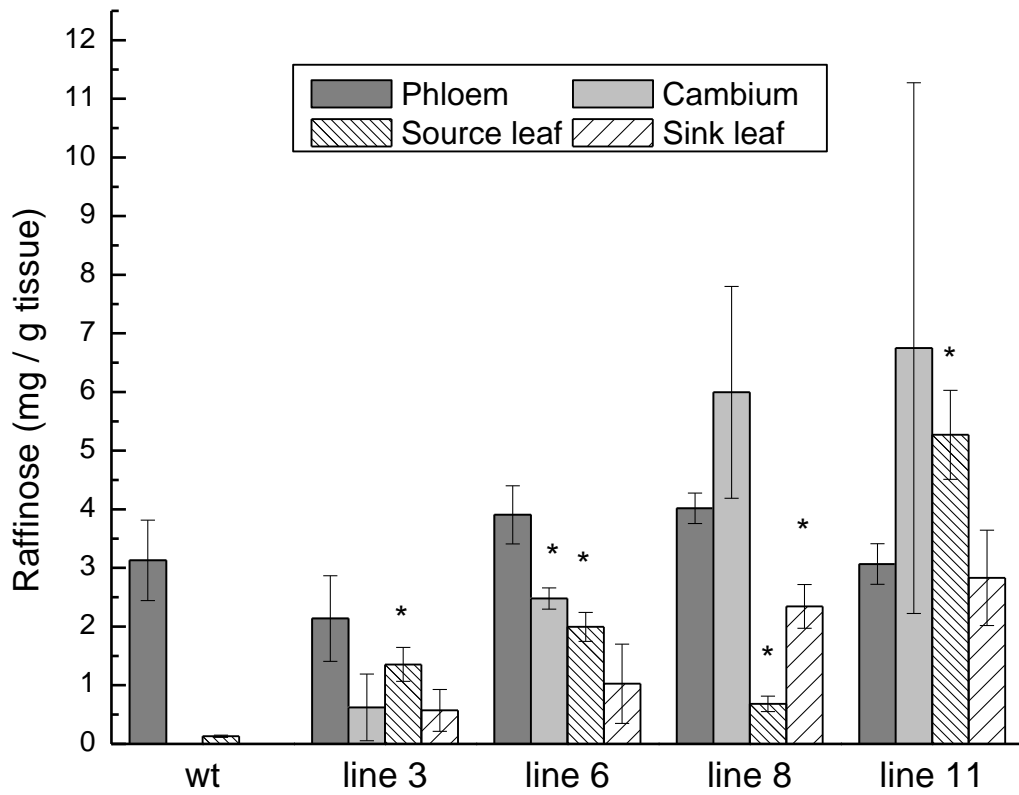


Figure 3.14 The concentration of *myo*-inositol in selected tissues of five-month old greenhouse-grown wild-type and *AtGols3* transgenic hybrid poplar. Bars represent the standard error of the mean (n=3). Asterisks represent statistical difference from wild type (wt) at 95% level.



**Figure 3.15** The concentration of sucrose in selected tissues of five-month old greenhouse-grown wild-type and *AtGols3* transgenic hybrid poplar. Bars represent the standard error of the mean (n=3). Asterisks represent statistical difference from wild type (wt) at 95% level.



**Figure 3.16** The concentration of raffinose in selected tissues of five-month old greenhouse-grown wild-type and *AtGols3* transgenic hybrid poplar. Bars represent the standard error of the mean (n=3). Asterisks represent statistical difference from wild type (wt) at 95% level.

Lines	Source leaf		Phloem		Sink leaf		Dev. xylem	
	%		%		%		%	
<b>wt</b>	9.03	(1.10)	5.65	(0.07)	7.06	(0.55)	2.88	(0.28)
<b>line 3</b>	4.67	(1.47)	5.73	(0.29)	5.79	(1.71)	3.41	(0.23)
<b>line 6</b>	6.16	(1.65)	12.96	(1.77)	5.30	(0.46)	<b>6.26</b>	<b>(0.96)</b>
<b>line 8</b>	6.90	(0.52)	<b>18.71</b>	<b>(0.19)</b>	<b>10.67</b>	<b>(0.54)</b>	4.68	(1.03)
<b>line 11</b>	6.30	(1.75)	10.67	(1.29)	6.81	(0.51)	1.88	(1.42)

**Table 3.5 Starch content % dry weight of five-month old wild-type and *AtGolS3* transgenic poplar trees. Values represent the mean and standard error of the mean in parenthesis with bold values corresponding to a statistical difference from wild type (wt) at 95% level (n=3).**

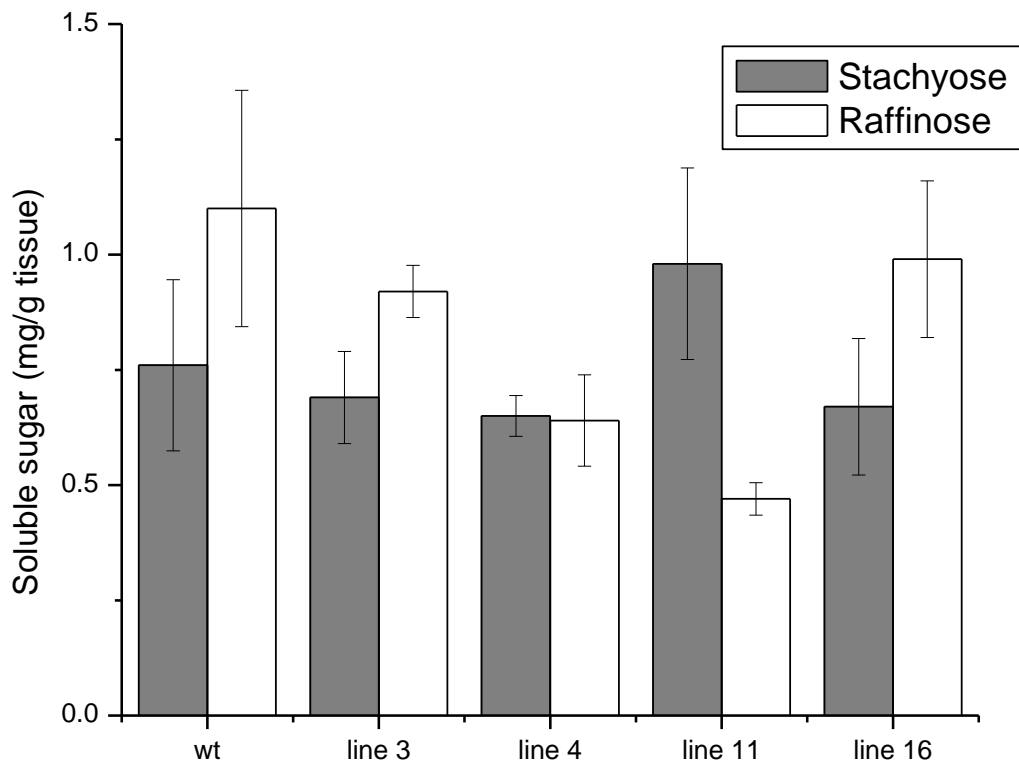


**Figure 3.17** The concentration of stachyose and raffinose in source leaf of six-month old greenhouse-grown wild-type and *GolSRNAi* transgenic hybrid poplar exposed to 2°C for 7 days. Bars represent the standard error of the mean (n=3).

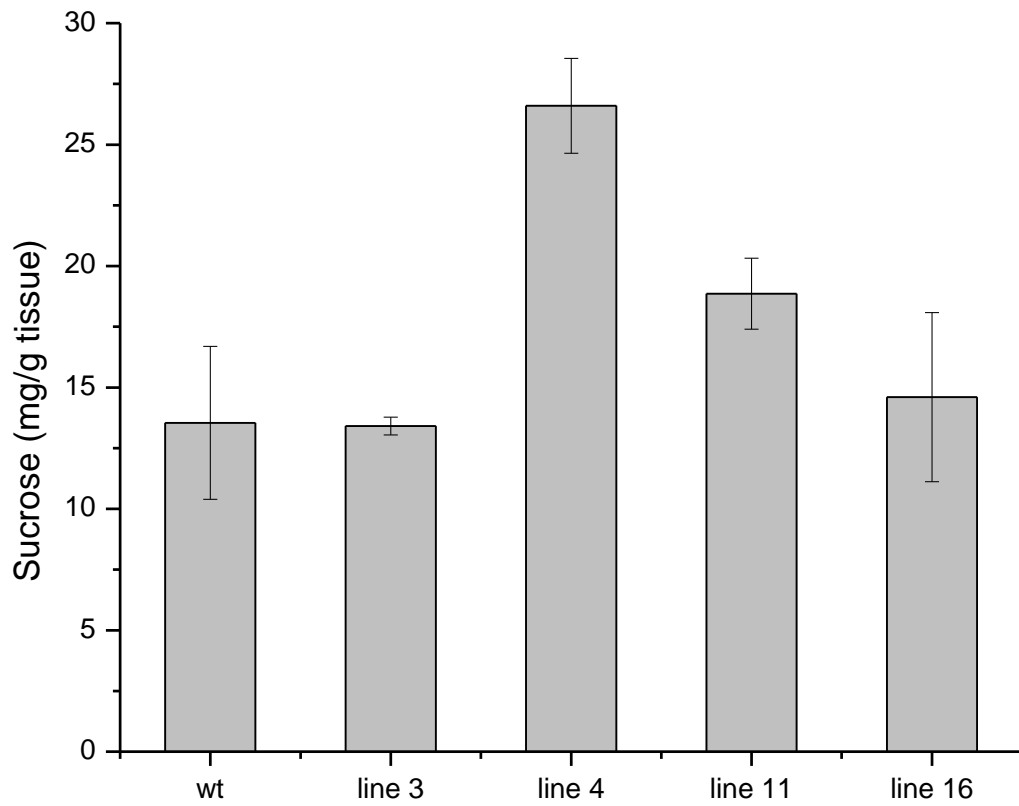


**Figure 3.18** The concentration of sucrose in source leaf of six-month old greenhouse-grown wild-type and *GolSRNAi* transgenic hybrid poplar exposed to 2°C for 7 days. Bars represent the standard error of the mean (n=3).

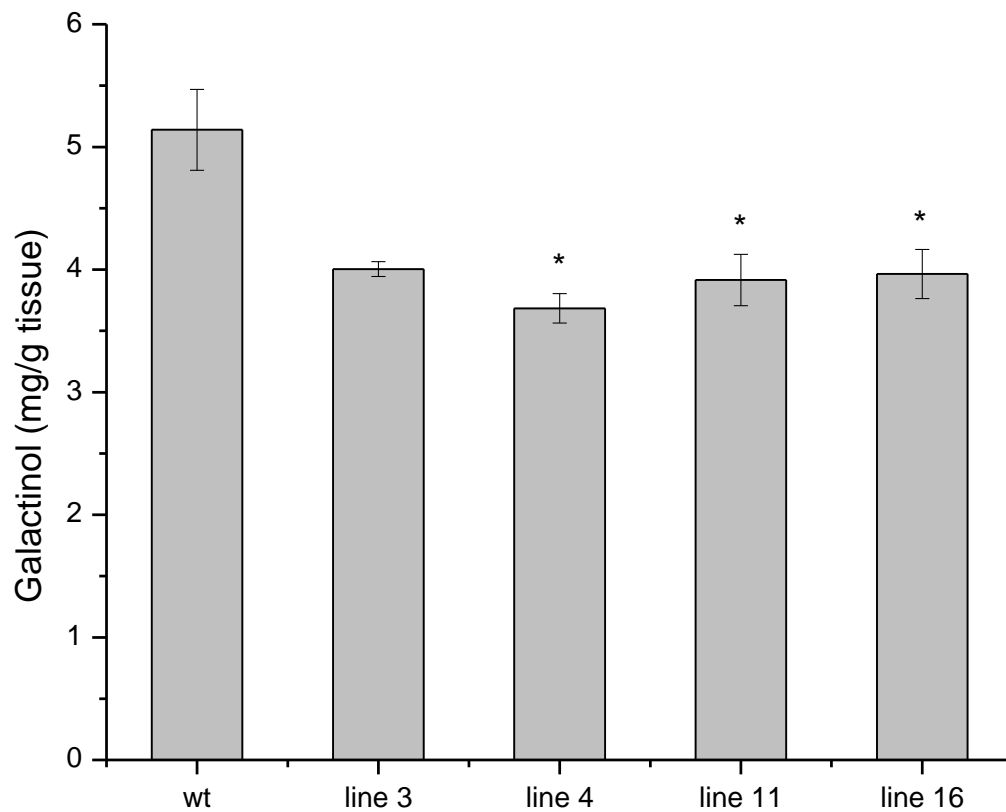


**Figure 3.19** The concentration of galactinol in source leaf of six-month old greenhouse-grown wild-type and *GoISRNAi* transgenic hybrid poplar exposed to 2°C for 7 days. Bars represent the standard error of the mean (n= 2-3). Asterisks represent statistical difference from wild type (wt) at 95% level.

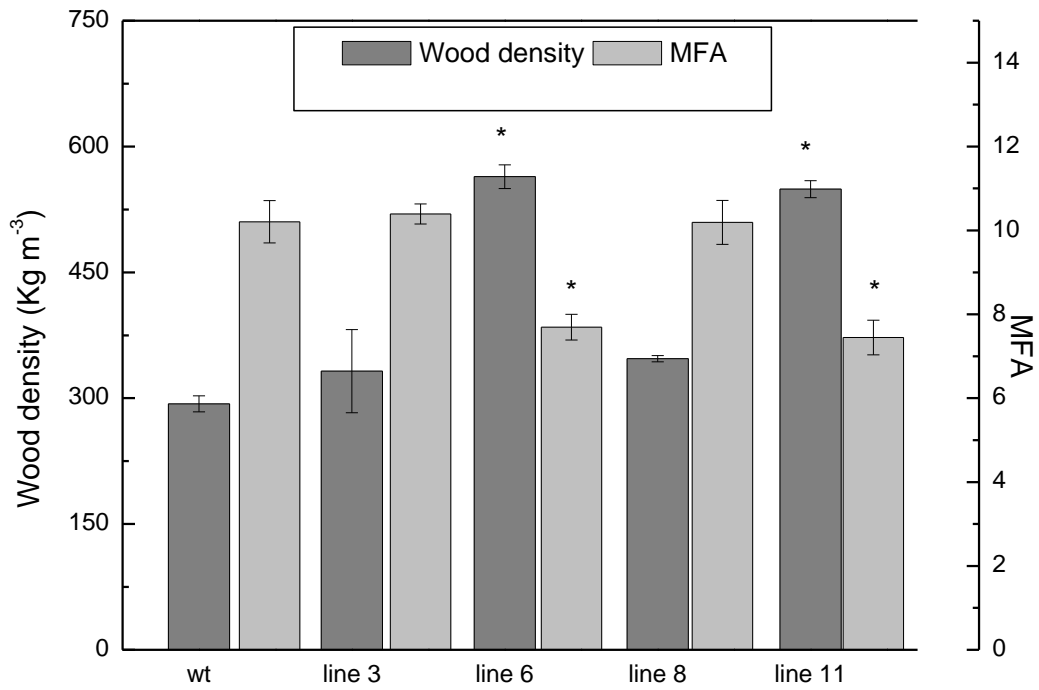


**Figure 3.20** Wood density and microfibre angle (MFA) of five-month old greenhouse-grown wild-type and *AtGols3* transgenic hybrid poplar. Bars represent the standard error of the mean (n=9). Asterisks represent statistical difference from wild type (wt) at 95% level.

<b>Lines</b>	<b>Crystallinity</b>	
	<b>%</b>	
<b>wt</b>	46.7	(1.2)
<b>line 3</b>	46.0	(1.5)
<b>line 6</b>	51.3	(3.4)
<b>line 8</b>	44.7	(0.9)
<b>line 11</b>	<b>55.0</b>	<b>(3.4)</b>

**Table 3.6 Crystallinity percentage of five-month old greenhouse-grown wild-type and *AtGolS3* transgenic hybrid poplar trees. Values represent the mean and standard error of the mean in parenthesis with bold values corresponding to a statistical difference from wild type (wt) at 95% level (n=3).**

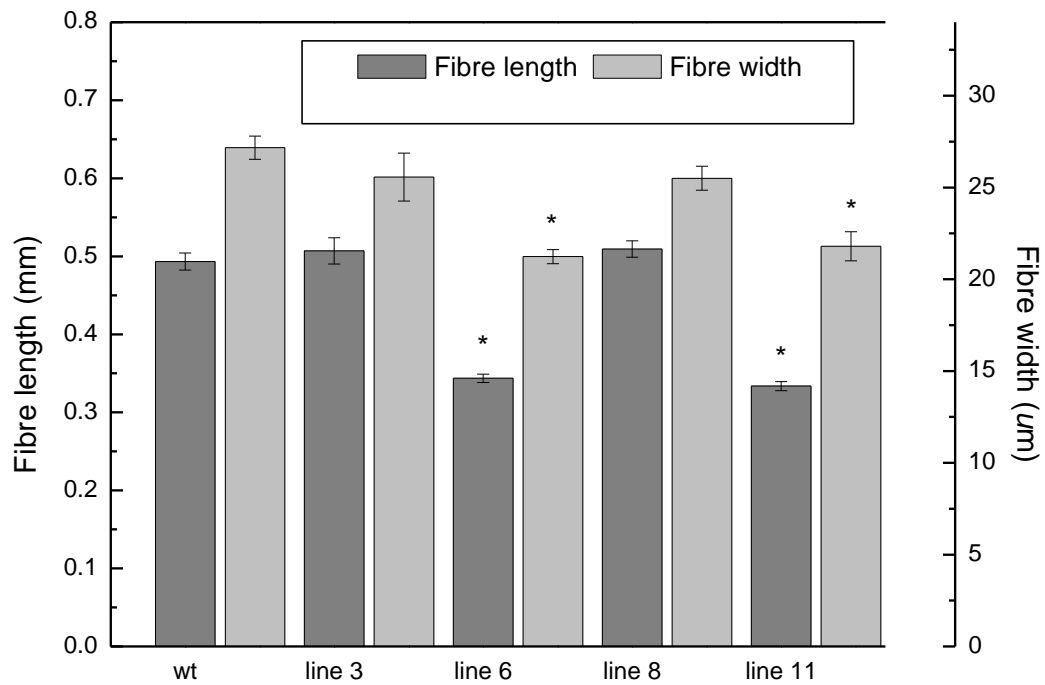


**Figure 3.21** Fibre length and width of five-month old greenhouse-grown wild-type and *AtGols3* transgenic hybrid poplar. Bars represent the standard error of the mean (n=3). Asterisks represent statistical difference from wild type (wt) at 95% level.

Line	N		P		Ca %		Mg		K		Cu		Zn		Fe ppm		Mn		B	
wt	2.98	(0.23)	0.30	(0.02)	1.08	(0.10)	0.22	(0.05)	1.30	(0.005)	7.00	(0.57)	80.00	(6.92)	204.3	(17.5)	120.00	(8.88)	73.00	(11.50)
line 6	<b>4.21</b>	<b>(0.06)</b>	<b>0.45</b>	<b>(0.02)</b>	0.77	(0.13)	0.13	(0.01)	<b>1.93</b>	<b>(0.14)</b>	<b>16.67</b>	<b>(1.33)</b>	73.00	(1.00)	151.0	(11.0)	<b>24.33</b>	<b>(1.20)</b>	<b>33.00</b>	<b>(1.00)</b>
line 8	3.35	(0.17)	0.30	(0.01)	0.95	(0.15)	0.16	(0.02)	1.26	(0.10)	7.33	(0.33)	65.00	(9.53)	163.6	(31.4)	<b>69.67</b>	<b>(9.49)</b>	69.67	(8.95)
line11	<b>4.31</b>	<b>(0.30)</b>	<b>0.54</b>	<b>(0.04)</b>	0.80	(0.07)	0.14	(0.003)	<b>2.86</b>	<b>(0.41)</b>	22.00	(5.85)	68.33	(7.17)	152.6	(20.1)	<b>19.67</b>	<b>(1.33)</b>	38.00	(6.35)

**Table 3.7 Leaf nutrient analysis of source leaves of five-month old wild-type and *AtGolS3* transgenic poplar trees. Values represent the mean and standard error of the mean in parenthesis with bold values corresponding to a statistical difference from wild type (wt) at 95% level (n=3).**

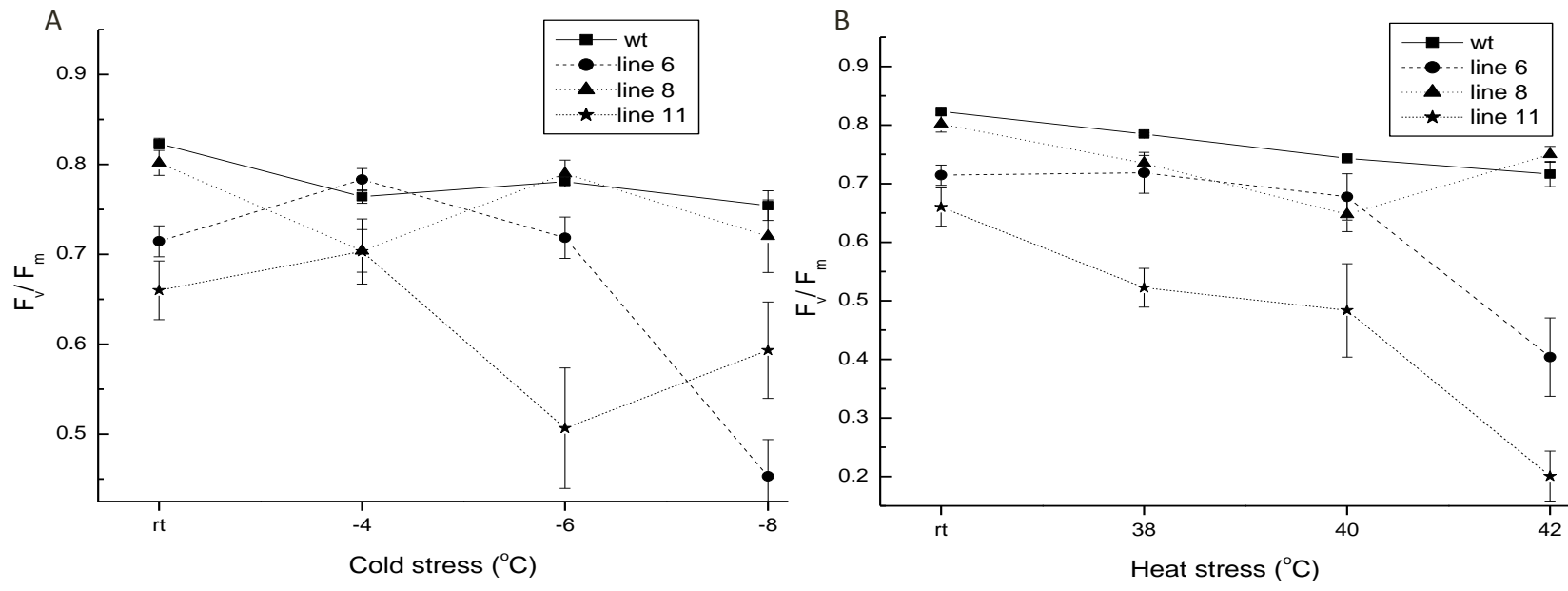


**Figure 3.22** The maximum quantum yield of PSII, as judged by  $F_v/F_m$  after stress treatment of leaf discs of *AtGols3* transgenic hybrid poplar and wild-type trees A) cold stress and B) heat stress. Bars represent the standard error of the mean (n=6).

## Chapter 4: **Over-expression of the *Cucumis sativus* raffinose synthase in hybrid poplar**

### **4.1 Introduction**

The raffinose family of oligosaccharides are almost universally found in plants and have been shown to accumulate extensively in a variety of seeds, where they have been ascribed three putative roles: acquisition of seed desiccation tolerance (Black *et al.*, 1996; Bailly *et al.*, 2001); regulating the longevity of seeds in the dry state (Koster, 1991; Buitink *et al.*, 1998); and providing a source of rapidly metabolizable carbohydrates during germination (Dirk *et al.*, 1999). Additionally, many functions have been specifically proposed for raffinose during abiotic stress. For example, raffinose has been suggested to act as a potential protectant of membranes during drying, which is a side effect of ice crystal formation in intercellular spaces (Hinch *et al.*, 2003). It has also been postulated that raffinose may act as a radical scavenger aiding in the detoxification of reactive oxygen species that are known to accumulate at low temperatures (Nishizawa *et al.*, 2008). Contrary to common thought, it has been suggested that raffinose is not essential for freeze tolerance in *Arabidopsis*; a conclusion that was drawn from results of work with a knockout mutant of the *RFS* gene, where the authors found no variation in the ability of mutant *Arabidopsis* plants to withstand freezing damage when compared to wild-type plants (Zuther *et al.*, 2004). In a more recent study, using the same *RFS* knockout mutant, Knaupp *et al.* (2011) revealed that the lack of raffinose does not affect electrolyte leakage from leaf cells; supporting the conclusion that raffinose may not be essential for protecting the plasma membrane. Nevertheless, *in situ* chlorophyll fluorescence indicated that that maximum quantum yield of PS II photochemistry of cold acclimated leaves in the *RFS* mutant was indeed

significantly affected, suggesting that raffinose is involved in stabilizing PS II against damage during freezing. Thus, the exact role of raffinose in abiotic stress remains inconclusive.

The biosynthesis of RFOs depends on the galactosyl transfer from a galactosyl donor to an acceptor, for instance, sucrose, raffinose or its higher homologues. Three types of galactosyl donors are involved in RFO metabolism: UDP-D-galactose, galactinol and the RFOs themselves. Raffinose synthase (EC 2.4.1.82) is the crucial enzyme that channels sucrose into the raffinose oligosaccharide pathway, which proceeds by the addition of a galactosyl unit to sucrose. The proposed dual role of raffinose synthase as a transglycosidase with some hydrolytic activity is in line with its classification as a family 36 glycoside hydrolase (Peterbauer *et al.*, 2002). However, its hydrolytic activity is probably of little physiological significance, because it is strongly inhibited by sucrose, which is usually present in high concentrations *in planta*. Raffinose can thereafter act as a substrate for the reversible synthesis of stachyose by the enzyme stachyose synthase where again a galactosyl unit is added to raffinose (Tanner & Kandler, 1968). To date, galactinol (*Gols*) and stachyose (*STS*) synthase have been fairly well characterized, and corresponding cDNA sequences have been cloned from several sources (Peterbauer & Richter, 2001). Alternatively, few studies have investigated the raffinose synthase families, likely because of the rapid turnover by the pathway. Raffinose synthase has, however, been purified from *Vicia faba* (Lehle & Tanner, 1973), and genes encoding other RFS have been reported in patents (Oosumi *et al.*, 1998; Watanabe & Oeda, 1998). Additionally, RFS from the leaves of *Ajuga reptans* was characterized from crude preparations (Bachmann *et al.*, 1994), and kinetic properties of pea RFS were reported from partially purified enzyme (Peterbauer *et al.*, 2002). Transgenic potato plants with constitutive or companion cell specific over-expression of the *Cucumis sativus Gols* or *Gols* plus *RFS* were studied to provide a better understanding of the

metabolism and transport of RFOs in plants (Hannah *et al.*, 2006). The transgenic potatoes were unable to transport large amounts of raffinose regardless of the elevated *RFS* expression and substrate concentration, which implies that there are additional features of the intermediary cells (cells in RFO transporting plants) required for synthesis and transport of RFOs.

In the present study, we report on the over-expression of *Cucumis sativus* raffinose synthase (*CsRFS*) in transgenic hybrid poplar trees (*Populus alba* × *grandidentata*). Transcription abundance of the *RFS* transgene increased significantly in all tissues analyzed, and the effect of the raffinose synthase over-expression on biomass, soluble and structural carbohydrate content, and the wood properties are reported herein.

## **4.2 Materials and methods**

### **4.2.1 Plasmid construction**

The *Cucumis sativus RFS* (AF073744) was cloned from leaf cDNA of greenhouse-grown cucumber plants using the following primers: *CsRFS2Fw* 5'-TTCTTCTCACAAATGGCTCCTAGTT-3' and *CsRFS2Rv* 5'-CAACAGCGACAACAACAATCATT-3'.

The raffinose synthase transformation vector was constructed by ligating the cloned *CsRFS* gene into the pSM3 vector (pCambia 1390 with double 35S promoter, Mansfield Lab, UBC) using the *BamHI* and *SacI* restriction enzymes. The vector was confirmed by genomic sequencing for correct frame and orientation, and then transformed into *Agrobacterium tumefaciens* (EHA-105 strain). This binary vector and *Agrobacterium* strain was then used for poplar transformation.

### **4.2.2 Hybrid poplar transformations**

*Populus alba* × *grandidentata* (P39) leaf discs were harvested from four week-old tissue culture-grown plants using a cork borer. Twenty plates containing 25 leaf discs (7 mm<sup>2</sup>) per genotype were co-cultivated with 30 ml of *Agrobacterium* culture in 50 ml Falcon tubes for 30 min at 28°

C in a gyratory shaker (100 rpm). Following co-cultivation, the explants were blotted dry on sterile filter paper and placed abaxially on WPM 0.1 NAA, 0.1 BA and 0.1 TDZ culture medium. The plates were cultured in the dark for two days at room temperature. On the third day, residual *Agrobacterium* culture was killed by transferring the leaf discs to WPM media supplemented with 250 mg l<sup>-1</sup> cefotaxime and 500 mg l<sup>-1</sup> carbenicillin. All plates were kept in the dark for an additional two days. Following this period, the explants were transferred to WPM selection media supplemented with 250 mg l<sup>-1</sup> cefotaxime, 500 mg l<sup>-1</sup> carbenicillin and 25 mg l<sup>-1</sup> hygromycin. After emergence, only one shoot per leaf disc was excised and placed on WPM selection media. After 6 weeks growth, explants were transferred to fresh medium with the same composition, and permitted to develop. Plants were confirmed as being transgenic by genomic DNA screening, and those identified as positive were then sub-cultured and multiplied on antibiotic-free WPM media.

#### **4.2.3 Plant growth**

Transgenic plants were multiplied on WPM media until approximately eight plants of each transgenic event (line), displaying the same size, were available. The plants were then moved from the tissue culture lab to the greenhouse and transplanted into 2 gallon pots containing perennial soil (50% peat, 25% fine bark and 25% pumice; pH 6.0). The trees were then maintained on flood tables with supplemental lighting (16 h days) and fertigated daily in the UBC greenhouse, Vancouver, BC. After five months plants were harvested using liquid N and kept in -80°C until used.

#### **4.2.4 Tissue collection**

Source leaf was collected using the leaf plastochron index (PI=5). Where PI=0 was defined as the first leaf greater than 5 cm in length and where PI=1 is the leaf immediately below PI=0.

Sink leaves are the smallest and not fully expanded leaves. Phloem tissue included the bark, phloem tissue and cambium cells. Developing xylem corresponded to slight scrapings of the stem.

#### **4.2.5 Molecular analysis**

##### **4.2.5.1 Genomic DNA extraction**

The CTAB DNA (Sigma-Aldrich Co.) extraction method was used to isolate DNA from hybrid poplar tissues. In short, the tissue was frozen with liquid N<sub>2</sub> and ground into powder with 1 ml extraction buffer (2% w/v CTAB, 1.4 M NaCl, 20 mM EDTA, 100 mM Tris-HCl, 1% PVP, and 0.2% v/v β-mercaptoethanol). The DNA concentration was measured with a ND1000 spectrophotometer (NanoDrop Technologies, Inc. DE, USA), and stored at -20° C until use.

##### **4.2.5.2 RNA isolation**

The RNA was isolated as per (Kolosova *et al.*, 2004), using source and sink leaves, phloem, and developing xylem tissue. The RNA concentration was measured using the ND1000 spectrophotometer. DNase I DIGEST kit (Ambion Inc.) was used to eliminate DNA contamination. RNA treated with DNase was quantified, and 1 µg was used to generate cDNA using the iScript™ cDNA Synthesis Kit (Bio-Rad Laboratories, CA, USA) as per the manufacturer's instructions. The resulting cDNA was stored at -20° C.

##### **4.2.5.3 PCR analysis of putative transformants**

Hybrid poplar plants that survived antibiotic selection were evaluated for the presence of the transgene. Successful transformation was demonstrated by PCR screening of genomic DNA using gene specific primers *HygFw* 5'-GGCAAACCTGTGATGGACGAC-3' and *HygRv* 5'-GCTGGGGCGTCGGTTTCC-3' targeting the hygromycin B phosphotransferase (hph) gene coding for hygromycin resistance.

#### 4.2.5.4 Real Time- RT PCR

Real Time RT-PCR reactions consisted of 10 µl of SsoFast Eva Green<sup>®</sup> Supermix (Bio-Rad Laboratories), 20 pmol of *CsRFSrtFw* 5'-TTTGGCATGCTTTGTGTGGATA-3' and *CsRFSrtRv* 5'-CAAAATCCTCCATCGTCATCT-3', 1µl of cDNA, and water to a total volume of 20 µl. RT-PCR was performed on a CFX 96 Real Time PCR System<sup>®</sup> (Bio-Rad Laboratories). The following thermal cycler conditions was used to amplify the 120 bp fragment of the *CsRFS* transcript: 1 cycle of 30 sec at 95° C, 39 cycles of 95° C for 5 seconds, and 58° C for 30 sec, followed by 1 cycle of 95° C for 30 sec, and a melt curve cycle of 58° C to 95° C increment of 0.5 ° C for 5 sec. Relative expression was calculated using the following equation  $\Delta ct = 2^{-(ct_{\text{target gene}} - ct_{\text{TIF5A}})}$ , where *TIF5A* is used as the reference gene (Coleman *et al.*, 2009).

#### 4.2.6 Phylogenetic analysis

Amino acid sequences obtained from GenBank and Phytozome were used for multiple sequence alignment employing the program MAFFT (<http://www.ebi.ac.uk/>). The evolutionary history was inferred using the Neighbor-Joining method (Saitou & Nei, 1987). The optimal tree with the sum of branch length = 5.18 is shown. The percentages of replicate trees in which the associated taxa clustered together in the bootstrap test (1000 replicates) are shown next to the branches (Felsenstein, 1985). The tree is drawn to scale, with branch lengths in the same units as those of the evolutionary distances used to infer the phylogenetic tree. The evolutionary distances were computed using the Poisson correction method (Zuckerka & Pauling, 1965), and are in the units of the number of amino acid substitutions per site. The analysis involved 32 amino acid sequences, and all positions containing gaps and missing data were eliminated. There were a total of 635 positions in the final dataset. Evolutionary analyses were conducted in MEGA5 (Tamura *et al.*, 2011). Amino acid percentage similarity was calculated in ClustalW.

Visualization of the alignment file to identify the conserved motifs (KxD and RxxxD) was run in MEGA.

#### **4.2.7 Phenotypic analyses**

##### **4.2.7.1 Growth measurements**

After six months of growth in the greenhouse, tree height was measured as the length from the root collar to the apex of the tree, while stem diameter was measured using digital calipers at 10 cm above the root collar.

##### **4.2.7.2 Structural chemistry analysis**

Dried wood samples from six months old greenhouse-grown trees were used to determine lignin and carbohydrate content following a modified Klason method (Cullis *et al.*, 2004). Samples were ground in a Wiley mill to pass a 40-mesh screen, extracted overnight with hot acetone using a Soxhlet, and then dried for 24 h at 105°C. Approximately 200 mg of dried extractive-free tissue was treated with 72% sulphuric acid for 2 h, diluted to 4% with deionized distilled water and autoclaved at 121°C for 60 min. The reaction was filtered through a medium coarseness crucible and the retentate collected and dried at 105°C to determine the acid-insoluble lignin gravimetrically. The acid-soluble lignin was estimated from the filtrate using an UV spectrophotometer at 205 nm.

Carbohydrate contents were determined by HPLC analysis of the same filtrate. Glucose, xylose, mannose, galactose, arabinose and rhamnose were analyzed using a Dx-600 anion-exchange HPLC (Dionex, Sunnyvale, CA, USA) fitted with a CarboPac PA1 column (Dionex) and eluted with water at 1 ml min<sup>-1</sup>. Detection was achieved with a pulsed amperometric detector with post-column addition of 200 mM NaOH at 0.5 ml min<sup>-1</sup>. Sugar concentrations were

calculated from standard curves created from external standards. Normalizations of the calculations were done using fucose as internal standard.

#### **4.2.7.3 Wood density determination**

Wood density was measured on a QDP-01X density profiler (QMS; Quntek Measurement System Inc. Knoxville, TN, USA) using 1.68 mm precision cut samples that were Soxhlet extracted with hot acetone overnight, and allowed to acclimate to 7% moisture before the analysis. Density was measured on both sides of the pith and averaged for each sample.

#### **4.2.7.4 Soluble sugar analysis**

Liquid nitrogen frozen phloem, developing xylem, source and sink leaf tissues were ground using a mortar and pestle in the presence of excess liquid nitrogen. Subsequently, the tissue was lyophilized for 24 h, weighed and treated with 4 ml of methanol:chloroform:water (M:C:W; 12:5:3) solution overnight at 4°C. The solution was centrifuged at  $2770 \times g$  for 10 min and the supernatant collected. The pellet was then washed twice with 4 ml of the same solution and supernatant was pooled (12 ml). The pellet was dried and kept for starch analysis. Water (5 ml) was added to the pooled supernatant, mixed thoroughly and centrifuged at  $2770 \times g$  for 5 min, which facilitated phase separation. An aliquot (1 ml) of the upper phase was collected and dried using a vacuum centrifuge. The pellet was re-suspended in 1 ml of water and analyzed for stachyose, raffinose sucrose, galactinol, *myo*-inositol, glucose, and fructose content using a HPLC fit with a Rezex RPM column (Phenomenex, CA, USA). Fucose or galactitol were added as internal standards.

#### **4.2.7.5 Starch analysis**

The pellet remaining from the soluble sugar analysis was dried overnight in a 50°C oven, weighed and incubated with 4% sulfuric acid, autoclaved at 121°C for 3.5 min, cooled and

centrifuged at  $20 \times g$  for 5 min. An aliquot of the supernatant was then analyzed using a Dx-600 anion-exchange HPLC (Dionex) to determine glucose release, which represents the starch that was hydrolyzed by the acid treatment. Fucose was added as internal standard.

## 4.3 Results

### 4.3.1 Phylogenetic analysis

The program MAFFT was used to align the putative sequences of 14 raffinose synthases (RFS) from *P. trichocarpa*, 5 RFS from *A. thaliana*, 2 RFS from *C. sativus*, *E. grandis*, and *P. vulgaris*, and a single RFS from *P. sativum*, *G. max*, *M. esculenta*, *B. hygrometrica*, *M. trunculata* and *O. sativa*. In order to root the tree with a distant sequence, the RFSs were BLAST against the *S. moellendorffii* genome. The best hit (XP\_002961660.1, with an e-value  $1.e^{-99}$ ) was then used to root the tree. A bootstrap value of 70 was used to define clades (Figure 4.1).

An alignment of all the RFS sequences revealed the presence of two common motifs (KxD and RxxxD) that are conserved in all members of the glycosyl hydrolase clan (GH-D). More specifically, in the case of all *P. trichocarpa* raffinose synthases the conserved motif was KVD, and five main clades were identified in the phylogenetic tree. The first clade has four PtRFS (POPTR\_0017s06440.1, POPTR\_0007s02450.1, POPTR\_0004s21770.1, and POPTR\_0015s09330.1), the first two sharing 88% similarity and suggesting that they may correspond to the genome duplication event (Tuskan *et al.*, 2006). The remaining two sequences shared similarities ranging between 72 to 85%. Additionally, this group has two *C. sativus* RFS with 99% similarity, as well as other raffinose synthases from various species, including: AtRFS5 (AT5G40390.1), *P. vulgaris* (ACZ74660.1), *B. hygrometrica* (AEP68101), *P. sativum* (CAD20127.2) and *G. max* (Glyma05G02510.1) that were placed in this group, but have rather low bootstrap values. The *O. sativa* RFS was also placed in this clade, and was shown to be more

similar to the POPTR\_0015s09330.1 than to any other RFS in the clade, with 64% similarity at the amino acid level.

The second clade is formed by two *P. trichocarpa* proteins with 88% similarity (POPTR\_0002s19450.1 and POPTR\_0014s11370.1), and two *E. grandis* RFS (71% similarity). Also, the raffinose synthases from *M. esculenta*, *P. vulgaris* (Phvul091000173), *M. truncatula* and AtRFS4 (AT4G01970.1) are part of this group. POPTR\_0015s09800.1 and POPTR\_0016s00410.1 form the third group; however, they only shared 58% similarity. The fourth clade is formed by three poplar raffinose synthases. Two of these sequences correspond to the same gene (POPTR\_0006s06460.1 and POPTR\_0006s06460.2) which is a duplicated gene, and the remaining PtRFS (POPTR\_0018s12670.1) shares 90% similarity. Additionally, AtRFS6 (AT5G20250) belongs to this group. The last clade is formed by three *P. trichocarpa* RFS, which show 92% similarity between two of the raffinose synthases (POPTR\_006s05130.1 and POPTR\_0016s05500), and two *A. thaliana* raffinose synthases, corresponding to AtRFS2 (AT3G57520.1) and AtRFS1 (AT1G55740.1), which share 60% similarity.

#### **4.3.2 Generation of transgenic poplar trees**

The full length coding sequence of the *Cucumis sativus* raffinose synthase was cloned and inserted into the binary vector pSM-3. *Agrobacterium*-mediated transformations yielded multiple *CsRFS* transformants that were verified through genomic screening. After several weeks of growth, RNA was isolated; cDNA generated using reverse transcriptase, and transcript abundance determined by Real Time RT-PCR. The five transgenic lines displaying the highest transcript abundance were transferred to antibiotic free-media and multiplied to obtain at least eight clonal trees per transgenic line.

The *CsRFS* transgenic plants were then transferred to the UBC greenhouse (August 2010), and after six months of growth the height and diameter of the stem were recorded and used for calculations of biomass. Relative expression analysis using Real Time RT-PCR was again checked on the greenhouse-grown plants. Transcripts were clearly detected in all five transgenic lines, but not in wild-type trees (Figure 4.2), as expected. The transcript level of the exogenous *CsRFS* was higher in leaf tissues in all lines when compared to the corresponding vascular tissue from the same plants. Of the tissues surveyed for transgene expression, the developing xylem tissue showed the least amount of the transgene abundance.

#### **4.3.3 Soluble sugar and starch analyses**

Soluble carbohydrates were analyzed in several tissues, including developing xylem, phloem, source and sink leaves. As expected, raffinose concentrations increased in all transgenic lines compared to wild type in all tissues; the incremental change was greatest in the phloem (Figure 4.3). Comparatively, sucrose was reduced in the phloem tissue of most transgenic lines, and more significantly in lines 9 and 13 compared to wild type (Figure 4.4). These biochemical findings are consistent with the transgene transcript profiling, which showed that line 13 had the highest expression in leaf. However, in leaf tissue, sucrose content was higher than in wild type. In addition, glucose was reduced in the phloem and developing xylem of all transgenic lines compared to wild type, and was more significant in lines 7, 8, 9 and 13 in the phloem tissue (Figure 4.5). Fructose was also reduced in vascular tissues of transgenic lines compared to wild-type trees (Figure 4.6).

Starch content was measured in the *CsRFS* transgenic hybrid poplar as hydrolyzed glucose liberated from the soluble carbohydrate extracted tissue pellet (Table 4.1). In source leaves the starch content was increased in all transgenic lines, with line 8 having a significantly

higher value, showing a greater than 3-fold increase in leaf starch content. On the other hand, no significant differences were found in starch content of phloem tissue.

#### **4.3.4 Carbohydrate and lignin analysis**

The structural chemistry of the stem was analyzed to explore the effects of transgene expression on xylem traits. The wild-type trees showed typical cell wall composition, with approximately 20% of the sugars being derived from hemicellulose associated carbohydrates (arabinose + rhamnose + galactose + xylose + mannose), and ~41% from glucose (largely cellulose), and ~22% total lignin (specifics in Table 4.2). Both the total lignin content and xylose moieties were slightly reduced in the transgenic plants, while the total amount of glucose was commensurately increased in the transgenic trees, ranging from a ~1 - 4% increase. In general, the other cell wall carbohydrates did not vary significantly from those of the wild-type trees (Table 4.2).

#### **4.3.5 Total biomass**

Total tree biomass was calculated using the volume of the stem ( $1/3 \pi r^2 h$ ) which was derived from the height and diameter estimates of individual trees, and the wood density determined by X-Ray densitometry (Table 4.3). Although no statistical differences were found for total biomass, all transgenic lines had an increase in total biomass compared to the wild-type trees. Among the transgenic lines, line 7 had substantially higher wood density ( $410.4 \text{ Kg m}^{-3}$ ) compared to wild type ( $367.4 \text{ Kg m}^{-3}$ ), while lines 8 and 9 had marginally increased wood densities showing averages of  $376.5$  and  $390.1 \text{ Kg m}^{-3}$ , respectively (Figure 4.7).

However, when combining the total biomass with the cell wall chemical analysis, it was apparent that total cellulose content was higher in *CsRFS* transgenic lines compared to wild-type trees (Table 4.3). Lines 2 and 7 showed statistically significant higher cellulose content with 19

and 20% more when compared to wild type. Other transgenic lines had also considerably higher quantities of cellulose, ranging between 11-19%.

## **4.4 Discussion**

### **4.4.1 Phylogenetic analysis**

Although few studies have reported on the characterization of raffinose synthase genes in the literature, the amino acid sequences for several putative RFS have been placed in NCBI and Phytozome, which facilitated the extensive phylogenetic analysis. The presence of two motifs, KxD and RxxxD, conserved in all members of the glycosyl hydrolase clan GH-D (Garman *et al.*, 2002; Fujimoto *et al.*, 2003; Lee *et al.*, 2004) was found in all the RFS proteins used in the comparative analysis. The aspartic acid residue in the KxD motif is thought to be the catalytic nucleophile used to generate a covalent glycosyl-enzyme intermediate in  $\alpha$ -galactosidases of family 27 (Hart *et al.*, 2000; Ly *et al.*, 2000). Conversely, the Asp residue in the RxxxD motif is thought to act as a catalytic acid-base that facilitates the actual hydrolysis of the carbohydrate by removing or adding a proton.

Of the limited raffinose synthases that have been described in the literature, two *A. thaliana* RFS corresponding to AtRFS2 (AT3G57520.1) and AtRFS1 (AT1G55740.1) that share 60% similarity, have been well characterized. For example, the transcript abundance of *AtRFS2* has been shown to be highly induced by the over-expression of the heat shock transcription factor A2 (*HsfA2*) (Nishizawa *et al.*, 2008). In the same study, the expression of *HsfA2*, *GolS1*, 2, 3, 4, and 8, and *RFS2*, 4, 5, and 6 was shown to be induced in wild-type plants exposed to oxidative stress and manifested in increased levels of galactinol and raffinose. The 14 putative raffinose synthases from *Populus* are distributed in five different clades; most of them are positioned in pairs following the pattern of genome duplication (Tuskan *et al.*, 2006). The *Pisum*

*sativum* RFS shared 67% similarity with the *Glycine max* RFS, and has been expressed in insect cells (Peterbauer *et al.*, 2002). The recombinant enzyme, a protein of glycoside hydrolase family 36, displayed similar kinetic properties to raffinose synthase partially purified from maturing seeds. Furthermore, steady-state kinetic analyses suggested that the recombinant raffinose synthase is a transglycosidase operating by a “ping-pong” reaction mechanism, and may also act as a glycoside hydrolase. The *Oryza sativa* RFS, which has 64% similarity with the *Populus* RFS (POPTR\_0015s09330.1), share similar enzymatic characteristics, including pH dependence, inhibition, and kinetic properties, to the ones reported for PsRFS (Peterbauer *et al.*, 2002).

#### **4.4.2 Structural carbohydrates and soluble sugars**

The *CsRFS* transgenic hybrid poplar trees had increased raffinose concentrations in all tissues analyzed when compared to wild-type plants. However, the raffinose content was higher in the phloem than in leaf tissue. This observation is in agreement with the hypothesis that raffinose is more effectively retained within the phloem than galactinol leading to higher transport efficiency (Ayre *et al.*, 2003). Commensurately, the amount of sucrose, glucose and fructose was slightly reduced in the phloem of most of the transgenic lines. Interestingly, the content of these sugars increases in leaf tissues, which we believe represents a homeostatic response. Briefly, it is possible that poplar trees sense a “pull” on the soluble sucrose pools in sink tissues as raffinose synthesis is elevated by the over-expression of the transgene, and in response increases the synthesis of sucrose in the source leaves. Basically, plants must achieve a balance between carbon assimilation, storage and growth, however little is known about how these mechanisms are regulated and controlled (Smith & Stitt, 2007). It is known that the direct products of photosynthetic carbon assimilation in the light are partitioned between sucrose, immediately available for growth, and starch which accumulates in the leaf through the day (Caspar *et al.*,

1985; Gibon *et al.*, 2004; Lu *et al.*, 2005). In our study, the increasing pools of sucrose in the source leaves of *CsRFS* transgenic trees resulted in an accumulation of leaf starch, which is in line with the proposed theory that the transgenic trees are responding to the depletion of sucrose in sink tissue.

Based on the soluble sugar profile of the phloem tissue, sucrose appears to be the major transport sugar in *Populus*. However, it is apparent that a small amount of raffinose was also present in phloem tissue of wild-type trees. Similar results have been shown in other angiosperm tree species, for example the phloem sap of *E. globulus* has been shown to be dominated by sucrose and raffinose (Pate & Arthur, 2000; Tausz *et al.*, 2008; Merchant *et al.*, 2010) suggesting that, at least in part, a symplastic loading mechanism is employed (Turgeon, 1996). Temperate tree species can exhibit high degrees of symplastic, plasmodesmatal connectivity between phloem companion cells and the mesophyll (Gamalei, 1989; Rennie & Turgeon, 2009). Rennie & Turgeon (2009) presented data that indicated that a large number of woody species load solutes passively by maintaining high concentrations of sucrose, and in some cases sugar alcohols, in mesophyll cells. The symplastic mechanism could be either active (polymer trapping) or passive (Turgeon, 2010). Additionally, plasmodesmata can provide an uninterrupted and relatively unrestricted pathway to replenish the companion cells and provide nutrients for sink tissues.

Interestingly, altering carbon partitioning, by increasing the demand on the sucrose in sink tissue by over-expressing an exogenous raffinose synthase gene, resulted in an increase in the total biomass of the transgenic lines compared to wild-type trees. Specifically, it seems that the overall increase in biomass is related to an increase in wood density in the transgenic lines. Additionally, the total cellulose content of all transgenic lines was higher than its corresponding

wild-type trees. The elevated concentration of soluble sugars found in leaf tissue appears to provide increased substrate for polymeric carbohydrate synthesis in the form of starch and cellulose, and consequently produce changes in the overall cell wall composition of the stem. Ultimately, when considering the biomass increases, transformations resulted in overall yields of as much 20% increases in the total cellulose content. Taken together, these results suggest that changes in the composition of the sugars loaded in the phloem by the over-expression of *RFS* can affect the source to sink relationship, and consequently the tree growth and xylem development. Remarkably, in chapter three the over-expression of the galactinol synthase gene in hybrid poplar, with its corresponding increase of galactinol, resulted in the alteration of wood formation, which we hypothesize happens as a consequence of galactinol serving as a signalling molecule culminating in global stress response that ends in the formation of what appears to be tension wood. In this study, increasing the raffinose content in hybrid poplar via the over-expression of a raffinose synthase gene did not have the same effect. These results support the hypothesis that the signal molecule for stress may be galactinol and not raffinose. Further research with the *RFS-OE* lines will be necessary to evaluate the role of this enzyme under stress conditions.

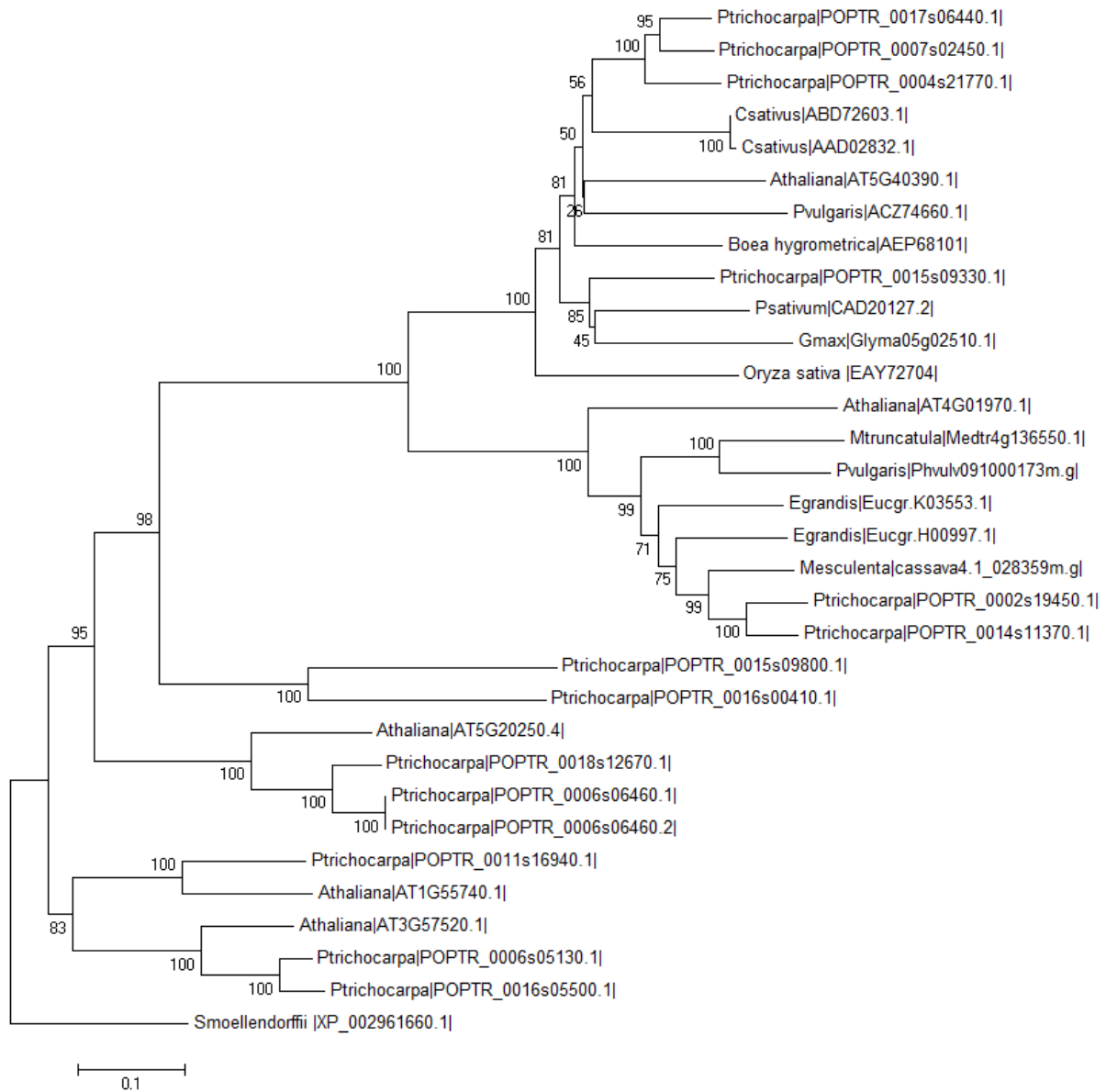


**Figure 4.1 Phylogenetic analyses using the Neighbour-Joining method and based on predicted amino acid sequences of confirmed and putative RFS proteins. Phytozome accession numbers are provided for the *Populus trichocarpa* RFS proteins and GenBank accession number are provided for the remaining proteins. Bootstrap values are based on 1000 replicates. Bars, 0.1 amino acid substitutions per site.**

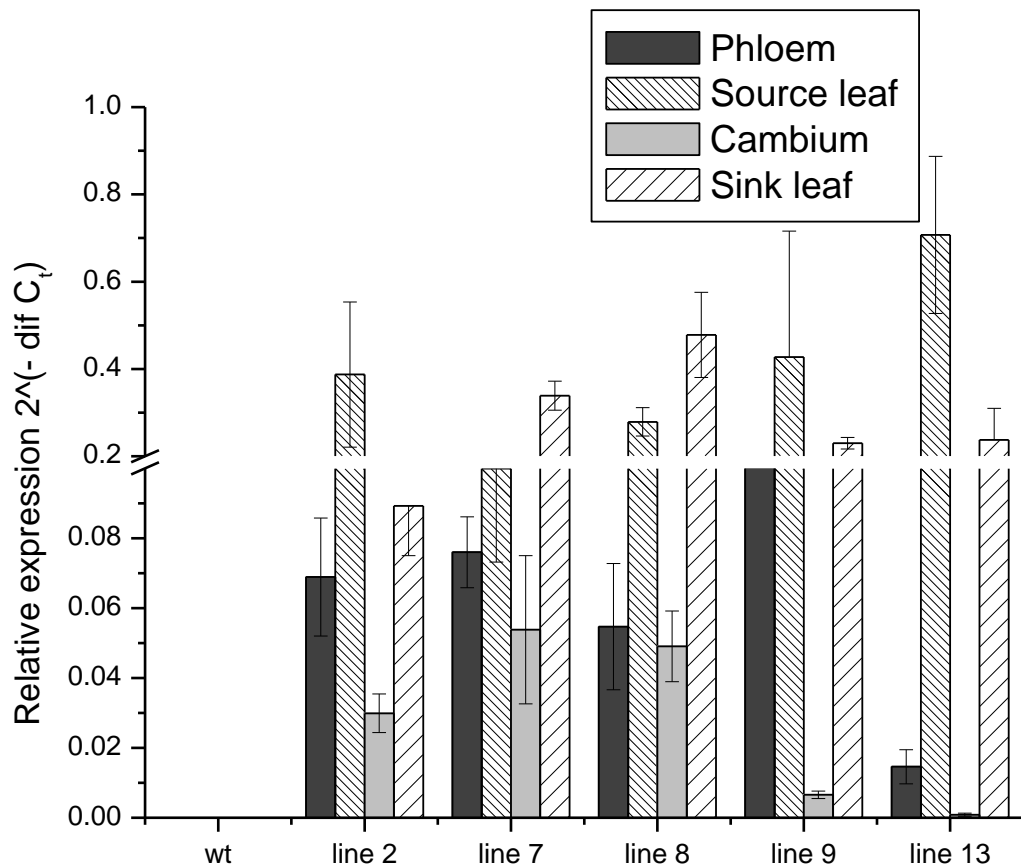
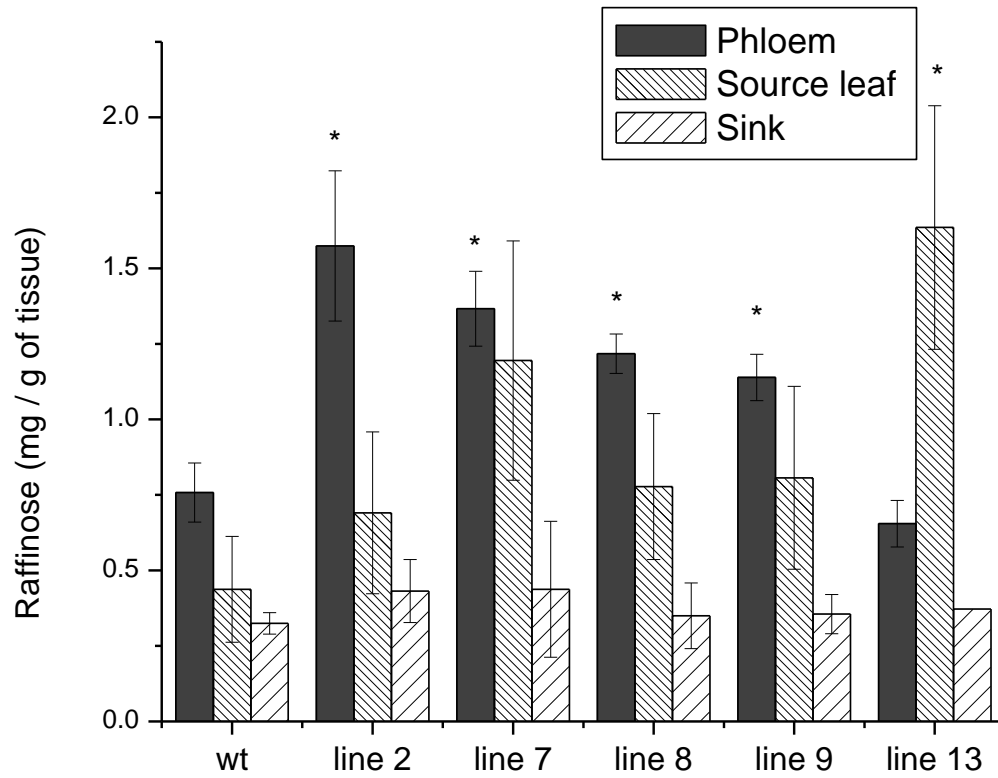
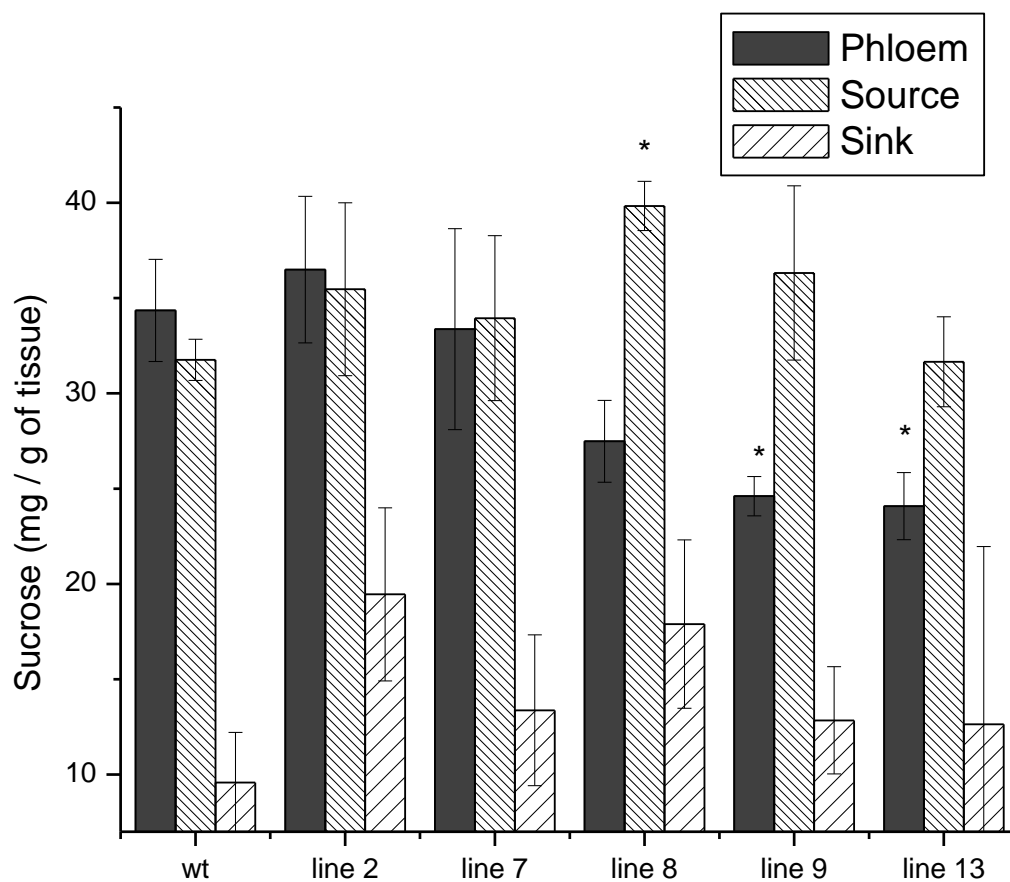


Figure 4.2 Transcript abundance of the *Cucumis sativus* raffinose synthase gene (*CsRFS*) in four tissue types of six months old greenhouse-grown hybrid poplar. Values presented are expression relative to the transcript abundance of translation initiation factor 5A (*TIF5A*= reference gene) using the formula  $2^{(-\Delta Ct)}$ . Bars represent the standard error of the mean (n=3).



**Figure 4.3** Concentration of raffinose in three tissue types of six-month old greenhouse-grown wild-type and *CsRFS* transgenic hybrid poplar. Bars represent the standard error of the mean (n=3). Asterisks represent statistical difference from wild type (wt) at 95% level.



**Figure 4.4** Concentration of sucrose in three tissue types of six-month old greenhouse-grown wild-type and *CsRFS* transgenic hybrid poplar. Bars represent the standard error of the mean (n=3). Asterisks represent statistical difference from wild type (wt) at 95% level.

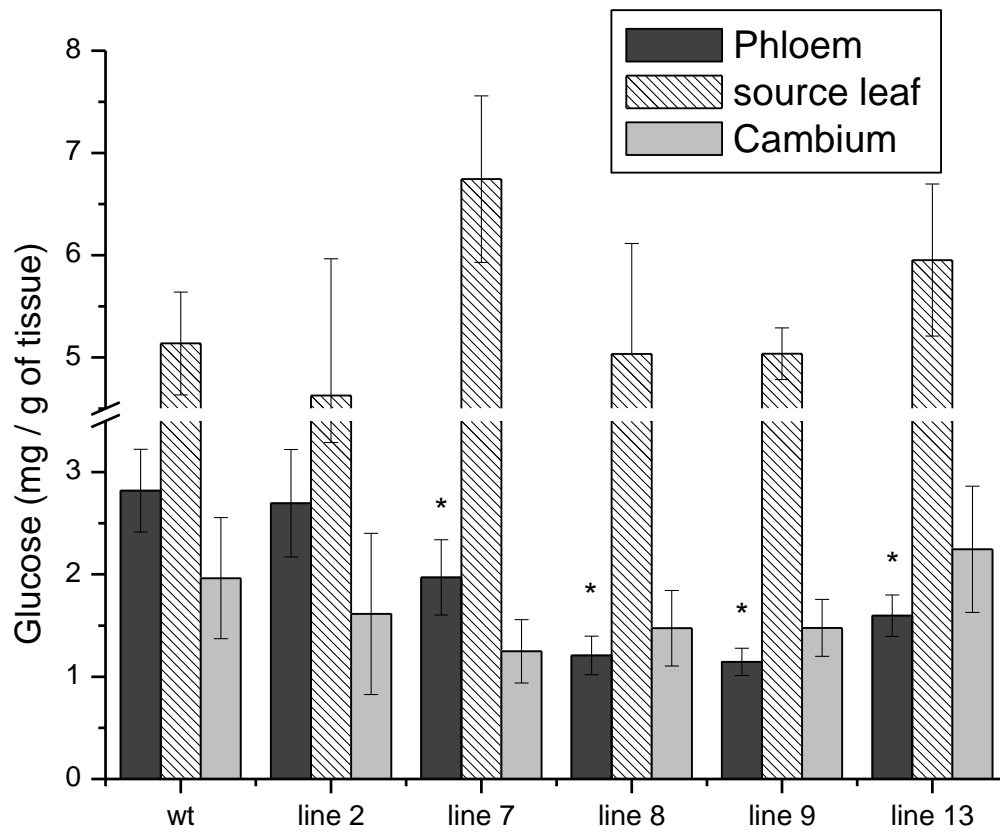


**Figure 4.5** Concentration of glucose in three tissue types of six-month old greenhouse-grown wild-type and *CsRFS* transgenic hybrid poplar. Bars represent the standard error of the mean (n=3). Asterisks represent statistical difference from wild type (wt) at 95% level.

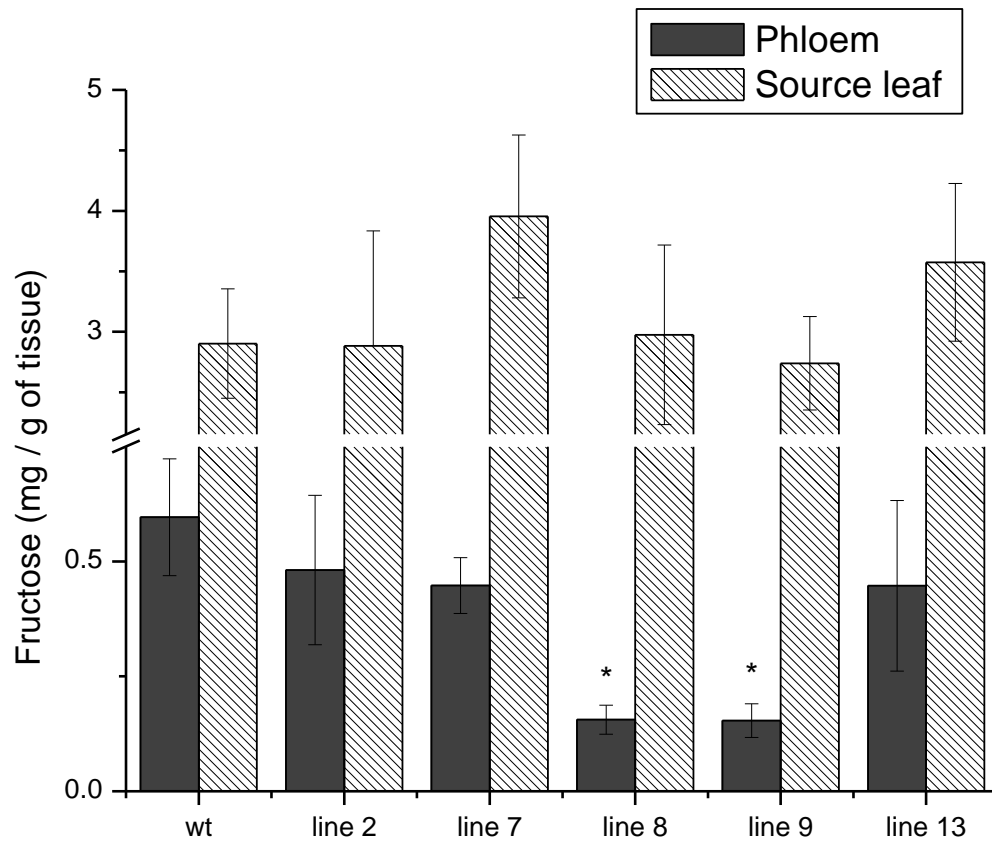


**Figure 4.6** Concentration of fructose in two tissue types of six-month old greenhouse-grown wild-type and *CsRFS* transgenic hybrid poplar. Bars represent the standard error of the mean (n=3). Asterisks represent statistical difference from wild type (wt) at 95% level.

<b>Lines</b>	<b>Source leaf %</b>	<b>Phloem %</b>
<b>wt</b>	2.05 (0.85)	1.32 (0.19)
<b>line 2</b>	4.41 (1.38)	1.06 (0.18)
<b>line 7</b>	3.25 (1.22)	1.11 (0.17)
<b>line 8</b>	<b>6.18 (0.91)</b>	1.42 (0.27)
<b>line 9</b>	6.36 (1.53)	1.03 (0.23)
<b>line 13</b>	3.12 (0.58)	1.63 (0.05)

**Table 4.1 Starch content (dry weight percentage) in source leaves and phloem tissues of six-month old wild-type and *CsRFS* transgenic poplar trees. Values represent the mean and standard error of the mean in parenthesis. Bold values represent statistical difference from wild type (wt) at 95% level (n=4).**

Lines	Arabinose		Rhamnose		Galactose		Glucose		Xylose		Mannose		Lignin	
	%		%		%		%		%		%		%	
<b>wt</b>	0.39	(0.05)	0.35	(0.06)	0.85	(0.02)	40.96	(1.47)	15.98	(0.46)	2.59	(0.08)	22.21	(0.40)
<b>line 2</b>	0.34	(0.05)	0.28	(0.08)	0.80	(0.18)	42.41	(1.94)	14.50	(1.17)	2.73	(0.28)	21.60	(0.51)
<b>line 7</b>	0.38	(0.06)	0.34	(0.07)	0.95	(0.06)	44.47	(0.89)	15.60	(1.09)	3.07	(0.29)	21.08	(0.36)
<b>line 8</b>	0.36	(0.02)	0.31	(0.05)	<b>0.73</b>	<b>(0.02)</b>	41.87	(1.64)	15.04	(0.52)	2.86	(0.10)	22.11	(0.54)
<b>line 9</b>	0.38	(0.02)	0.37	(0.04)	0.82	(0.04)	42.25	(2.19)	15.93	(0.76)	2.74	(0.14)	21.96	(0.62)
<b>line 13</b>	0.34	(0.03)	0.36	(0.07)	0.88	(0.06)	44.80	(0.71)	14.16	(1.31)	<b>3.55</b>	<b>(0.14)</b>	20.58	(0.80)

**Table 4.2 Structural cell wall carbohydrates and total lignin content of six-month old wild-type and *CsRFS* transgenic poplar trees. Values represent the mean and standard error of the mean in parenthesis. Bold values corresponding to a statistical difference from wild type (wt) at 95% level (n=4).**

Lines	Biomass		Total cellulose	
	vol (m <sup>3</sup> ) × density (kg m <sup>-3</sup> )		biomass × % cellulose	
	Kg		Kg	
<b>wt</b>	0.0337	(0.002)	0.01281	(0.0005)
<b>line 2</b>	0.0338	(0.002)	<b>0.01426</b>	<b>(0.0002)</b>
<b>line 7</b>	0.0355	(0.002)	<b>0.01542</b>	<b>(0.0007)</b>
<b>line 8</b>	0.0348	(0.002)	0.01464	(0.0012)
<b>line 9</b>	0.0340	(0.003)	0.01429	(0.0010)
<b>line 13</b>	0.0341	(0.002)	0.01530	(0.0010)

**Table 4.3 Biomass and total cellulose content of six-month old wild-type and *CsRFS* transgenic poplar trees. Biomass was calculated using the volume of the stem ( $1/3 \pi r^2 h$ ) and the wood density. Total cellulose was calculated based on the biomass and the percentage of glucose from the chemical analysis. Values represent the mean and standard error of the mean in parenthesis. Bold values correspond to a statistical difference from wild type (wt) at 95% level (n=3).**

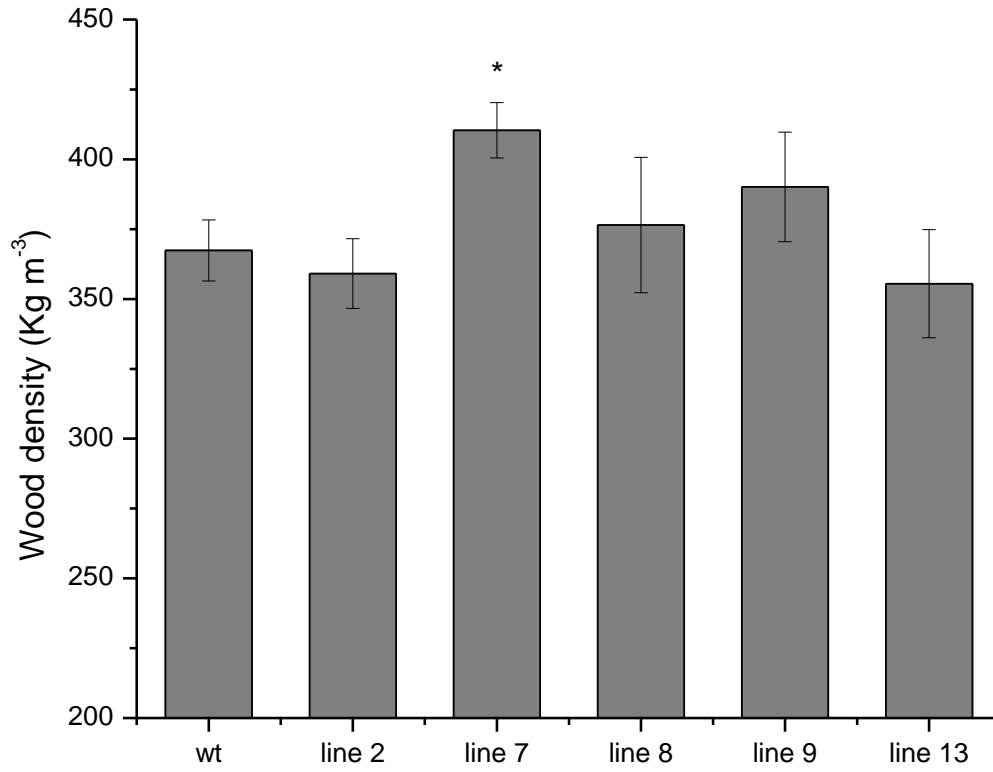


**Figure 4.7** Wood density of six-month old greenhouse-grown wild-type and *CsRFS* transgenic hybrid poplar. Bars represent the standard error of the mean (n=9). Asterisks represent statistical difference from wild type (wt) at 95% level.

## Chapter 5: Conclusion

### 5.1 Thesis summary

Members of the raffinose family of oligosaccharides serve as transport carbohydrates in the phloem, storage compounds in sink tissues, and metabolic agents to combat both abiotic and biotic stress in several plant species (Taji *et al.*, 2002; Cunningham *et al.*, 2003; Panikulangara *et al.*, 2004; Philippe *et al.*, 2010; Kim *et al.*, 2008). This pathway has been studied mostly in seeds and in plant species known to have raffinose as the primary transport photosynthate (Lehle & Tanner, 1973; Bachmann *et al.*, 1994; Peterbauer *et al.*, 2002). To-date, few studies have investigated this pathway in woody species, and none have investigated the impact of mis-regulation of the genes that code for enzymes in this pathway in trees. The main goal of this research project was to understand the function(s) of the enzymes that are involved in the biosynthesis of the raffinose family of oligosaccharides (RFO) in hybrid poplar (*Populus alba* × *grandidentata*). To achieve this objective the research was divided into three main studies.

In the first part of this research I identified and characterized two cDNAs encoding galactinol synthases from hybrid poplar (Chapter two), enzymes known to catalyze the first step in the biosynthesis of the RFOs. Phylogenetic comparisons of the *Pa* × *g*GalS isoforms with other known galactinol synthases suggested a putative role for these enzymes during biotic or abiotic stress in hybrid poplar. The two isoforms were cloned into a heterologous *Pichia pastoris* system to produce recombinant enzyme. The protein analysis showed that the two isoforms are indeed true, catalytically functional galactinol synthases; however, *Pa* × *g*GalSI possesses a broader pH and temperature range than *Pa* × *g*GalSII. Furthermore, an examination of the spatial and temporal expression patterns of the isoforms revealed that the

*Pa×gGolSII* transcript levels varied seasonally, implying a temperature-regulated transcriptional control of this gene in addition to the observed thermosensitivity of the respective enzyme. The cumulative results suggest that *Pa×gGolSI* may be involved in basic metabolic activities (*i.e.* storage), while *Pa×gGolSII* is likely involved in seasonal mobilization of carbohydrates.

To further understand the function of the galactinol synthase *in planta*, I investigated the effects of the mis-regulation of a *GolS* gene in hybrid poplar (Chapter three). For this, I inserted the *A. thaliana GolS3* gene (Taji *et al.*, 2002) in an over-expression construct; in addition a *Pa×gGolSRNAi*-suppression construct was created and tested in hybrid poplar under normal growth and stress conditions. *AtGolS3* over-expression transgenic lines 6 and 11, which had the highest transgene expression in vascular tissues, showed a clear growth phenotype. They were severely stunted and had numerous lateral stems that grew like vines and possessed noticeably chlorotic leaves. Furthermore, the stunted *AtGolS3* over-expressive lines had cell wall traits characteristic of tension wood. For example, cross section histochemical analyses revealed a significant increase in the number of vessels in the xylem tissue, as well as the presence of a G-layer in the fibres. These same transgenic lines showed a reduction in the microfibril angle and an increase in the percentage of cell wall crystallinity, while the chemical analysis showed an increase in glucose, implying higher cellulose content. Additionally, these lines showed a massive reduction in mannose content. Similar changes in the carbohydrate composition have been documented for tension wood G fibres compared to normal wood fibres (Gustafsson *et al.*, 1952; Schwerin, 1958; Meier, 1962 ; Hedenstrom *et al.*, 2009). Finally, total lignin percentage of the phenotypic transgenic lines was reduced compared to wild-type trees and the 2D NMR analysis indicated the absence of

the *p*-hydroxybenzoates group in the transgenic lines, which are common of poplar, aspen, willow and palm (Meyermans *et al.*, 2000; Landucci & Ralph, 2001). Although, soluble galactinol and raffinose content increased in the over-expressive transgenic lines, they did not improve the stress tolerance of leaf discs subjected to abiotic treatments. Furthermore, it seems that the efficiency of PSII ( $F_v/F_m$ ) in these extreme lines was affected before the stress treatments were applied. Given these results, I hypothesized that the over-expression of galactinol synthase or its resulting product, galactinol, may be a signal molecule to initiate a complex array of metabolic changes aimed at combating global stress. Consequently, it may also be involved in the initiation of tension wood formation, a cell wall alteration known to occur in response to environmental stimuli, such as gravity, which often results in stem reorientation to the upright position. The possibility that galactinol is a signal molecule was previously proposed in plants subjected to biotic stress (Kim *et al.*, 2008; Cho *et al.*, 2010). Similarly, Valluru & Van den Ende (2011) presented a model suggesting that galactinol and the RFOs maintain reactive oxygen species (ROS) homeostasis in plants, and proposed that these sugars may function as endogenous signals acting downstream of ROS signalling. These studies are in line with the hypothesis that I present here, since it is apparent that biotic and abiotic elicitors share a substantial proportion of features in their stress mechanisms with the formation of tension wood, a specialized xylem tissue, being a possible response to global stress. The main finding from the down-regulation of the *Pa×gGolS* experiment was the difference in expression of the *Pa×gGolS* isoforms under varied stress conditions. For example, the *Pa×gGolSII* increased more than 1000 times its expression when cold treatment was applied compared to normal growth conditions, confirming that this isoform is temperature sensitive, which was alluded to in the monthly endogenous expression

experiment (Chapter two). Additionally, a water stress treatment failed to alter the transcript abundance of *Pa×gGolsII* in the source leaves of wild-type trees. The relative expressions of the other isoforms (*Pa×gGolsIV*, *III* and *I*) were markedly lower compared to *Pa×gGolsII* when the trees were monitored under cold stress. Similar results were shown for *Arabidopsis*, as *AtGols3* was induced by cold stress but not by drought or salt stress (Taji *et al.*, 2002). By contrast, *AtGols1* and *2* were induced by drought and salinity stress, but not by cold stress (Taji *et al.*, 2002). Additionally, galactinol and raffinose content was reduced in the *Pa×gGols* RNAi lines; however no visible phenotype was found.

To further expand our knowledge of the biosynthesis of these metabolites, an over-expression construct of the *Cucumis sativus* raffinose synthase (*CsRFS*) was inserted into hybrid poplar (Chapter four) to study the effects of raffinose synthesis on carbon allocation and wood chemistry, by using a gene later in the pathway. The alteration in carbon partitioning found in the transgenic lines resulted in an increase in the total biomass when compared to wild-type trees. In addition, the total cellulose content of all transgenic lines was higher than its corresponding wild-type trees. The results in chapter four suggest that changes in the composition of the sugars loaded in the phloem by the over-expression of *RFS* can affect the carbon allocation, and consequently the xylem development and tree growth. Interestingly, the over-expression of *RFS* and the accumulation of its corresponding product, raffinose, did not have the signalling effect in hybrid poplar as witnessed in the *Gols* over-expression, suggesting that the signal molecule for stress response may be galactinol and not raffinose.

## **5.2 Future research**

The results obtained from this thesis, which focused on the raffinose family of oligosaccharides in *Populus*, contribute substantially to our fundamental understanding of the importance of the raffinose family of oligosaccharides in plant growth and development, as impacted by carbon allocation. The results from the over-expression of the galactinol synthase (Chapter three) suggest that this enzyme or its biochemical product, galactinol, could play a significant role in stress signalling. Additionally, the over-expression of the raffinose synthase and/or the accumulation of raffinose has an effect in carbon allocation and consequently in tree growth (Chapter four), but no evidence for a general signalling. Although highly informative, the results of this thesis have also generated several additional questions, and opportunities for future research. The most obvious are listed below.

### **5.2.1 Use of different promoters to drive the expression of *GolS***

In the present study the enhanced tandem cauliflower mosaic virus (2x35S) promoter was used to over-express the *A. thaliana* galactinol synthase gene (Chapter three). This is a constitutive promoter that drives the expression of the gene in all plant tissues. The ensuing *AtGolS3* transgenic lines showed a phenotype in the xylem tissue, with the formation of what appears to be tension wood. A parallel study to investigate the impact of targeted over-expression of galactinol synthase in xylem tissue should be a natural progression. For example, the CesA promoters that will drive expression of the transgene in secondary cell wall would be suitable. Furthermore, recent studies have identified xylem-specific (DX; Developing xylem) promoters based on transcriptome analysis of poplar (Ko *et al.*, 2012) that would be equally suitable. The GUS expression patterns of the transgenic plants in this study showed that the DX promoters were active in the xylem cells at early seedling growth

and had strongest expression in the developing xylem cells at later growth stages of poplar. Using this approach may minimize the impact of the galactinol synthesis in leaf tissue, and thus not stimulate the preserved global stress response, culminating in a stunted phenotype.

### **5.2.2 Application of a cold stress treatment on *Gols* and *RFS* over-expression lines**

The results in chapter three showed that leaf discs of galactinol synthase over-expressive lines were more susceptible (measured by the efficiency of PSII-  $F_v/F_m$ ) to cold stress than its corresponding wild-type samples. Taking account of these results, future work should analyze the effects of a cold and freezing stress treatments applied to the whole tree, measuring the stress tolerance of the galactinol synthase transgenic lines. Additionally, the main alteration in the raffinose synthase transgenic lines was in carbon allocation resulting in an increase in biomass under normal growth conditions (Chapter four), and as such it would be interesting to compare the pattern of carbohydrate partitioning when the trees are subjected to cold stress.

### **5.2.3 Double transformation of the *AtGols3* phenotypic lines with a *RFS* construct**

In chapter three I suggested that galactinol may be a signal molecule for global stress response. This hypothesis can be further confirmed if the extreme *AtGols3* transgenic lines are used as the starting plant material for a stacking strategy to create double transformants with the raffinose synthase gene. The hypothesis of this experiment is that the additional galactinol produced by the transgenic lines, that resulted in the xylem phenotype, will be rapidly metabolized to raffinose and not accumulate and thus should “rescue” the xylem phenotype observed in the *Gols* transgenic poplar plants.

#### **5.2.4 Grafting experiments using the *AtGols3* phenotypic lines and wild-type trees**

Wild-type and *AtGols3* transgenic hybrid poplar trees could be used for reciprocal grafting experiments. This approach would test the effects of grafting the extreme phenotypic *AtGols3* lines with wild type and studying the cell wall characteristics to further elucidate whether or not galactinol is indeed a signalling molecule in trees, and more specifically what pathways may be stimulated by the accumulation of this sugar alcohol in poplar trees.

## References

- Amiard, V., Mueh, K., Demmig-Adams, B., Ebbert, V., Turgeon, R., & Adams, W. (2005). Anatomical and photosynthetic acclimation to the light environment in species with differing mechanisms of phloem loading. *Proceedings of the National Academy of Sciences of the United States of America*, *102*(36), 12968-12973.
- Anderson, C., & Kohorn, B. (2001). Inactivation of *Arabidopsis* SIP1 leads to reduced levels of sugars and drought tolerance. *Journal of Plant Physiology*, *158*(9), 1215-1219.
- Andersson-Gunneras, S., Mellerowicz, E. J., Love, J., Segerman, B., Ohmiya, Y., Coutinho, P. M., *et al.* (2006). Biosynthesis of cellulose-enriched tension wood in *Populus*: Global analysis of transcripts and metabolites identifies biochemical and developmental regulators in secondary wall biosynthesis. *Plant Journal*, *45*(2), 144-165.
- Ayre, B. G., Blair, J. E., & Turgeon, R. (2003). Functional and phylogenetic analyses of a conserved regulatory program in the phloem of minor veins. *Plant Physiology*, *133*(3), 1229-1239.
- Bachmann, M., & Keller, F. (1995). Metabolism of the raffinose family oligosaccharides in leaves of *Ajuga reptans* L - intercellular and intracellular compartmentation. *Plant Physiology*, *109*(3), 991-998.
- Bachmann, M., Matile, P., & Keller, F. (1994). Metabolism of the raffinose family oligosaccharides in leaves of *Ajuga reptans* L - cold-acclimation, translocation, and sink to source transition - discovery of chain elongation enzyme. *Plant Physiology*, *105*(4), 1335-1345.
- Bailly, C., Audigier, C., Ladonne, F., Wagner, M. H., Coste, F., Corbineau, F., *et al.* (2001). Changes in oligosaccharide content and antioxidant enzyme activities in developing bean seeds as related to acquisition of drying tolerance and seed quality. *Journal of Experimental Botany*, *52*(357), 701-708.
- Beebe, D. U., & Turgeon, R. (1992). Localization of galactinol, raffinose, and stachyose synthesis in *Cucurbita pepo* leaves. *Planta*, *188*(3), 354-361.
- Bento dos Santos, T., Budzinski, I. G. F., Marur, C. J., Petkowicz, C. L. O., Pereira, L. F. P., & Vieira, L. G. E. (2011). Expression of three galactinol synthase isoforms in *Coffea arabica* L. and accumulation of raffinose and stachyose in response to abiotic stresses. *Plant Physiology and Biochemistry*, *49*(4), 441-448.

- Bentum, A.L.K., Cote, W.A., Day, A.C., & Timell, T.E. (1969). Distribution of lignin in normal and tension wood. *Wood Sci.Technol.*, 3, 3: 218
- Black, M., Corbineau, F., Grzesik, M., Guy, P., & Come, D. (1996). Carbohydrate metabolism in the developing and maturing wheat embryo in relation to its desiccation tolerance. *Journal of Experimental Botany*, 47(295), 161-169.
- Blackman, S. A., Obendorf, R. L., & Leopold, A. C. (1992). Maturation proteins and sugars in desiccation tolerance of developing soybean seeds. *Plant Physiology*, 100(1), 225-230.
- Bloch, A., Grenier-de March, G., Sourdioux, M., Peterbauer, T., & Richter, A. (2005). Induction of raffinose oligosaccharide biosynthesis by abscisic acid in somatic embryos of alfalfa (*Medicago sativa* L.). *Plant Science*, 168(4), 1075-1082.
- Blokhina, O., Virolainen, E., & Fagerstedt, K. (2003). Antioxidants, oxidative damage and oxygen deprivation stress: A review. *Annals of Botany*, 91(2), 179-194.
- Bolwell, G., Bindschedler, L., Blee, K., Butt, V., Davies, D., Gardner, S., *et al.* (2002). The apoplastic oxidative burst in response to biotic stress in plants: A three-component system. *Journal of Experimental Botany*, 53(372), 1367-1376.
- Bowling, A. J., & Vaughn, K. C. (2008). Immunocytochemical characterization of tension wood: Gelatinous fibers contain more than just cellulose. *American Journal of Botany*, 95(6), 655-663.
- Brenac, P., Horbowicz, M., Downer, S. M., Dickerman, A. M., Smith, M. E., & Obendorf, R. L. (1997). Raffinose accumulation related to desiccation tolerance during maize (*Zea mays* L) seed development and maturation. *Journal of Plant Physiology*, 150(4), 481-488.
- Brunner, A. M., Busov, V. B., & Strauss, S. H. (2004). Poplar genome sequence: Functional genomics in an ecologically dominant plant species. *Trends in Plant Science*, 9(1), 49-56.
- Buitink, J., Claessens, M. M. A. E., Hemminga, M. A., & Hoekstra, F. A. (1998). Influence of water content and temperature on molecular mobility and intracellular glasses in seeds and pollen. *Plant Physiology*, 118(2), 531-541.
- Burgert, I., & Fratzl, P. (2009). Plants control the properties and actuation of their organs through the orientation of cellulose fibrils in their cell walls. *Integrative and Comparative Biology*, 49(1), 69-79.
- Caffrey, M., Fonseca, V., & Leopold, A. C. (1988). Lipid-sugar interactions - relevance to anhydrous biology. *Plant Physiology*, 86(3), 754-758.

Cao, P., Song, J., Zhou, C., Weng, M., Liu, J., Wang, F., *et al.* (2009). Characterization of multiple cold induced genes from *Ammopiptanthus mongolicus* and functional analyses of gene *AmEBP1*. *Plant Molecular Biology*, 69(5), 529-539.

Carpenter, J. F., & Crowe, J. H. (1989). An infrared spectroscopic study of the interactions of carbohydrates with dried proteins. *Biochemistry*, 28(9), 3916-3922.

Caspar, T., Huber, S. C., & Somerville, C. (1985). Alterations in growth, photosynthesis, and respiration in a starchless mutant of *Arabidopsis thaliana* (L) deficient in chloroplast phosphoglucomutase activity. *Plant Physiology*, 79(1), 11-17.

Castonguay, Y., & Nadeau, P. (1998). Enzymatic control of soluble carbohydrate accumulation in cold-acclimated crowns of alfalfa. *Crop Science*, 38(5), 1183-1189.

Castonguay, Y., Nadeau, P., Lechasseur, P., & Chouinard, L. (1995). Differential accumulation of carbohydrates in alfalfa cultivars of contrasting winter hardiness. *Crop Science*, 35(2), 509-516.

Chiou, T., & Bush, D. (1998). Sucrose is a signal molecule in assimilate partitioning. *Proceedings of the National Academy of Sciences of the United States of America*, 95(8), 4784-4788.

Cho, S. M., Kang, E. Y., Kim, M. S., Yoo, S. J., Im, Y. J., Kim, Y. C., *et al.* (2010). Jasmonate-dependent expression of a galactinol synthase gene is involved in priming of systemic fungal resistance in *Arabidopsis thaliana*. *Botany-Botanique*, 88(5), 452-461.

Choi, S., Zhang, Y., Ito, H., Stephens, K., Winder, T., Edwards, G., *et al.* (1998). Increasing rice productivity by manipulation of starch biosynthesis during seed development. In D. Armstrong, R. Riley & J. Waterlow (Eds.), *Feeding a world population of more than eight billion people: A challenge to science* (pp. 137-149). New York: Oxford University Press.

Cisneros, H. A., Belanger, L., Gee, W. Y., Watson, P. A., & Hatton, J. V. (1996). Wood and fibre properties of hybrid poplars from southern British Columbia. *1996 Pulping Conference, Books 1 and 2*, 675-685.

Clair, B., Almeras, T., Pilate, G., Jullien, D., Sugiyama, J., & Riekkel, C. (2011). Maturation stress generation in poplar tension wood studied by synchrotron radiation microdiffraction. *Plant Physiology*, 155(1), 562-570.

Clair, B., Almeras, T., & Sugiyama, J. (2006). Compression stress in opposite wood of angiosperms: Observations in chestnut, mani and poplar. *Annals of Forest Science*, 63(5), 507-510.

- Coleman, H. D., Yan, J., & Mansfield, S. D. (2009). Sucrose synthase affects carbon partitioning to increase cellulose production and altered cell wall ultrastructure. *Proceedings of the National Academy of Sciences of the United States of America*, 106(31), 13118-13123.
- Cooke, J. E. K., & Rood, S. B. (2007). Trees of the people: The growing science of poplars in Canada and worldwide. *Canadian Journal of Botany-Revue Canadienne De Botanique*, 85(12), 1103-1110.
- Cox, S. E., & Stushnoff, C. (2001). Temperature-related shifts in soluble carbohydrate content during dormancy and cold acclimation in *Populus tremuloides*. *Canadian Journal of Forest Research-Revue Canadienne De Recherche Forestiere*, 31(4), 730-737.
- Cullis, I. F., Saddler, J. N., & Mansfield, S. D. (2004). Effect of initial moisture content and chip size on the bioconversion efficiency of softwood lignocellulosics. *Biotechnology and Bioengineering*, 85(4), 413-421.
- Cunningham, S. M., Nadeau, P., Castonguay, Y., Laberge, S., & Volenec, J. J. (2003). Raffinose and stachyose accumulation, galactinol synthase expression, and winter injury of contrasting alfalfa germplasms. *Crop Science*, 43(2), 562-570.
- Daly, R., & Hearn, M. T. W. (2005). Expression of heterologous proteins in *Pichia pastoris*: A useful experimental tool in protein engineering and production. *Journal of Molecular Recognition*, 18(2), 119-138.
- Dastidar, K., Maitra, S., Goswami, L., Roy, D., Das, K., & Majumder, A. (2006). An insight into the molecular basis of salt tolerance of L-*myo*-inositol 1-P synthase (PcINO1) from *Porteresia coarctata* (roxb.) Tateoka, a halophytic wild rice. *Plant Physiology*, 140(4), 1279-1296.
- Dinant, S., & Lemoine, R. (2010). The phloem pathway: New issues and old debates. *Comptes Rendus Biologies*, 333(4), 307-319.
- Dirk, L. M. A., van der Krol, A. R., Vreugdenhil, D., Hilhorst, H. W. M., & Bewley, J. D. (1999). Galactomannan, soluble sugar and starch mobilization following germination of *Trigonella foenum-graecum* seeds. *Plant Physiology and Biochemistry*, 37(1), 41-50.
- Downie, B., Gurusinghe, S., Dahal, P., Thacker, R. R., Snyder, J. C., Nonogaki, H., *et al.* (2003). Expression of a galactinol synthase gene in tomato seeds is up-regulated before maturation desiccation and again after imbibition whenever radicle protrusion is prevented. *Plant Physiology*, 131(3), 1347-1359.

- Eveland, A. L., & Jackson, D. P. (2012). Sugars, signalling, and plant development. *Journal of Experimental Botany*, 63(9), 3367-3377.
- Fang, C., Clair, B., Gril, J., & Liu, S. (2008). Growth stresses are highly controlled by the amount of G-layer in poplar tension wood. *Iawa Journal*, 29(3), 237-246.
- Faruya, N., Takahashi, S., & Miazaki, H. (1970). The chemical composition of the gelatinous layer from the tension wood of *Populus euramericana*. *J. Jap. Wood Res. Soc.*, 16, 26-30.
- Felsenstein, J. (1985). Confidence-limits on phylogenies - an approach using the bootstrap. *Evolution*, 39(4), 783-791.
- Fisher, D., & Cash-Clark, C. (2000). Sieve tube unloading and post-phloem transport of fluorescent tracers and proteins injected into sieve tubes via severed aphid stylets. *Plant Physiology*, 123(1), 125-137.
- Fiske, C. H., & Subbarow, Y. (1925). The colorimetric determination of phosphorus. *Journal of Biological Chemistry*, 66(2), 375-400.
- Fowler, S., & Thomashow, M. (2002). *Arabidopsis* transcriptome profiling indicates that multiple regulatory pathways are activated during cold acclimation in addition to the CBF cold response pathway. *Plant Cell*, 14(8), 1675-1690.
- Foyer, C. H., & Shigeoka, S. (2011). Understanding oxidative stress and antioxidant functions to enhance photosynthesis. *Plant Physiology*, 155(1), 93-100.
- Fu, Q., Cheng, L., Guo, Y., & Turgeon, R. (2011). Phloem loading strategies and water relations in trees and herbaceous plants. *Plant Physiology*, 157(3), 1518-1527.
- Fujimoto, Z., Kaneko, S., Momma, M., Kobayashi, H., & Mizuno, H. (2003). Crystal structure of rice alpha-galactosidase complexed with D-galactose. *Journal of Biological Chemistry*, 278(22), 20313-20318.
- Gaffney, S. H., Haslam, E., Lilley, T. H., & Ward, T. R. (1988). Homotactic and heterotactic interactions in aqueous-solutions containing some saccharides. Experimental results and an empirical relationship between saccharide solvation and solute solute interactions. *Journal of the Chemical Society-Faraday Transactions*, 84, 2545-2552.
- Gamalei, Y. (1989). Structure and function of leaf minor veins in trees and herbs a taxonomic review. *Trees-Structure and Function*, 3(2), 96-110.

Garman, S. C., Hannick, L., Zhu, A., & Garboczi, D. N. (2002). The 1.9 angstrom structure of alpha-N-acetylgalactosaminidase: Molecular basis of glycosidase deficiency diseases. *Structure*, 10(3), 425-434.

Gibon, Y., Blasing, O. E., Palacios-Rojas, N., Pankovic, D., Hendriks, J. H. M., Fisahn, J., *et al.* (2004). Adjustment of diurnal starch turnover to short days: Depletion of sugar during the night leads to a temporary inhibition of carbohydrate utilization, accumulation of sugars and post-translational activation of ADP-glucose pyrophosphorylase in the following light period. *Plant Journal*, 39(6), 847-862.

Gilbert, G., Wilson, C., & Madore, M. (1997). Root-zone salinity alters raffinose oligosaccharide metabolism and transport in *Coleus*. *Plant Physiology*, 115(3), 1267-1276.

Gilmour, S., Sebolt, A., Salazar, M., Everard, J., & Thomashow, M. (2000). Overexpression of the *Arabidopsis* CBF3 transcriptional activator mimics multiple biochemical changes associated with cold acclimation. *Plant Physiology*, 124(4), 1854-1865.

Gleave, A. P. (1992). A versatile binary vector system with a T-DNA organizational-structure conducive to efficient integration of cloned DNA into the plant genome. *Plant Molecular Biology*, 20(6), 1203-1207.

Gomez-Ariza, J., Campo, S., Rufat, M., Estopa, M., Messeguer, J., San Segundo, B., *et al.* (2007). Sucrose-mediated priming of plant defense responses and broad-spectrum disease resistance by overexpression of the maize pathogenesis-related PR protein in rice plants. *Molecular Plant-Microbe Interactions*, 20(7), 832-842.

Gorshkova, T. A., Gurjanov, O. P., Mikshina, P. V., Ibragimova, N. N., Mokshina, N. E., Salnikov, V. V., *et al.* (2010). Specific type of secondary cell wall formed by plant fibers. *Russian Journal of Plant Physiology*, 57(3), 328-341.

Goswami, L., Dunlop, J. W. C., Jungnikl, K., Eder, M., Gierlinger, N., Coutand, C., *et al.* (2008). Stress generation in the tension wood of poplar is based on the lateral swelling power of the G-layer. *Plant Journal*, 56(4), 531-538.

Groover, A., Nieminen, K., Helariutta, Y., & Mansfield, S. D. (2010). Wood formation in *Populus*. In S. Jansson, R. P. Bhalerao & A. Groover (Eds.), *Genetics and genomics of Populus*. 8 ed., (pp: 201-224). New York: Springer.

Gustafsson, C., Ollinmaa, P. J., & Saarnio, J. (1952). The carbohydrates in birchwood. *Acta Chemica Scandinavica*, 6(8), 1299-1300.

- Gustavsson, M., Bengtsson, M., Gatenholm, P., Glasser, W., Teleman, A., & Dhlman, O. (2001). Isolation, characterization and material properties of 4-O-methylglucuronoxylan from aspen. In E. Chiellini, H. Gil, G. Braunegg, J. Buchert, p. Gatenholm & M. vander Zee (Eds.), *Biorelated polymers-sustainable polymer science and technology* (pp. 41-52). New York: Kluwer Academy/Plenon.
- Hannah, M. A., Zuther, E., Buchel, K., & Heyer, A. G. (2006). Transport and metabolism of raffinose family oligosaccharides in transgenic potato. *Journal of Experimental Botany*, 57(14), 3801-3811.
- Haritatos, E., Ayre, B., & Turgeon, R. (2000). Identification of phloem involved in assimilate loading in leaves by the activity of the galactinol synthase promoter. *Plant Physiology*, 123(3), 929-937.
- Hart, D. O., He, S. M., Chany, C. J., Withers, S. G., Sims, P. F. G., Sinnott, M. L., *et al.* (2000). Identification of asp-130 as the catalytic nucleophile in the main alpha-galactosidase from *Phanerochaete chrysosporium*, a family 27 glycosyl hydrolase. *Biochemistry*, 39(32), 9826-9836.
- Hedenstrom, M., Wiklund-Lindstrom, S., Oman, T., Lu, F., Gerber, L., Schatz, P., *et al.* (2009). Identification of lignin and polysaccharide modifications in *Populus* wood by chemometric analysis of 2D NMR spectra from dissolved cell walls. *Molecular Plant*, 2(5), 933-942.
- Hellgren, J. M., Olofsson, K., & Sundberg, B. (2004). Patterns of auxin distribution during gravitational induction of reaction wood in poplar and pine. *Plant Physiology*, 135(1), 212-220.
- Helliwell, C., & Waterhouse, P. (2003). Constructs and methods for high-throughput gene silencing in plants. *Methods*, 30(4), 289-295.
- Higuchi, T. (1997). *Biochemistry and molecular biology of wood*. New York: Springer-Verlag.
- Hillis, W. E., Evans, R., & Washusen, R. (2004). An unusual formation of tension wood in a natural forest *Acacia sp.* *Holzforschung*, 58(3), 241-245.
- Hincha, D. K., Zuther, E., & Heyer, A. G. (2003). The preservation of liposomes by raffinose family oligosaccharides during drying is mediated by effects on fusion and lipid phase transitions. *Biochimica Et Biophysica Acta-Biomembranes*, 1612(2), 172-177.

- Hinesley, L., Pharr, D., Snelling, L., & Funderburk, S. (1992). Foliar raffinose and sucrose in 4 conifer species - relationship to seasonal temperature. *Journal of the American Society for Horticultural Science*, 117(5), 852-855.
- Hirsh, A. (1987). Vitrification in plants as a natural form of cryoprotection. *Cryobiology*, 24(3), 214-228.
- Hirsh, A., Williams, R., & Meyerman, H. (1985). A novel method of natural cryoprotection - intracellular glass-formation in deeply frozen *Populus*. *Plant Physiology*, 79(1), 41-56.
- Horbowicz, M. and Obendorf, R.L. (1994). Seed desiccation tolerance and storability: Dependence on flatulence-producing oligosaccharides and cyclitols. *Seed Science Research*, 4, 385-405.
- Huber, S. C. (1983). Role of sucrose-phosphate synthase in partitioning of carbon in leaves. *Plant Physiology*, 71(4), 818-821.
- Jansson, S., & Douglas, C. J. (2007). *Populus*: A model system for plant biology. *Annual Review of Plant Biology*, 58, 435-458.
- Joersbo, M., Pedersen, S., Nielsen, J., Marcussen, J., & Brunstedt, J. (1999). Isolation and expression of two cDNA clones encoding UDP-galactose epimerase expressed in developing seeds of the endospermous legume guar. *Plant Science*, 142(2), 147-154.
- Johansson, T., & Karacic, A. (2011). Increment and biomass in hybrid poplar and some practical implications. *Biomass & Bioenergy*, 35(5), 1925-1934.
- Joo, J., Bae, Y., & Lee, J. (2001). Role of auxin-induced reactive oxygen species in root gravitropism. *Plant Physiology*, 126(3), 1055-1060.
- Jourez, B. (1997). Tension wood 1. Definition and distribution in the tree. *BASE: Biotechnologie, Agronomie, Société Et Environnement*, 1, 100-112.
- Jourez, B., Riboux, A., & Leclercq, A. (2001). Anatomical characteristics of tension wood and opposite wood in young inclined stems of poplar (*Populus euramericana* cv 'ghoy'). *Iawa Journal*, 22(2), 133-157.
- Kaku, T., Serada, S., Baba, K., Tanaka, F., & Hayashi, T. (2009). Proteomic analysis of the G-layer in poplar tension wood. *Journal of Wood Science*, 55(4), 250-257.
- Kandler, O., & Hopf, H. (1982). Oligosaccharides based on sucrose (sucrosyl oligosaccharides). *Encyclopedia of plant physiology (new series)* (pp. 348-383)

- Karner, U., Peterbauer, T., Raboy, V., Jones, D., Hedley, C., & Richter, A. (2004). Myo-inositol and sucrose concentrations affect the accumulation of raffinose family oligosaccharides in seeds. *Journal of Experimental Botany*, 55(405), 1981-1987.
- Keller, F., & Pharr, D. (1996). Metabolism of carbohydrates in sinks and sources: Galactosyl-sucrose oligosaccharides. In Zamski E, & Schaffer AA (Eds.), *Photoassimilate distribution in plants and crops* (pp. 115-184). New York: Marcel Dekker.
- Kim, M. S., Cho, S. M., Kang, E. Y., Im, Y. J., Hwangbo, H., Kim, Y. C., *et al.* (2008). Galactinol is a signaling component of the induced systemic resistance caused by *Pseudomonas chlororaphis* O6 root colonization. *Molecular Plant-Microbe Interactions*, 21(12), 1643-1653.
- Knaupp, M., Mishra, K. B., Nedbal, L., & Heyer, A. G. (2011). Evidence for a role of raffinose in stabilizing photosystem II during freeze-thaw cycles. *Planta*, 234(3), 477-486.
- Ko, J., Kim, H., Hwang, I., & Han, K. (2012). Tissue-type-specific transcriptome analysis identifies developing xylem-specific promoters in poplar. *Plant Biotechnology Journal*, 10(5), 587-596.
- Kolosova, N., Miller, B., Ralph, S., Ellis, B. E., Douglas, C., Ritland, K., *et al.* (2004). Isolation of high-quality RNA from gymnosperm and angiosperm trees. *BioTechniques*, 36(5), 821-824.
- Koster, K. L. (1991). Glass-formation and desiccation tolerance in seeds. *Plant Physiology*, 96(1), 302-304.
- Kuo, C. M., & Timell, T. E. (1969). Isolation and characterization of a galactan from tension wood of american beech (*Fagus grandifolia* ehrl). *Svensk Papperstidning-Nordisk Cellulosa*, 72(21), 703.
- Landucci, L. L., & Ralph, S. A. (2001). Reaction of p-hydroxycinnamyl alcohols with transition metal salts. IV. tailored syntheses of beta-O-4 trimers. *Journal of Wood Chemistry and Technology*, 21(1), 31-52.
- Larson, P. (1994). *The vascular cambium*. New York: Springer-Verlag.
- Lautner, S., Ehling, B., Windeisen, E., Rennenberg, H., Matyssek, R., & Fromm, J. (2007). Calcium nutrition has a significant influence on wood formation in poplar. *New Phytologist*, 173(4), 743-752.

- Lee, R. H., Lin, M. C., & Chen, S. C. G. (2004). A novel alkaline alpha-galactosidase gene is involved in rice leaf senescence. *Plant Molecular Biology*, 55(2), 281-295.
- Lehle, L., & Tanner, W. (1973). Biosynthesis of raffinose. *Hoppe-Seylers Zeitschrift Fur Physiologische Chemie*, 354(10-1), 1217-1217.
- Li, S. H., Li, T. P., Kim, W. D., Kitaoka, M., Yoshida, S., Nakajima, M., *et al.* (2007). Characterization of raffinose synthase from rice (*Oryza sativa* L. var. nipponbare). *Biotechnology Letters*, 29(4), 635-640.
- Liu, J. J. J., Odegard, W., & Delumen, B. O. (1995). Galactinol synthase from kidney bean cotyledon and zucchini leaf - purification and N-terminal sequences. *Plant Physiology*, 109(2), 505-511.
- Lohaus, G., Winter, H., Riens, B., & Heldt, H. (1995). Further-studies of the phloem loading process in leaves of barley and spinach - the comparison of metabolite concentrations in the apoplastic compartment with those in the cytosolic compartment and in the sieve tubes. *Botanica Acta*, 108(3), 270-275.
- Lu, Y., Gehan, J. P., & Sharkey, T. D. (2005). Daylength and circadian effects on starch degradation and maltose metabolism. *Plant Physiology*, 138(4), 2280-2291.
- Ly, H. D., Howard, S., Shum, K., He, S. M., Zhu, A., & Withers, S. G. (2000). The synthesis, testing and use of 5-fluoro-alpha-D-galactosyl fluoride to trap an intermediate on green coffee bean alpha-galactosidase and identify the catalytic nucleophile. *Carbohydrate Research*, 329(3), 539-547.
- Mansfield, S. D., Kim, H., Lu, F., & Ralph, J. (2012). Whole plant cell wall characterization using solution-state 2D NMR. *Nature Protocols*, 7(7), 1-11.
- Mansfield, S. D., & Weineisen, H. (2007). Wood fiber quality and kraft pulping efficiencies of trembling aspen (*Populus tremuloides* michx) clones. *Journal of Wood Chemistry and Technology*, 27(3-4), 135-151.
- McDermitt, D. (1990). Sources of error in the estimation of stomatal conductance and transpiration from porometer data. *HortScience*, 25(12), 1538-1548.
- Megraw, R., Leaf, G., & Bremer, D. (1998). Longitudinal shrinkage and microfibril angle in loblolly pine. in microfibril angle in wood: *Proceedings of the IAWA/IUFRO International Workshop on the Significance of Microfibril Angle to Wood Quality*, Westport, N.Z. University of Canterbury Press, Canterbury, N.Z. pp. 27-61.

- Meier, H. (1962). Studies on a galactan from tension wood of beech (*Fagus silvatica* L.). *Acta Chemica Scandinavica*, 16(9), 2275-&.
- Mellerowicz, E. J., Baucher, M., Sundberg, B., & Boerjan, W. (2001). Unravelling cell wall formation in the woody dicot stem. *Plant Molecular Biology*, 47(1-2), 239-274.
- Mellerowicz, E. J., & Gorshkova, T. A. (2012). Tensional stress generation in gelatinous fibres: A review and possible mechanism based on cell-wall structure and composition. *Journal of Experimental Botany*, 63(2), 551-565.
- Mellerowicz, E. J., Immerzeel, P., & Hayashi, T. (2008). Xyloglucan: The molecular muscle of trees. *Annals of Botany*, 102(5), 659-665.
- Merchant, A., Tausz, M., Keitel, C., & Adams, M. A. (2010). Relations of sugar composition and delta <sup>13</sup>C in phloem sap to growth and physiological performance of *Eucalyptus globulus* (labill). *Plant Cell and Environment*, 33(8), 1361-1368.
- Meyermans, H., Morreel, K., Lapierre, C., Pollet, B., De Bruyn, A., Busson, R., *et al.* (2000). Modifications in lignin and accumulation of phenolic glucosides in poplar xylem upon down-regulation of caffeoyl-coenzyme A O-methyltransferase, an enzyme involved in lignin biosynthesis. *Journal of Biological Chemistry*, 275(47), 36899-36909.
- Mooney, C., Stolle-Smits, T., Schols, H., & de Jong, E. (2001). Analysis of retted and non retted flax fibres by chemical and enzymatic means. *Journal of Biotechnology*, 89(2-3), 205-216.
- Munch, E. (1927). Dynamik der saftstromtungen. *Ber. Deut. Bot. Ges.*, 44, 69-71.
- Muzquiz, M., Burbano, C., Pedrosa, M., Folkman, W., & Gulewicz, K. (1999). Lupins as a potential source of raffinose family oligosaccharides - preparative method for their isolation and purification. *Industrial Crops and Products*, 9(3), 183-188.
- Nadwodnik, J., & Lohaus, G. (2008). Subcellular concentrations of sugar alcohols and sugars in relation to phloem translocation in *Plantago major*, *Plantago maritima*, *Prunus persica*, and *Apium graveolens*. *Planta*, 227(5), 1079-1089.
- Nishikubo, N., Awano, T., Banasiak, A., Bourquin, V., Ibatullin, F., Funada, R., *et al.* (2007). Xyloglucan endo-transglycosylase (XET) functions in gelatinous layers of tension wood fibers in poplar - A glimpse into the mechanism of the balancing act of trees. *Plant and Cell Physiology*, 48(6), 843-855.

- Nishizawa, A., Yabuta, Y., & Shigeoka, S. (2008). Galactinol and raffinose constitute a novel function to protect plants from oxidative damage. *Plant Physiology*, *147*(3), 1251-1263.
- Nobuchi T. & Fujita M. (1972). Cytological structure of differentiating tension wood fibres of *Populus euroamericana* × *canadensis*). *Journal of the Japan Wood Research Society*, *18*, 3: 137-144.
- Noiraud, N., Maurousset, L., & Lemoine, R. (2001). Identification of a mannitol transporter, *AgMaT1*, in celery phloem. *Plant Cell*, *13*(3), 695-705.
- Norberg,P.H. & Meier,H. (1966). Physical and chemical properties of gelatinous layer in tension wood fibres of aspen (*Populus tremula* L). *Holzforschung*, *20*, 6: 174.
- Okuyama, T., Yamamoto, H., Yoshida, M., Hattori, Y., & Archer, R. R. (1994). Growth stresses in tension wood - role of microfibrils and lignification. *Annales Des Sciences Forestieres*, *51*(3), 291-300.
- Oosumi, C., Nozaki, J., & Kida, T. (1998). *Raffinose synthetase gene, method of producing raffinose and transgenic plant* International Patent Publication WO98/49273, PCT/JP97/03879.
- Ottow, E. A., Brinker, M., Teichmann, T., Fritz, E., Kaiser, W., Brosche, M., *et al.* (2005). *Populus euphratica* displays apoplastic sodium accumulation, osmotic adjustment by decreases in calcium and soluble carbohydrates, and develops leaf succulence under salt stress. *Plant Physiology*, *139*(4), 1762-1772.
- Panikulangara, T. J., Eggers-Schumacher, G., Wunderlich, M., Stransky, H., & Schoffl, F. (2004). Galactinol synthase1. A novel heat shock factor target gene responsible for heat-induced synthesis of raffinose family oligosaccharides in *Arabidopsis*. *Plant Physiology*, *136*(2), 3148-3158.
- Pate, J. S., & Arthur, D. J. (2000). Uptake, partitioning and utilization of carbon and nitrogen in the phloem bleeding tree, tasmanian blue gum (*Eucalyptus globulus*). *Australian Journal of Plant Physiology*, *27*(8-9), 869-884.
- Pence, V., & Clark, J. (2005). Desiccation, cryopreservation and germination of seeds of the rare wetland species, *Plantago cordata* lam. *Seed Science and Technology*, *33*(3), 767-770.
- Peterbauer, T., Lahuta, L. B., Blochl, A., Mucha, J., Jones, D. A., Hedley, C. L., *et al.* (2001). Analysis of the raffinose family oligosaccharide pathway in pea seeds with contrasting carbohydrate composition. *Plant Physiology*, *127*(4), 1764-1772.

Peterbauer, T., Mach, L., Mucha, J., & Richter, A. (2002). Functional expression of a cDNA encoding pea (*Pisum sativum* L.) raffinose synthase, partial purification of the enzyme from maturing seeds, and steady-state kinetic analysis of raffinose synthesis. *Planta*, 215(5), 839-846.

Peterbauer, T., Mucha, J., Mayer, U., Popp, M., Glossl, J., & Richter, A. (1999). Stachyose synthesis in seeds of adzuki bean (*Vigna angularis*): Molecular cloning and functional expression of stachyose synthase. *Plant Journal*, 20(5), 509-518.

Peterbauer, T., & Richter, A. (2001). Biochemistry and physiology of raffinose family oligosaccharides and galactosyl cyclitols in seeds. *Seed Science Research*, 11(3), 185-197.

Peters, S. (2007). Protection mechanisms in the resurrection plant *Xerophyta viscosa* (baker): Both sucrose and raffinose family oligosaccharides (RFOs) accumulate in leaves in response to water deficit. *Journal of Experimental Botany*, 58(8), 1947.

Peterson, E. B., & Peterson, N. M. (1995). *Aspen managers' handbook for British Columbia* (Canada–British Columbia Partnership Agreement on Forest Resource Development FRDA II and BC Ministry of Forests No. FRDA Report No. 230). Victoria, BC:

Philippe, R. N., Ralph, S. G., Mansfield, S. D., & Bohlmann, J. (2010). Transcriptome profiles of hybrid poplar (*Populus trichocarpa x deltoides*) reveal rapid changes in undamaged, systemic sink leaves after simulated feeding by forest tent caterpillar (*Malacosoma disstria*). *New Phytologist*, 188(3), 787-802.

Plomion, C., Leprovost, G., & Stokes, A. (2001). Wood formation in trees. *Plant Physiology*, 127(4), 1513-1523.

Popper, Z. A., & Fry, S. C. (2008). Xyloglucan-pectin linkages are formed intraprotoplasmically, contribute to wall-assembly, and remain stable in the cell wall. *Planta*, 227(4), 781-794.

Ramsperger-Gleixner, M., Geiger, D., Hedrich, R., & Sauer, N. (2004). Differential expression of sucrose transporter and polyol transporter genes during maturation of common plantain companion cells. *Plant Physiology*, 134(1), 147-160.

Rennie, E. A., & Turgeon, R. (2009). A comprehensive picture of phloem loading strategies. *Proceedings of the National Academy of Sciences of the United States of America*, 106(33), 14162-14167.

- Ribeiro, M., Felix, C. R., & De Paulino Lozzi, S. (2000). Soybean seed galactinol synthase activity as determined by a novel colorimetric assay. *Revista Brasileira De Fisiologia Vegetal*, 12(3), 203-212.
- Richardson, J., Cooke, J. E. K., Isebrands, J. G., Thomas, B. R., & Van Rees, K. C. J. (2007). Poplar research in Canada - a historical perspective with a view to the future. *Canadian Journal of Botany-Revue Canadienne De Botanique*, 85(12), 1136-1146.
- Rolland, F., Moore, B., & Sheen, J. (2002). Sugar sensing and signaling in plants. *Plant Cell*, 14, S185-S205.
- Romo, S., Labrador, E., & Dopico, B. (2001). Water stress-regulated gene expression in *Cicer arietinum* seedlings and plants. *Plant Physiology and Biochemistry*, 39(11), 1017-1026.
- Ruel, K., & Barnoud, F. (1978). Researches on quantitative-determination of tension wood of beech - validity of criterion amount of galactose. *Holzforschung*, 32(5), 149-156.
- Russin, W., & Evert, R. (1985). Studies on the leaf of *Populus deltoides* (Salicaceae) - ultrastructure, plasmodesmatal frequency, and solute concentrations. *American Journal of Botany*, 72(8), 1232-1247.
- Saitou, N., & Nei, M. (1987). The Neighbor-Joining method - a new method for reconstructing phylogenetic trees. *Molecular Biology and Evolution*, 4(4), 406-425.
- Saravitz, D. M., Pharr, D. M., & Carter, T. E. (1987). Galactinol synthase activity and soluble sugars in developing seeds of 4 soybean genotypes. *Plant Physiology*, 83(1), 185-189.
- Schneider, T., & Keller, F. (2009). Raffinose in chloroplasts is synthesized in the cytosol and transported across the chloroplast envelope. *Plant and Cell Physiology*, 50(12), 2174-2182.
- Schwerin, G. (1958). The chemistry of reaction wood part II. The polysaccharides of *Eucalyptus goniocalyx* and *Pinus radiata*. *Holzforschung*, 12, 43-48.
- Smirnoff, N., & Cumbes, Q. (1989). Hydroxyl radical scavenging activity of compatible solutes. *Phytochemistry*, 28(4), 1057-1060.
- Smith, A. M., & Stitt, M. (2007). Coordination of carbon supply and plant growth. *Plant Cell and Environment*, 30(9), 1126-1149.

Smith, P. T., Kuo, T. M., & Crawford, C. G. (1991). Purification and characterization of galactinol synthase from mature zucchini squash leaves. *Plant Physiology*, 96(3), 693-698.

Sprenger, N., & Keller, F. (2000). Allocation of raffinose family oligosaccharides to transport and storage pools in *Ajuga reptans*: The roles of two distinct galactinol synthases. *Plant Journal*, 21(3), 249-258.

Stewart, J. J., Kadla, J. F., & Mansfield, S. D. (2006). The influence of lignin chemistry and ultrastructure on the pulping efficiency of clonal aspen (*Populus tremuloides* michx.). *Holzforschung*, 60(2), 111-122.

Stitt, M., & Krapp, A. (1999). The interaction between elevated carbon dioxide and nitrogen nutrition: The physiological and molecular background. *Plant Cell and Environment*, 22(6), 583-621.

Stoop, J., Williamson, J., & Pharr, D. (1996). Mannitol metabolism in plants: A method for coping with stress. *Trends in Plant Science*, 1(5), 139-144.

Sugiyama, K., Okuyama, T., Yamamoto, H., & Yoshida, M. (1993). Generation process of growth stresses in cell-walls - relation between longitudinal released strain and chemical-composition. *Wood Science and Technology*, 27(4), 257-262.

Taji, T., Ohsumi, C., Iuchi, S., Seki, M., Kasuga, M., Kobayashi, M., *et al.* (2002). Important roles of drought- and cold-inducible genes for galactinol synthase in stress tolerance in *Arabidopsis thaliana*. *Plant Journal*, 29(4), 417-426.

Takahashi, R., Joshee, N., & Kitagawa, Y. (1994). Induction of chilling resistance by water-stress, and cDNA sequence-analysis and expression of water stress-regulated genes in rice. *Plant Molecular Biology*, 26(1), 339-352.

Tamura, K., Peterson, D., Peterson, N., Stecher, G., Nei, M., & Kumar, S. (2011). MEGA5: Molecular evolutionary genetics analysis using maximum likelihood, evolutionary distance, and maximum parsimony methods. *Molecular Biology and Evolution*, 28(10), 2731-2739.

Tanner, W., & Kandler, O. (1968). Myo-inositol a cofactor in biosynthesis of stachyose. *European Journal of Biochemistry*, 4(2), 233-&.

Tausz, M., Merchant, A., Kruse, J., Samsa, G., & Adams, M. A. (2008). Estimation of drought-related limitations to mid-rotation aged plantation grown *Eucalyptus globulus* by phloem sap analysis. *Forest Ecology and Management*, 256(4), 844-848.

- Teleman, A., Nordstrom, M., Tenkanen, M., Jacobs, A., & Dahlman, O. (2003). Isolation and characterization of O-acetylated glucomannans from aspen and birch wood. *Carbohydrate Research*, 338(6), 525-534.
- Telewski, F., Aloni, R., & Sauter, J. (1996). Physiology of secondary tissues of *Populus*. In R. Stettler, H. Bradshaw, P. Heilman & T. Hinckley (Eds.), *Biology of Populus and its implications for management and conservation* (pp. 301-323). Ottawa, Ontario, Canada: NRC Research Press,.
- Telewski, F. W. (2006). A unified hypothesis of mechanoperception in plants. *American Journal of Botany*, 93(10), 1466-1476.
- Teskey, R. O., Fites, J. A., Samuelson, L. J. & Bongarten, B. C.(1986). Stomatal and nonstomatal limitations to net photosynthesis in *Pinus taeda* L. under different environmental conditions. *Tree Physiol.*, 2 (1-3), 131-142.
- Timell, T. E. (1986). *Compression wood in gymnosperms*. Heidelberg: Springer- Verlag.
- Truernit, E. (2001). Plant physiology: The importance of sucrose transporters. *Current Biology*, 11(5), R169-R171.
- Turgeon, R., & Medville, R. (2004). Phloem loading. A reevaluation of the relationship between plasmodesmatal frequencies and loading strategies. *Plant Physiology*, 136(3), 3795-3803.
- Turgeon, R. (1996). Phloem loading and plasmodesmata. *Trends in Plant Science*, 1(12), 418-423.
- Turgeon, R. (2010). The role of phloem loading reconsidered. *Plant Physiology*, 152(4), 1817-1823.
- Turgeon, R., & Wolf, S. (2009). Phloem transport: Cellular pathways and molecular trafficking. *Annual Review of Plant Biology*, 60, 207-221.
- Tuskan, G. A., DiFazio, S., Jansson, S., Bohlmann, J., Grigoriev, I., Hellsten, U., *et al.* (2006). The genome of black cottonwood, *Populus trichocarpa* (Torr. & Gray). *Science*, 313, 1596-1604.
- Unda, F., Canam, T., Preston, L., & Mansfield, S. D. (2012). Isolation and characterization of galactinol synthases from hybrid poplar. *Journal of Experimental Botany*, 63(5), 2059-2069.

- Uraki, Y., Nakamura, A., Kishimoto, T., & Ubukata, M. (2007). Interaction of hemicelluloses with monolignols. *Journal of Wood Chemistry and Technology*, 27(1), 9-21.
- Valluru, R., & Van den Ende, W. (2011). Myo-inositol and beyond - emerging networks under stress. *Plant Science*, 181(4), 387-400.
- Van Bel, A. J. E. (2003). The phloem, a miracle of ingenuity. *Plant Cell and Environment*, 26(1), 125-149.
- Vinocur, B., & Altman, A. (2005). Recent advances in engineering plant tolerance to abiotic stress: Achievements and limitations. *Current Opinion in Biotechnology*, 16(2), 123-132.
- Volk, G. M., Haritatos, E. E., & Turgeon, R. (2003). Galactinol synthase gene expression in melon. *Journal of the American Society for Horticultural Science*, 128(1), 8-15.
- Volk, G., Turgeon, R., & Beebe, D. (1996). Secondary plasmodesmata formation in the minor-vein phloem of *Cucumis melo* L and *Cucurbita pepo* L. *Planta*, 199(3), 425-432.
- Vonk, C. G. (1973). Computerization of rulands X-ray method for determination of crystallinity in polymers. *Journal of Applied Crystallography*, 6(APR1), 148-152.
- Wakiuchi, N., Shiomi, R., & Tamaki, H. (2003). Production of galactinol from sucrose by plant enzymes. *Bioscience Biotechnology and Biochemistry*, 67(7), 1465-1471.
- Wang, Z. I., Li, P. H., Fredricksen, M., Gong, Z. H., Kim, C. S., Zhang, C. Q., *et al.* (2004). Expressed sequence tags from *Thellungiella halophila*, a new model to study plant salt-tolerance. *Plant Science*, 166(3), 609-616.
- Wang, Z., Zhu, Y., Wang, L., Liu, X., Liu, Y., Phillips, J., *et al.* (2009). A WRKY transcription factor participates in dehydration tolerance in *Boea hygrometrica* by binding to the W-box elements of the galactinol synthase (*BhGolS1*) promoter. *Planta*, 230(6), 1155-1166.
- Wardrop, A. B., & Dadswell, H. E. (1948). The nature of reaction wood 1. the structure and properties of tension wood fibres. *Australian Journal of Scientific Research Series B-Biological Sciences*, 1(1), 3-16.
- Washusen, R., Evans, R., & Southerton, S. (2005). A study of *Eucalyptus grandis* and *Eucalyptus globulus* branch wood microstructure. *Iawa Journal*, 26(2), 203-210.
- Watanabe, E., & Oeda, K. (1998). *Raffinose synthase genes and use thereof*. European Patent Application EPO849359, 97122417.5.

Westermarck, U. (1982). Calcium promoted phenolic coupling by superoxide radical - a possible lignification reaction in wood. *Wood Science and Technology*, 16(1), 71-78.

Wilkins, O., Waldron, L., Nahal, H., Provart, N. J., & Campbell, M. M. (2009). Genotype and time of day shape the *Populus* drought response. *The Plant Journal*, 60(4), 715.

Wimmers, L., & Turgeon, R. (1991). Transfer cells and solute uptake in minor veins of *Pisum sativum* leaves. *Planta*, 186(1), 2-12.

Wu, X., Kishitani, S., Ito, Y., & Toriyama, K. (2009). Accumulation of raffinose in rice seedlings overexpressing *OsWRKY11* in relation to desiccation tolerance. *Plant Biotechnology*, 26(4), 431-434.

Zhao, T. Y., Thacker, R., Corum, J. W., Snyder, J. C., Meeley, R. B., Obendorf, R. L., *et al.* (2004). Expression of the maize galactinol synthase gene family: (I) expression of two different genes during seed development and germination. *Physiologia Plantarum*, 121(4), 634-646.

Zobel, B., & van Buijtenen, J. (1989). Wood variation: Its causes and control. In T. E. Timell (Ed.). Heidelberg: Springer-Verlag.

Zuckerka, E., & Pauling, L. (1965). Molecules as documents of evolutionary history. *Journal of Theoretical Biology*, 8(2), 357

Zuther, E., Buchel, K., Hundertmark, M., Stitt, M., Hinch, D. K., & Heyer, A. G. (2004). The role of raffinose in the cold acclimation response of *Arabidopsis thaliana*. *FEBS Letters*, 576(1-2), 169-173.